NASA Technical Paper 2485

June 1985

Static and Dynamic Pressure Measurements on a NACA 0012 Airfoil in the Ames High Reynolds Number Facility

John B. McDevitt
and Arthur F. Okuno

NASA

NASA Technical Paper 2485

1985

Static and Dynamic Pressure Measurements on a NACA 0012 Airfoil in the Ames High Reynolds Number Facility

John B. McDevitt
and Arthur F. Okuno

Ames Research Center
Moffett Field, California

NASA
National Aeronautics
and Space Administration

Scientific and Technical Information Branch

NOMENCLATURE

b	span of airfoil, cm (in.)
c	chord of airfoil, cm (in.)
c_n	section normal force coefficient, $\int_0^1 (C_{p_\ell} - C_{p_u}) d(x/c)$
c_p	pressure coefficient $(p - p_\infty)/q_\infty$
c_p^*	pressure coefficient at sonic velocity
f	frequency, Hz
$\bar{f}$	reduced frequency, $2\pi fc$ divided by free-stream velocity
$\dot{m}_{(1)}, \dot{m}_{(2)}$	mass flow rates through sidewall boundary-layer removal panels (see fig. 4)
$\dot{m}_T$	tunnel mass flow rate
M	Mach number
p	static pressure, N/m^2 (lb/ft^2)
P_t	pitot pressure, N/m^2 (lb/ft^2)
P_T, PT	total pressure, N/m^2 (lb/ft^2)
q	dynamic pressure, N/m^2 (lb/ft^2)
Re	Reynolds number
$Re_{c,\infty}$	Reynolds number based on airfoil chord and free-stream conditions
u,v	local velocities in x,z directions
x,z	airfoil coordinates, see figure 1, cm (in.)
x_{sh}	shock location
$\bar{X},Z$	test section coordinates, see figure 4, cm (in.)
y	distance from wall, cm (in.)
ΔP	(instantaneous pressure) - (mean static pressure)
$\Delta(\ )$	incremental quantity
$\langle\langle(\ )\rangle\rangle$	rms value
α	angle of attack, deg
δ^*	sidewall boundary-layer displacement thickness
δ_0^*	sidewall boundary-layer displacement thickness for $\dot{m}_{(1)} = \dot{m}_{(2)} = 0$

Subscripts

B	conditions at buffet onset
ℓ	lower surface
N	nominal or design value
u	upper surface
∞	free-stream value

SUMMARY

An experimental study has been conducted of the supercritical flows at high subsonic speeds over a NACA 0012 airfoil in order to acquire aerodynamic data suitable for evaluating numerical-flow codes. The measurements consisted primarily of static and dynamic pressures on the airfoil and test-channel walls. Shadowgraphs were also taken of the flow field near the airfoil. The tests were performed at free-stream Mach numbers from approximately 0.7 to 0.8, at angles of attack sufficient to include the onset of buffet, and at Reynolds numbers (based on airfoil chord) from 1 million to 14 million. A unique test section was employed which was designed specifically to obtain two-dimensional airfoil data with a minimum of wall interference effects. Boundary-layer suction panels were used to minimize sidewall interference effects. Flexible upper and lower walls allowed test-channel area-ruling to nullify Mach number changes induced by the mass removal, to correct for longitudinal boundary-layer growth, and to provide contouring compatible with the streamlines of the model in free air.

INTRODUCTION

The rapid advances in computer technology have prompted similar advancements in computational methods to the extent that computers are now routinely used to complement the wind tunnel in the development of new aerospace vehicles. However, the continued development of computational methods requires experimental studies to suggest better turbulence models and to provide test cases for evaluating new codes. In response to this need Ames Research Center has acquired the High Reynolds Number Facility, which is being used to perform basic fluid dynamic studies in support of numerical code developments. This facility consists of two major test channels, HRC-1 and HRC-2, which are described in detail in references 1 and 2. The present experimental study documents the high subsonic, locally supercritical, flows about a two-dimensional airfoil.

Two-dimensional airfoil test data at moderate to large Reynolds numbers (where natural transition is far forward on the airfoil) which are sufficiently accurate to be useful in evaluating numerical codes are virtually nonexistent. The primary problem is wall interference. Usually, test results are assigned "corrected" Mach numbers and angles of attack. This procedure is undesirable if the data are to be used in critical assessments of numerical methods. To correct this situation the first test section for use with the facility HRC-2 channel was designed to minimize wall-interference effects. Sidewall boundary-layer removal is used to minimize the sidewall interference effects. The shapes of the upper and lower walls are adjustable so that Mach number changes associated with the sidewall mass removal and boundary-layer displacement effects can be nullified and to allow streamline contouring compatible with the airfoil in free air. The success of this approach was demonstrated in reference 2. The first airfoil chosen for testing in the facility was the NACA 0012, which has long been a standard for evaluating wind tunnel test techniques and computational methods and for making comparisons between data obtained in different wind tunnels throughout the world.

The present tests were confined to high subsonic speeds at which the airfoil creates locally supersonic flows terminated by shock waves. The test program included both mean and dynamic pressure measurements so that the often overlooked unsteady flow aspects could be included. In particular, the onset of buffet at high subsonic speeds was carefully delineated.

APPARATUS AND TECHNIQUES

Model

The symmetrical NACA 0012 profile is shown in figure 1 together with a tabulation of the streamwise locations where measurements of static and dynamic pressures were made. As noted in this figure, the model deviates from the theoretical shape near the trailing edge for practical reasons. A sketch of the model installed in the test section is shown in figure 2. The angle-of-attack rotation is about the airfoil midchord.

The model was machined from stainless steel. The deviation between measured (near the midspan where the pressure orifices were located) and design coordinates was small, never exceeding $\Delta z/c = 0.0005$ and usually less than 0.0002. These small deviations should not noticeably affect the results. The static pressure orifices were 0.03 cm in diameter and connected to individual differential pressure transducers located

in insulated containers vented to the atmosphere. These containers were located as near as possible to the test section, and the length of tubing from orifice to transducer was less than 0.6 m. The dynamic pressure transducers were buried in the model with the diaphragm about 0.13 cm from the surface, and the orifice diameter was about 0.18 cm. The reference pressure sides for these transducers were connected to adjacent (same x/c) static pressure orifices by employing sufficient lengths of tubing to provide adequate damping so that the transducers responded only to deviations from the mean.

Facility

The facility and techniques for obtaining two-dimensional airfoil data with a minimum of wall interference effects is described in reference 2. A brief review is presented here.

The facility is of the blowdown type, discharging into a large vacuum sphere for low total pressure runs (P_T below about 2 atm) and into the atmosphere for large total pressure runs (P_T above about 2 atm). A schematic of the new facility is shown in figure 3, and details of the airfoil test section are presented in figure 4. The test Mach number is controlled by the adjustable throat at the downstream end of the test section. Sidewall vent panels (perforated plates) located just upstream of this throat maintain the "test cabin" pressure essentially at free-stream static pressure. This alleviates the structural strength and rigidity requirements for the test-section walls and facilitates the use of large viewing ports for making shadowgraphs and laser velocimeter measurements.

Upper and lower wall interference effects on the airfoil flow field can be eliminated, at least in principle, by contouring the walls to follow the streamlines in free air at a specific test condition. For the present tests an airfoil code was used to compute the streamline shapes for walls initially located 1.5 airfoil chords above and below the model. No attempt was made to further adjust the wall contours based on experimental measurements, as is done in the "adaptive wall" approach. However, since solid walls are involved, the appropriate boundary conditions can easily be incorporated in numerical methods when the test data are used to evaluate codes.

Sidewall interference effects are reduced by thinning the sidewall boundary layer by suction at two sets of porous panels (one set near the entrance to the test section and the other as near as possible to the model), each set operating separately from the other. The suction is provided by the low pressure in the downstream diffuser; the mass-removal rate is controlled by throttling valves and monitored at venturi sections (see lower right-hand portion of fig. 3). Mass removal alters the longitudinal Mach number distribution in the test channel, but this can be nullified by appropriate adjustments in the upper and lower wall contours (refs. 2 and 3).

The source of high-pressure dry air is the 930-m^3 Ames Underground Air Storage Facility, pressurized to 2×10^7 N/m^2 (3,000 psi) and maintained at ambient temperature. With the present test section, the maximum mass flow rate available is about 360 Kg/sec (800 lb/sec), for which the unit Reynolds number at subsonic speeds is about 10^8/m and airfoil test data can be acquired in the Reynolds number range, based on chord length of 20.3 cm (8 in.), from about 1×10^6 to 20×10^6. The corresponding available test run times range from about 5 min to 1 min. High-frequency pressure transducers and hot wire anemometers were used to measure pressure and velocity fluctuations in the test section. Typical results are presented in table 1.

A single-pass shadowgraph system was installed as shown in figure 5. Because of the limited space available inside the test cabin, the light source (steady illumination for motion pictures, spark illumination for still photography) was located outside the cabin, the light entering through a small window. The light beam is collimated by a spherical mirror, folded once, and then directed into the test section. For spark-illuminated shadowgraphs a motor-driven film magazine from an aerial-type camera (20-cm by 23-cm photographs) was mounted near the test section window as shown in figure 5. For motion pictures the light beam exits by traversing a similar path on the far side of the test section with the camera located outside the test cabin.

Tests and Procedures

The flow phenomenon chosen for study here is the supercritical flow about the airfoil at high subsonic speeds. An important and necessary part of the investigation was the determination of the onset of unsteady flow (buffet) as affected by test Mach number, Reynolds number, and model angle of attack. For each test condition the experimental technique used required that the upper and lower walls be adjusted mechanically at the seven jacking stations shown in figure 4. Since the wall contours could not be changed while the tunnel was running, the test program evolved around a series of nominal test conditions, referred to as "data sets," as shown in figure 6. The data sets are numbered in the chronological order that the test program progressed.

Measurements were made at Reynolds numbers (based on chord) ranging from 1 to at least 10 million. No attempt was made to fix transition on the model. However, a few oil-film runs were made which provide qualitative information regarding transition Reynolds number. A thin oil film was applied to the model surface, and post-run inspection indicated turbulent transition wedges (easily recognized by their 10° spreading angle) occurred in the vicinity of small roughness elements or surface irregularities near the model leading edge for a certain range of Reynolds number. Based on these observations the transition Reynolds number for the present tests was estimated to occur between Reynolds numbers of

1 and 2 million. Since the condition of the model surface is critical in maintaining laminar flow, changes with time, and is difficult to monitor, particularly in the absence of boundary-layer surveys, the emphasis in this study will be on the data acquired at high Reynolds numbers. Specifically, the test data at $Re_{c,\infty}$ = 10 million will be considered to be the most appropriate for use in evaluating codes.

A detailed description and calibration of the test section is given in reference 2. The recommended mass removal rates for the sidewall suction panels (see fig. 4) are 3% of the tunnel mass-flow rate at the first station ($\dot{m}_{(1)} = 0.03\ \dot{m}_T$) and 0.8% at the second station ($\dot{m}_{(2)} = 0.008\ \dot{m}_T$). The effectiveness of the mass removal in reducing the sidewall displacement thickness of the boundary layer is illustrated in figures 7 and 8.

The upper and lower wall contours used for the six data sets required inputs from three sources: First, a mean shape correction was required to offset the test section boundary layer growth in the model testing region. For Mach number and Reynolds number ranges of the present tests, ramp angles of 0.38° were to be applied as shown in figure 9. Second, wall changes were necessary to offset the effects of sidewall mass removal. These changes (see figs. 9 and 10) vary with the test Mach number, but were not sensitive to Reynolds number, at least within the accuracy of the calibrations tests of reference 2, provided that the mass removal rates are large, as in the present case. Third, the walls were contoured to conform to the streamlines of the model in free air, at a height of approximately 1.5 chords, as computed by Deiwert's method (refs. 4 and 5) for a Reynolds number of 10 million (see fig. 11 and tabulated values in table 2).

The free-stream test Mach number (corresponding to $x/c = -\infty$) was determined as follows: The local Mach number near the side wall of the test channel directly ahead of the wing and at station $\bar{X}/c$ = -3 (fig. 4) was evaluated from measurements of total and static pressures. A Mach number more representative of that near the center of the test channel was then obtained by correcting for a slight variation in local Mach number across the channel (a residual effect from the uneven flow in the bellmouth entrance to the test section). This correction was ΔM = -0.003. Finally, the influence of the test model on the measurements at tunnel station $\bar{X}/c$ = -3 was estimated by Deiwert's numerical method and the appropriate corrections (see table 3) were applied.

The measurement of airfoil static pressure employed transducers located outside the test section, but close to the airfoil (see discussion in "Model" section), and the response time (to reach 99.9% of the true value) was about 1 sec. Two transducers of exceptional accuracy were used to measure the test channel static and total pressures at station $\bar{X}/c$ = -3 (fig. 4) and were also used to calibrate the remaining transducers immediately before each test run. Error analyses indicated that the airfoil pressure measurements were accurate to ±0.002 P_T and the free-stream Mach number was accurate to ±0.002.

The onset of buffet was determined by recording on tape the signal output from the dynamic pressure transducers (fig. 1) as the model angle of attack ("α sweep") or Mach number ("Mach sweep") was changed. Post-run displays of the signals using various combinations of tape- and chart-recording speeds were made to view the signal envelopes and wave forms (see example presented in fig. 12). The onset of buffet is easily discernable by this technique since the envelope of the dynamic pressure measurements when the flow becomes unsteady (as verified by high-speed shadowgraph movies) grows in essentially linear fashion with angle of attack. "Buffetting" (structural response) was not involved in the present tests.

RESULTS AND DISCUSSION

The experimental results of this investigation consist of surface pressure measurements, surveys to define the onset of buffet, and flow-field shadowgraphs. Separate presentations will be made beginning with the surface pressure measurements, which were all conducted in the steady flow domain.

Surface Pressure Measurements

Surface static-pressure measurements on the model and at the test-channel sidewall for the six data sets (fig. 6) are presented in figures 13-18. It is important to note that for the airfoil data presentations the origin of x is at the airfoil leading edge whereas for the sidewall measurements the origin for $\bar{X}$ is at the airfoil midchord (center of rotation) (see figs. 1 and 4). The nominal Mach number, angle of attack, and Reynolds number (M_N, α_N, $Re_{c,\infty,N}$) in figures 13-18 refer to the values used in defining the test channel upper and lower wall contours (see earlier discussion in Tests and Procedures section). The effect of Reynolds number on airfoil pressure distributions is large at low values of Reynolds number but quite small above about 6 or 8 million. Since the streamline shapes used as a basis for wall contouring were estimated for a Reynolds number of 10 million, and since the accuracy of the test program increases with increasing total pressure, it is recommended that the Reynolds number test data for 10 million be used in evaluating numerical codes. The data at low Reynolds numbers have been included as a matter of interest and to show primarily where Reynolds number effects are large and where effects are small.

A few test runs were made at conditions "off-design" with regard to the upper and lower wall contouring to obtain a feeling for the sensitivity of the present airfoil pressure measurements to wall contouring. The effects of being off-design in the angle of attack or in the Mach number are shown in figures 19(a) and (b), respectively. For the test results presented in figure 19(a) the wall contouring used was based on

the streamlines shown in figure 11(a). The open data symbols in figure 19(a) represent "on-design" test data in that the test values of Mach number, angle of attack, and Reynolds number agree with the nominal values (design values) used to obtain the streamlines employed in the wall contouring (the data set 1 streamlines of fig. 11(a)). The closed symbols in figure 19(a) represent off-design test data since the test angle of attack ($\alpha = 2^\circ$) differed from the nominal value ($\alpha_N = 0^\circ$) used in obtaining the streamlines (data set 2 of fig. 11(a)) for the wall contouring. The test data reflect the appreciable differences in wall contouring. For figure 19(b) the streamline input to the wall contouring were those shown in figure 11(c) and the $\alpha = 2^\circ$ streamlines of figure 11(a). The open symbols in figure 19(b) represent on-design test data (the test Mach number, angle of attack, and Reynolds number agree with the design values) while the closed symbols represent off-design test data since the test Mach number ($M_\infty = 0.775$) differed from the design value ($M_N = 0.750$). In this case the differences in contouring were small and the experimental pressure measurements reflect this. The test results presented in figure 19 could be used as test cases in numerical studies of wall interference effects. It should be kept in mind that solid test channel walls can easily be included in numerical methods and that it is not necessary for the test data to represent free-air conditions in order to be useful in evaluating numerical methods. However, the availability of "free-air" (or nearly so) data is to be preferred to avoid dealing with the uncertainties of wall-interference effects.

The sidewall boundary-layer effect on the airfoil pressure measurements was evaluated by comparing test results with and without the use of the sidewall mass removal systems. The normal force coefficient

$$C_n = \int_0^1 (C_{p_\ell} - C_{p_u}) \mathrm{d}(x/c)$$

is easily integrated with good accuracy and when it is normalized with respect to the angle of attack it may be used as shown in figure 20 to demonstrate the loss in lift due to the presence of the sidewall boundary layers. The displacement thickness values, δ^*, were the average of the values (deduced from pitot rake surveys) measured just ahead of, and behind, the airfoil (see fig. 4). The basic data presented in this report (figs. 13-18) were obtained with $\dot{m}_{(1)} = 0.03\ \dot{m}_T$ and $\dot{m}_{(2)} = 0.008\ \dot{m}_T$, and the normal force coefficient is about 3% low, assuming that extrapolation to $\delta^* = 0$ is permissible. When no sidewall mass removal is made ($\dot{m}_{(1)} = \dot{m}_{(2)} = 0$), the normal force is in error about 15%.

The normal-force coefficients, per degree of angle of attack, taken from data sets 1, 4, 5, and 6 for $Re_{c,\infty} \approx 10 \times 10^6$, are presented in figure 21 and are compared with corrected data from reference 6. Also included in this figure is a theoretical incompressible flow prediction with Karman-Tsien scaling (applicable only for subcritical flows) taken from reference 7. The corrected data from reference 6 provides a reasonable estimate for free-air values of C_n/α. The present tests give slightly lower values, but by about the amount of a small sidewall interference effect discussed above.

Buffet

The present technique for determining the onset of unsteady flow was illustrated in figure 12. The envelope of the dynamic pressure measurements grows in essentially linear fashion with angle of attack in the unsteady flow regime so that the angle of attack where buffet started is easily discernible.

The buffet onset surveys were made at all of the test setups (data sets) shown in figure 6 except for setup no. 2. The nominal or "design" angles of attack for data sets 4, 5, and 6 are very close to the buffet region, and the buffet onset data should not be subject to appreciable off-design effects. Typical post-run data displays are presented in figures 22-24 for data set 5 ($M_N = 0.775, \alpha_N = 2^\circ$). Envelopes of the pressure deviations from the mean and the model angle of attack are presented in figure 22(f) for upper surface measurements at $x/c = 0.5$ and 0.8. Wave forms at $\alpha = 4^\circ$, which is well into the unsteady domain, are presented in figure 23 and a comparison of upper and lower surface wave forms is presented in figure 24. All of the buffet onset measurements made at Reynolds numbers from 1 to 10 million are summarized in figure 25. These measurements were obtained from "α sweeps" except for the two points at $\alpha = 0^\circ$ included in figures 25(e) and 25(f), which were obtained by "Mach number sweeps." Although the angle of attack remained fixed (exactly at 0°) during the Mach number sweeps, the test Mach number did vary slightly during the α sweeps because of the change in stream momentum which affects the behavior of the speed control (see fig. 4). In figure 25 the open symbols refer to data obtained with the midchord ($x/c = 0.5$) sensor and the closed symbols refer to the sensor near the trailing edge ($x/c = 0.8$). During pitchup α sweeps at low Reynolds numbers, the midchord sensor signals buffet onset before the aft sensor responds, indicating that the origin of the unsteady phenomenon is nearer to the midchord than to the trailing edge. However, at high Reynolds numbers (greater than about 6 million) both sensors respond in similar fashion. High-speed shadowgraph motion pictures show that an intermittent shock-induced separation of the boundary layer occurs near the midchord at angles of attack coincident with the buffet onset measurements. Thus it would be appropriate to label the buffet phenomena observed here as "shock-induced." In figure 25 the unflagged symbols refer to model pitchup, the flagged symbols to pitchdown. A hysteresis effect is not discernible from these tests.

The pressure wave forms in the buffet region were invariably erratic at low Reynolds numbers (less than about 6 million), but at large Reynolds numbers the cyclic nature and frequency were well defined. The reduced frequency parameter $2\pi fc/U_\infty$ measured during buffet at a Reynolds number of 10 million are tabulated in table 4.

Shadowgraphs

Spark-illuminated shadowgraphs of the upper, aft flow fields at Reynolds numbers ranging from 1 to 10 million are presented in figures 26-30. The clarity of the photographs diminish markedly with increasing Reynolds number because of the increased turbulent activity, particularly at the edges of the sidewall boundary layers. Shadowgraphs illustrating the effect of angle of attack on the flow fields are presented in figures 31-33. The nominal (or "design") test Mach number and angle of attack (M_N, α_N) for which the upper and lower walls were contoured are included in the figure titles together with the angle of attack for buffet onset (from fig. 25).

Although the clarity with which these photographs display the flow phenomenon diminishes with departure from the nominal angle of attack, α_N, some observations can reasonably be made. First of all, these photographs, as well as high-speed motion pictures, show that the onset of buffet coincides with the change from normal shock to an intermittent shock-induced separation of the boundary layer. When the airfoil is in the steady flow regime, but near buffet onset, an increase in either the free-stream Mach number or angle of attack will increase the local Mach number ahead of the normal shock until, ultimately, the boundary layer can no longer tolerate the shock-induced pressure recovery, and separation occurs. With separation an oblique shock wave forms and, in effect, the airfoil shape is altered (akin to the upward deflection of a trailing-edge flap), which tends to slow down the upper flow field. This causes the flow field to return to its original configuration – hence the intermittent phenomena. At moderate to large angles of attack, the intermittent, shock-induced separation phenomena may only occur on the leeward surface, as the windward flow field is too far removed from buffet onset to separate (in fact, in some cases the lower flow field may be everywhere subcritical), although the consequences of the upper flow field oscillations are felt globally. When buffet occurs at, or near, $\alpha = 0^\circ$, the unsteady phenomena are similar in the upper and lower flow fields, but 180° out of phase.

The effect of angle of attack on the chordwise location of the base of the shock wave in the steady flow regime is shown in figure 34. The shock location was deduced from flow-field shadowgraphs and from pressure measurements. When the angle of attack is increased from zero, the shock first moves downstream, then upstream, and eventually buffet begins.

CONCLUDING REMARKS

The tests described were performed to obtain data suitable for evaluating numerical flow-simulation codes. Emphasis was placed on measurements at high subsonic speeds near the buffet region. The onset of the buffet, as affected by free-stream Mach number, angle of attack, and Reynolds number, was included in the study, and this information also can be used as a test case for evaluating codes. Test data were obtained over a wide range of Reynolds numbers, but the measurements at Reynolds numbers of 10 million are considered to be the most appropriate for evaluating codes.

The tests were performed in a new test leg for the Ames High Reynolds Number Facility, and a unique test section was used which has provisions for minimizing wall interference effects. By using sidewall suction the boundary-layer displacement in the vicinity of the test model was reduced by about 75% and the reduction in airfoil normal force due to sidewall boundary layers was determined to be less than about 3%. Interference by the upper and lower walls was minimized by contouring to conform with streamlines of the model in free air as estimated by an airfoil code that includes viscous effects. Since solid walls were used, the representation boundary condition of tangential flow can easily be included in the numerical methods. Comparisons of solutions with and without wall boundaries would be helpful in determining, qualitatively at least, if appreciable interference effects are present. It is not necessary, of course, to use free-air data to evaluate codes, but this is to be preferred to avoid dealing with the uncertainties of wall-interference effects. It should be understood that the wall shapes to be used as inviscid boundaries in numerical simulations are the streamlines presented in figure 11 and are not the actual wall shapes used, which included inputs from the test-section calibration (internal area ruling to offset longitudinal Mach number changes due to mass removal and boundary layer displacement growth) performed to obtain a uniform test medium.

Ames Research Center
National Aeronautics and Space Administration
Moffett Field, California 94035, February 1985

REFERENCES

1. McDevitt, J. B.; Levy, L. L., Jr.; and Deiwert, G. S.: "Transonic Flow About a Thick Circular-Arc Airfoil," AIAA J., vol. 14, no. 5, May 1976, pp. 606-613.
2. McDevitt, J. B.; Polek, T. E., and Hand, L. A.: "A New Facility and Technique for Two-Dimensional Aerodynamic Testing," AIAA J. Aircraft, vol. 20, no. 6, June 1983, pp. 543-551.
3. Bernard-Guelle, R.: "Influence of Wind Tunnel Wall Boundary Layers on Two-Dimensional Transonic Tests." NASA TT F17, 255, 1975.
4. Deiwert, G. S.: "Numerical Simulation of Reynolds Number Transonic Flows," AIAA J., vol. 13, Oct. 1975, pp. 1354-1359.
5. Deiwert, G. S.: "Computation of Separated Transonic Turbulent Flows," AIAA J., vol. 14, June 1976, pp. 735-740.
6. Harris, C. D.: "Two-Dimensional Aerodynamic Characteristics of the NACA C012 Airfoil in the Langley 8-Foot Transonic Pressure Tunnel," NASA TM 81927, 1981.
7. Vidal, R. J.; Catlin, P. A.; and Chudyk, D. W.: "Two-Dimensional Subsonic Experiments with an NACA 0012 Airfoil," Calspan Report No. RK-5070-A-3, Calspan, 1973.

TABLE 1.– TEST-SECTION PRESSURE AND VELOCITY LEVELS,[a] $M_\infty = 0.8$

P_T, N/m^2	$\langle p \rangle / q_\infty$	$\langle u \rangle / U_\infty$
1.4×10^5	0.02	0.0046
2.8×10^5	0.02	0.0050

[a]Measurements by F. K. Owen of Complere, Inc.; NASA Contract NAS2-10859.

TABLE 2.– FREE-AIR STREAMLINES (see fig. 11)

$\bar{X}/c$	$\Delta z/c$		$\bar{X}/c$	$\Delta z/c$	
	Upper wall	Lower wall		Upper wall	Lower wall
Data set 1; $M_N = 0.75$, $\alpha_N = 2°$			Data set 4; $M_N = 0.80$, $\alpha_N = 1°$		
-4.25	0	0	-4.25	0	0
-2.50	.0063	.0050	-2.50	.0050	.0013
-1.25	.0200	.0110	-1.25	.0154	.0018
-.50	.0308	.0070	-.50	.0250	-.0041
0	.0308	.0025	0	.0269	-.0085
.50	.0210	0	.50	.0194	-.0079
1.25	.0045	-.0030	1.25	.0066	-.0056
2.50	-.0138	-.0150	2.50	-.0075	-.0081
3.55	-.0230	-.0235	3.55	-.0133	-.0115
4.79	-.0320	-.0300	4.79	-.0183	-.0159
Data set 2; $M_N = 0.75$, $\alpha_N = 0°$			Data set 5; $M_N = 0.775$, $\alpha_N = 2°$		
-4.25	0	0	-4.25	0	0
-2.50	.0031	-.0031	-2.50	.0063	.0056
-1.25	.0080	-.0080	-1.25	.0209	.0115
-.50	.0145	-.0145	-.50	.0321	.0074
0	.0180	-.0180	0	.0321	.0026
.50	.0145	-.0145	.50	.0220	0
1.25	.0080	-.0080	1.25	.0048	-.0031
2.50	.0038	-.0038	2.50	.0138	-.0150
3.55	.0012	-.0012	3.55	-.0240	-.0246
4.79	.0010	-.0010	4.79	-.0322	-.0328
Data set 3; $M_N = 0.80$, $\alpha_N = 0°$			Data set 6; $M_N = 0.725$, $\alpha_N = 4°$		
-4.25	0	0	-4.25	0	0
-2.50	.0034	-.0034	-2.50	.0094	.0088
-1.25	.0088	-.0088	-1.25	.0308	.0288
-.50	.0160	-.0160	.50	.0451	.0274
0	.0199	-.0199	0	.0418	.0216
.50	.0160	-.0160	.50	.0264	.0138
1.25	.0088	-.0088	1.25	.0038	0013
2.50	.0040	-.0040	2.50	-.0238	-.0250
3.55	.0014	-.0014	3.55	-.0438	-.0451
4.79	.0012	-.0012	4.79	-.0594	-.0600

TABLE 3.– CORRECTIONS TO MEASURED MACH NUMBER AT TUNNEL STATION $\bar{X}/c = -3$ (see fig. 4) DUE TO PRESENCE OF MODEL

M_∞	α, deg	ΔM	M_∞	α, deg	ΔM
0.725	0	0.0046	0.775	0	0.0050
	2	.0048		2	.0053
	4	.0051		4	.0057
0.75	0	0.0048	0.80	0	0.0053
	2	.0050		2	.0056
	4	.0053		4	.0061

TABLE 4.– SHOCK-OSCILLATION FREQUENCY PARAMETER $\bar{f} = 2\pi fc/U_\infty$ IN BUFFET REGION, $Re_{c,\infty} = 10^7$

M_N	α_N, deg	M_∞	α, deg	$\bar{f}$
0.725	4	0.72	6	0.55
.750	2	.75	4	.47
.775	2	.77	4	.44
.800	1	.80	4	.38

$$\pm\frac{z}{c} = 0.17814\sqrt{\frac{x}{c}} - 0.07560\frac{x}{c} - 0.21096\left(\frac{x}{c}\right)^2 + 0.17058\left(\frac{x}{c}\right)^3 - 0.06090\left(\frac{x}{c}\right)^4$$

LEADING-EDGE RADIUS = 0.0158 c

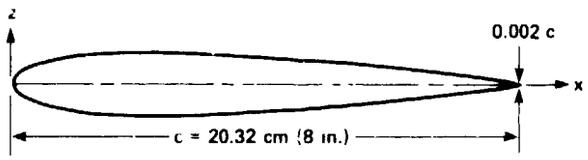

	STATIC PRESSURE ORIFICES		DYNAMIC PRESSURE TRANSDUCERS	
x/c	UPPER	LOWER	UPPER	LOWER
0	•			
0.025	•	•		
0.05	•	•		
0.075	•			
0.10	•	•		
0.15	•			
0.20	•	•	•	•
0.25	•			
0.30	•	•		
0.35	•			
0.40	•	•		
0 45	•			
0 50	•	•	•	•
0.55	•			
0.60	•	•		
0.65	•			
0.70	•	•		
0 75	•			
0.80	•	•	•	•
0.85	•	•		
0 90	•	•		
0.925	•	•		
0.95	•	•		
0.975	•	•		
1.00	•			

Figure 1.– NACA 0012 profile and location of pressure orifices.

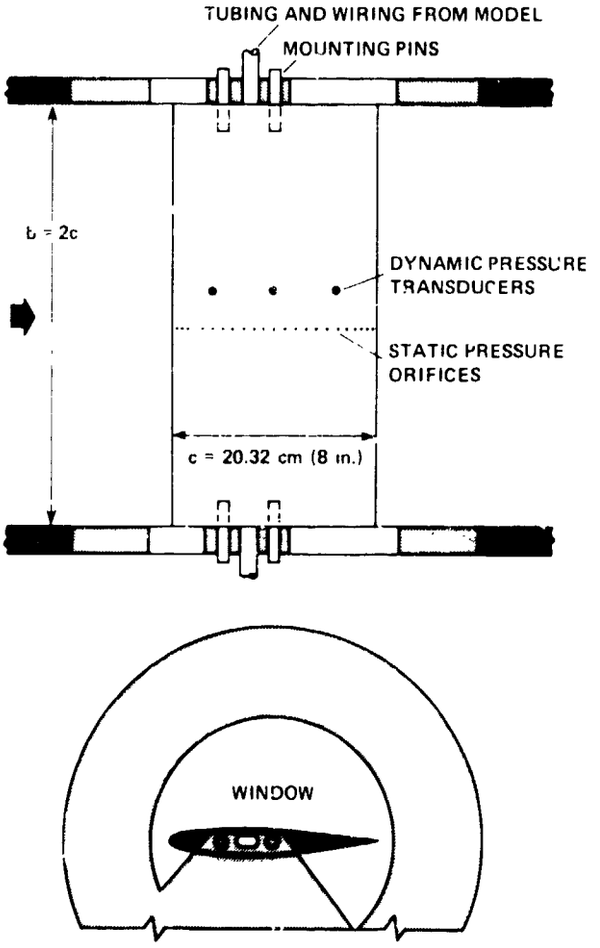

Figure 2. Sketch of model installed in tunnel.

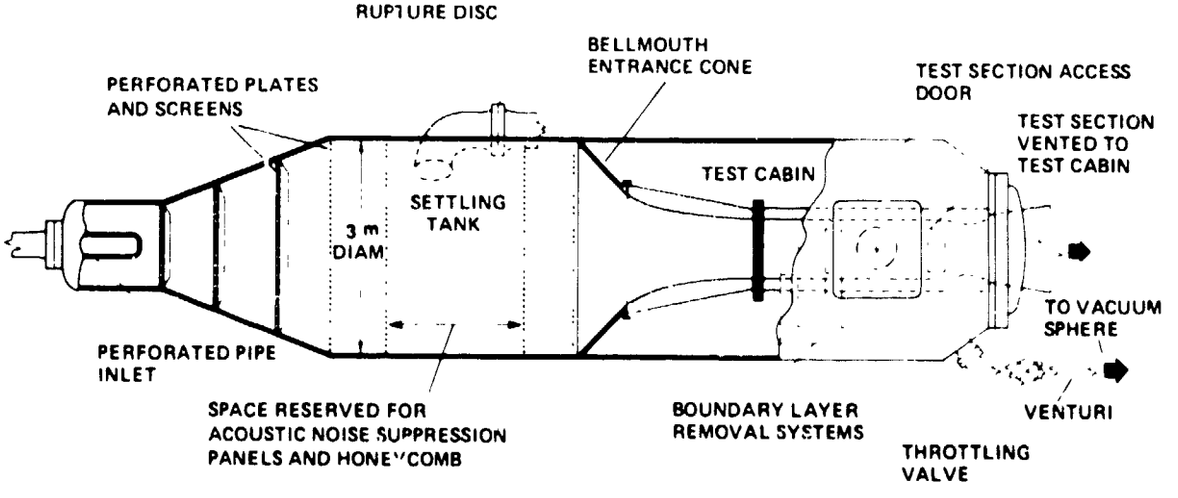

Figure 3.– Schematic of HRC-2 and airfoil test section.

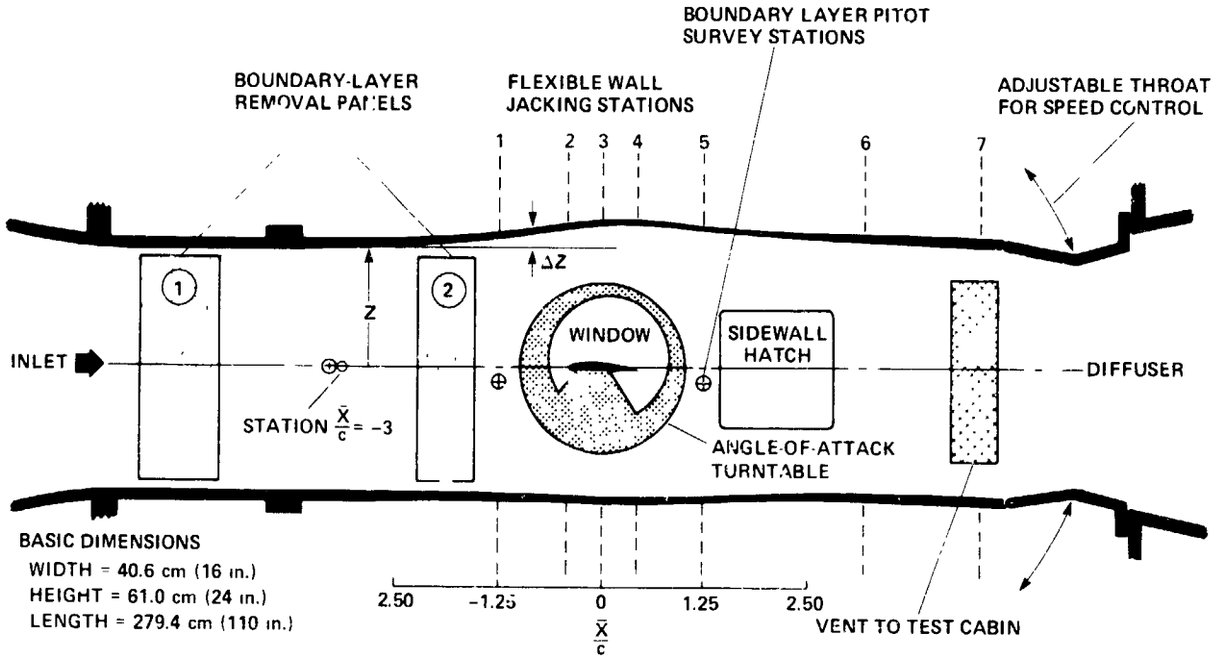

Figure 4.– Test section schematic.

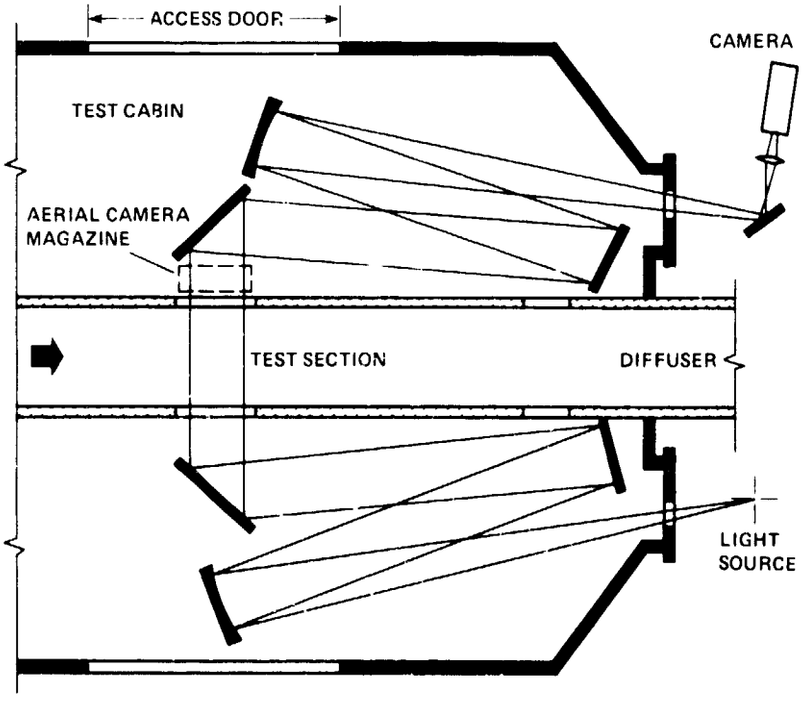

Figure 5.– Schematic of shadowgraph system (cross-sectional view from above).

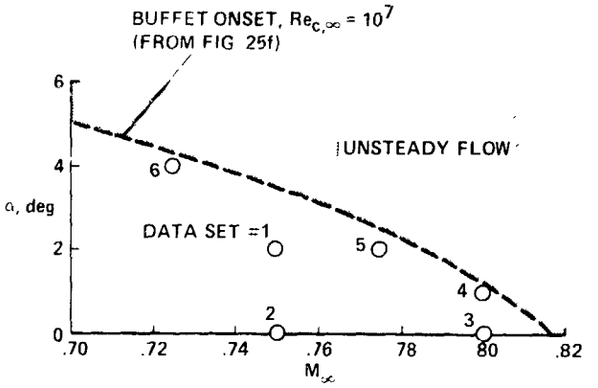

Figure 6.– Test matrix.

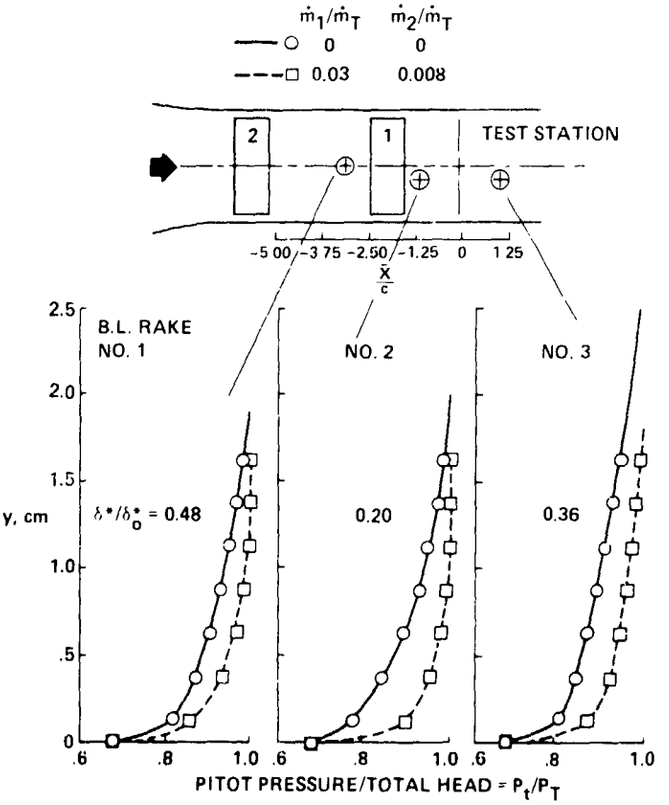

Figure 7.– Typical sidewall boundary-layer pitot surveys, $M_\infty = 0.775$, $Re_{c,\infty} = 10^7$.

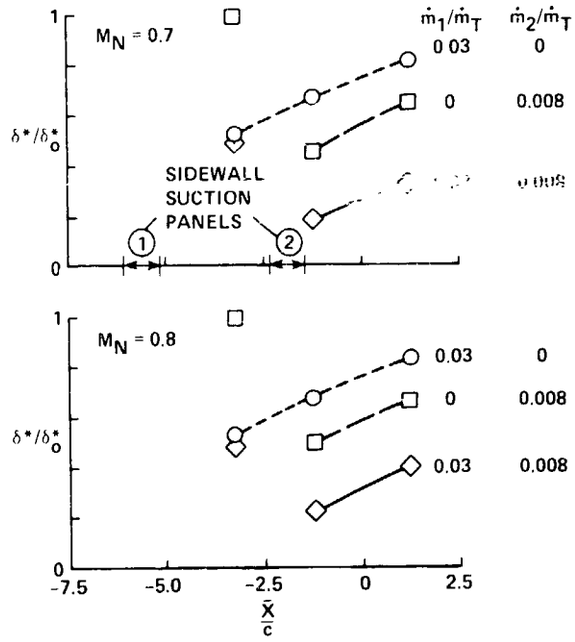

Figure 8.– Typical longitudinal variations in sidewall boundary-layer displacement thickness, $Re_{c,\infty} = 10^7$.

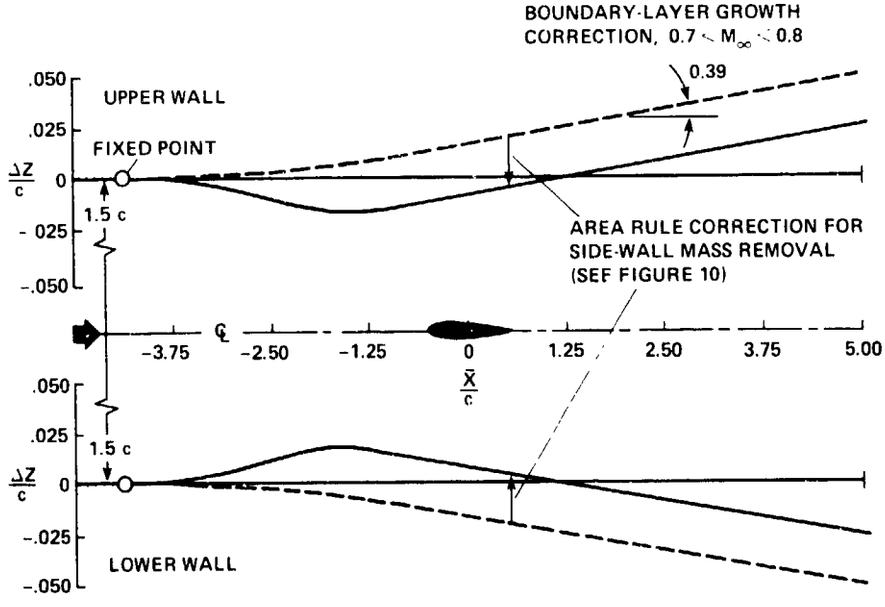

Figure 9.– Upper and lower wall contouring to offset channel boundary-layer growth and sidewall mass removal.

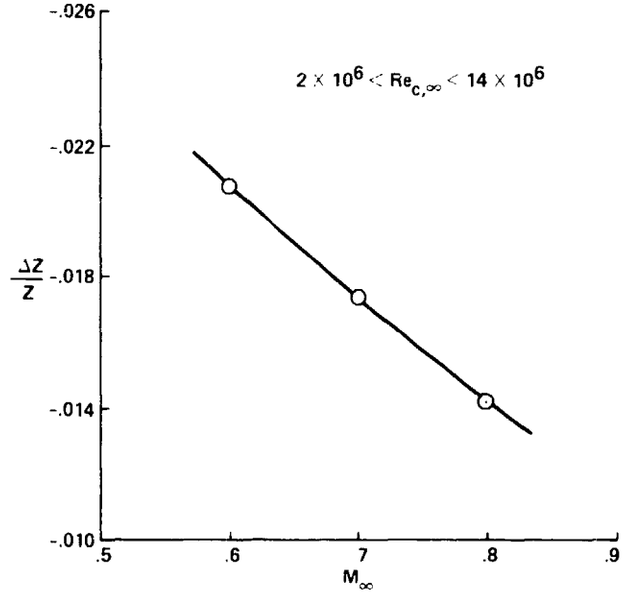

Figure 10.– Test channel cross-sectional area change required to offset effects of sidewall mass removal; $\dot{m}_{(1)} = 0.03\ \dot{m}_T$, $\dot{m}_{(2)} = 0.008\ \dot{m}_T$.

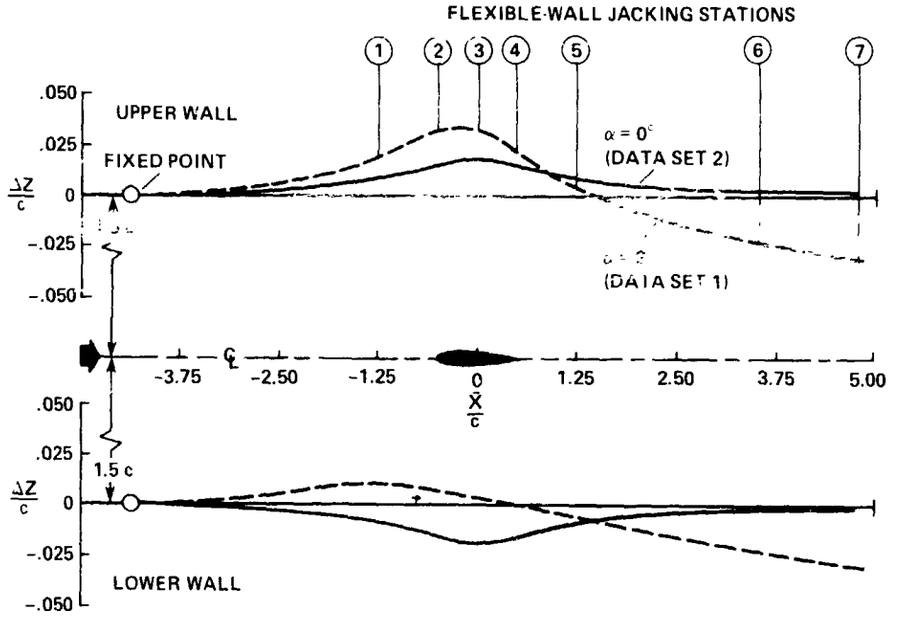

(a) $M_\infty = 0.75; Re_{c,\infty} = 10^7; \alpha = 0°, 2°$ (Data Sets 2 and 1).

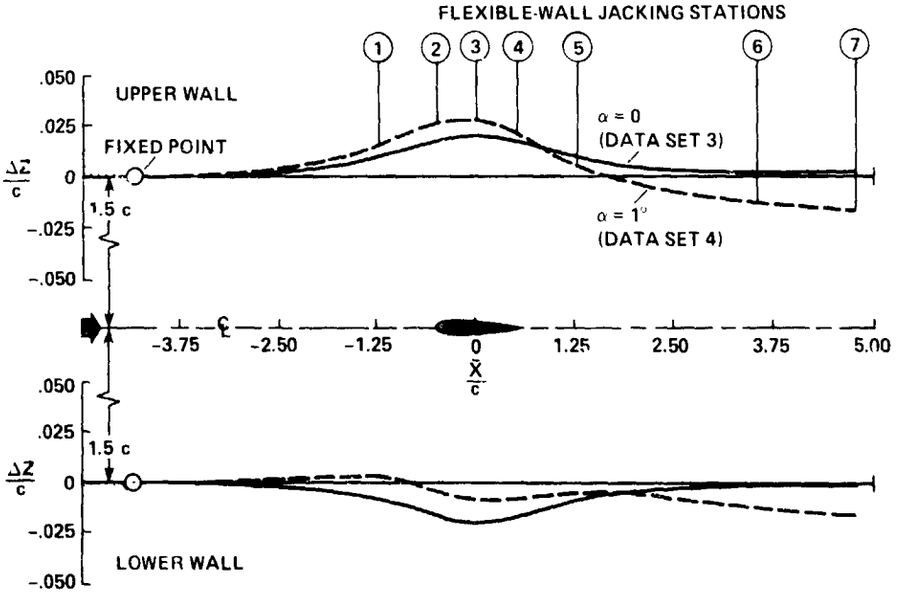

(b) $M_\infty = 0.80; Re_{c,\infty} = 10^7; \alpha = 0°, 1°$ (Data Sets 3 and 4).

Figure 11.– Streamlines of the airfoil in free air.

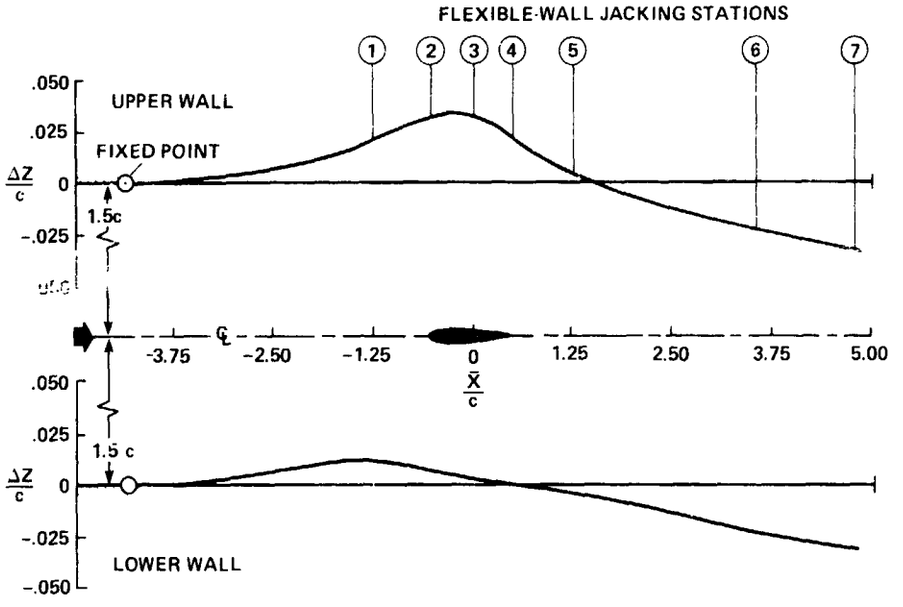

(c) $M_\infty = 0.775$; $Re_{c,\infty} = 10^7$; $\alpha = 2°$ (Data Set 5).

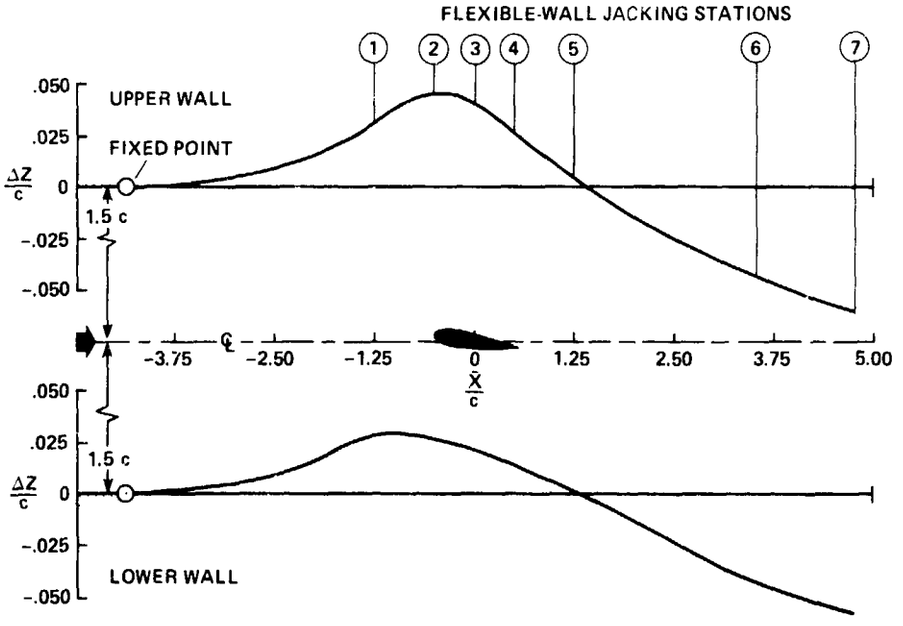

(d) $M_\infty = 0.725$; $Re_{c,\infty} = 10^7$; $\alpha = 4°$ (Data Set 6).

Figure 11.- Concluded.

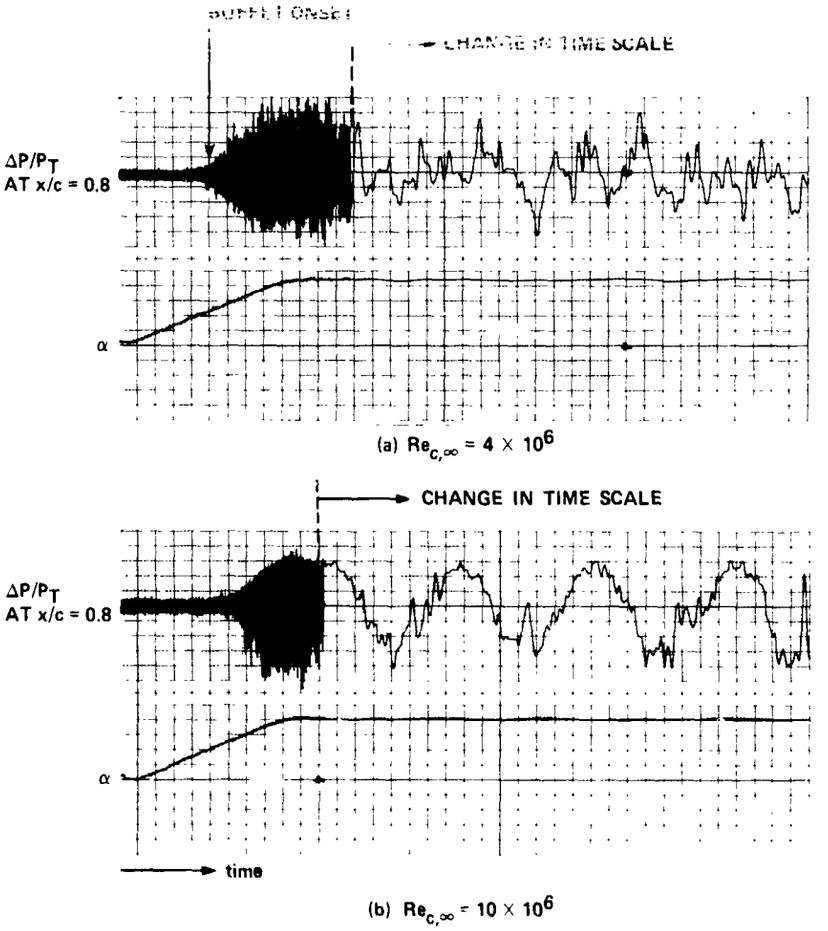

Figure 12.– Typical post run displays of dynamic pressure measurements showing onset of buffet (sensor at midchord).

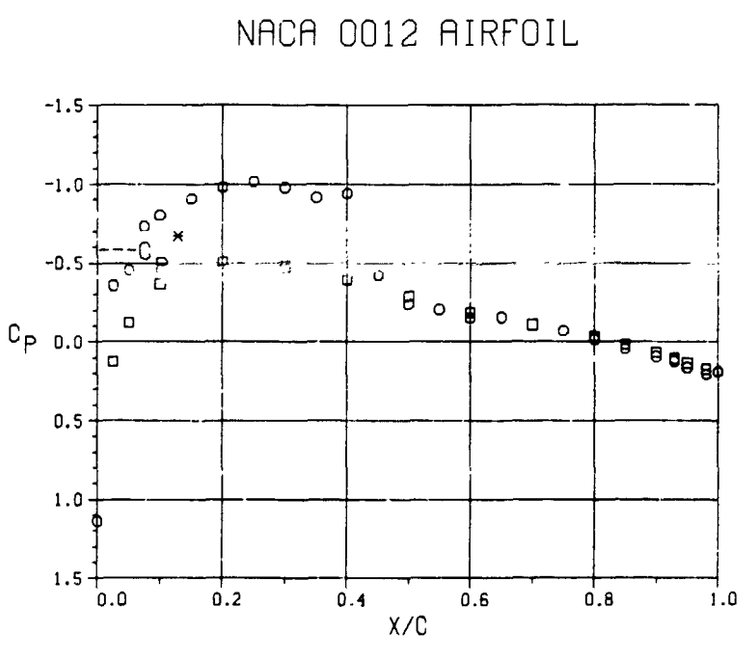

o - AIRFOIL UPPER SURFACE

X/C	C_P	P/PT	M
0.000	1.136	0.996	0.079
0.025	-0.357	0.585	0.909
0.050	-0.455	0.558	0.952
0.075	-0.732	0.482	1.076
0.100	-0.804	0.462	1.110
0.150	-0.909	0.434	1.161
0.200	-0.984	0.413	1.199
0.250	-1.019	0.403	1.217
[illegible]	[illegible]	0.414	1.197
[illegible]	[illegible]	0.421	[illegible]
0.400	[illegible]	[illegible]	[illegible]
0.450	-0.424	0.567	0.938
0.500	-0.238	0.618	0.859
0.550	-0.209	0.626	0.846
0.600	-0.152	0.642	0.822
0.650	-0.156	0.641	0.824
0.700			
0.750	-0.071	0.664	0.788
0.800	-0.017	0.679	0.765
0.850	0.043	0.695	0.740
0.900	0.093	0.709	0.718
0.930	0.121	0.717	0.707
0.950	0.161	0.728	0.689
0.980	0.205	0.740	0.670
1.000	0.189	0.735	0.677

□ - AIRFOIL LOWER SURFACE

X/C	C_P	P/PT	M
0.025	0.125	0.720	0.701
0.050	-0.123	0.650	0.810
0.100	-0.370	0.582	0.915
0.200	-0.509	0.547	0.969
0.300	-0.478	0.552	0.962
0.400	-0.397	0.578	0.921
0.500	-0.292	0.603	0.882
0.600	-0.187	0.635	0.832
0.700	-0.110	0.653	0.804
0.800	-0.036	0.676	0.769
0.850	0.014	0.687	0.752
0.900	0.067	0.705	0.725
0.930	0.105	0.712	0.713
0.950	0.132	0.722	0.698
0.980	0.174	0.731	0.684

SIDEWALL, Z=0

$\bar{X}$/C	C_P	P/PT	M
-3.75	0.061	0.702	0.729
-3.00	0.021	0.689	0.749
-1.25	0.067	0.703	0.727
1.25	0.036	0.695	0.740
3.75	-0.004	0.684	0.757

SIDEWALL, Z/C= 1.375

$\bar{X}$/C	C_P	P/PT	M
-3.75	0.054	0.701	0.731
-2.50	0.023	0.693	0.743
-2.00	0.027	0.694	0.742
-1.50	0.024	0.693	0.743
-1.00	-0.009	0.684	0.757
-0.50	-0.058	0.671	0.777
0.00	-0.017	0.682	0.760
0.50	-0.030	0.678	0.766
1.00	-0.012	0.683	0.758
1.50	-0.071	0.667	0.783
2.00	0.012	0.690	0.748
2.50	0.007	0.688	0.750
3.75	0.039	0.697	0.737

SIDEWALL, Z/C=-1.375

$\bar{X}$/C	C_P	P/PT	M
-3.75	0.058	0.702	0.729
-1.00	-0.005	0.685	0.755
-0.50	-0.256	0.617	0.862
0.00	-0.015	0.682	0.760
0.50	0.022	0.692	0.744
1.00	0.003	0.687	0.752
1.50	0.010	0.689	0.749
2.00	0.007	0.688	0.750
2.50	0.032	0.695	0.740
3.75	0.032	0.695	0.740

(a) $M_\infty = 0.753$, $\alpha = 2.02°$, $Re_{c,\infty} = 1.2 \times 10^6$.

Figure 13.– Airfoil and test section sidewall pressure measurements, Data Set 1 ($M_N = 0.75$, $\alpha_N = 2°$).

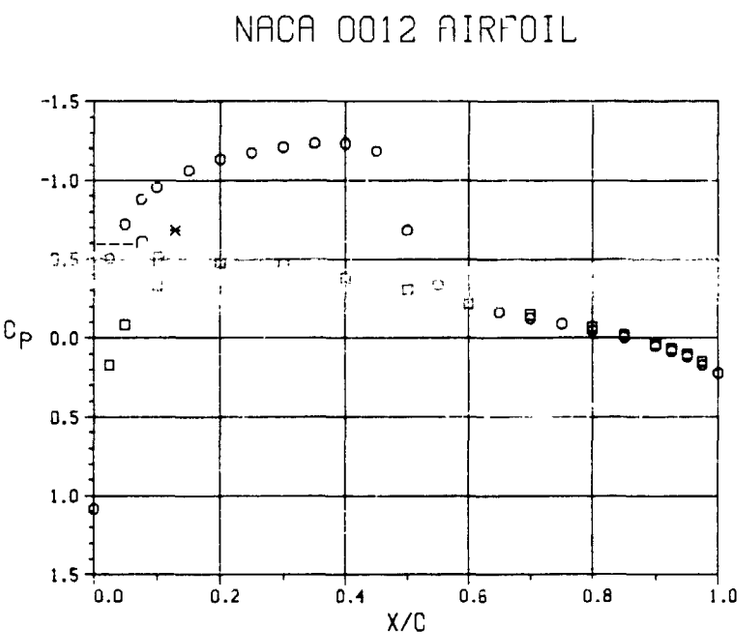

o - AIRFOIL UPPER SURFACE

X/C	C_P	P/PT	M
0.000	1.081	0.982	0.161
0.025	-0.507	0.552	0.962
0.050	-0.721	0.494	1.056
0.075	-0.881	0.451	1.130
0.100	-0.956	0.431	1.166
0.150	-1.064	0.402	1.220
0.200	-1.135	0.382	1.257
0.250	-1.175	0.371	1.279
0.300	-1.211	0.362	1.298
0.350	-1.236	0.355	1.312
[illegible]	[illegible]	[illegible]	[illegible]
0.450	-1.187	0.368	1.285
0.500	-0.683	0.505	1.039
0.550	-0.340	0.597	0.891
0.600	-0.219	0.630	0.840
0.650	-0.165	0.645	0.817
0.700	-0.126	0.655	0.801
0.750	-0.093	0.664	0.787
0.800	-0.049	0.676	0.769
0.850	-0.006	0.688	0.751
0.900	0.049	0.703	0.728
0.925	0.082	0.711	0.715
0.950	0.115	0.720	0.701
0.975	0.169	0.735	0.678
1.000	0.222	0.749	0.656

□ - AIRFOIL LOWER SURFACE

X/C	C_P	P/PT	M
0.025	0.172	0.736	0.676
0.050	-0.087	0.666	0.785
0.100	-0.335	0.599	0.888
0.200	-0.476	0.562	0.947
0.300	-0.468	0.563	0.945
0.400	-0.380	0.587	0.906
0.500	-0.305	0.607	0.876
0.600	-0.220	0.631	0.839
0.700	-0.149	0.649	0.811
0.800	-0.072	0.670	0.778
0.850	-0.020	0.684	0.757
0.900	0.036	0.700	0.733
0.925	0.066	0.707	0.721
0.950	0.101	0.717	0.706
0.975	0.149	0.730	0.686

SIDEWALL, Z=0

$\bar{X}$/C	C_P	P/PT	M
-3.75	0.027	0.697	0.737
-3.00	-0.012	0.686	0.754
-1.25	0.030	0.698	0.735
1.25	-0.007	0.688	0.751
3.75	-0.015	0.686	0.754

SIDEWALL, Z/C= 1.375

$\bar{X}$/C	C_P	P/PT	M
-3.75	0.013	0.694	0.742
-2.50	-0.036	0.681	0.762
-2.00	-0.028	0.683	0.759
-1.50	-0.031	0.682	0.760
-1.00	-0.071	0.671	0.777
-0.50	-0.137	0.653	0.804
0.00	-0.130	0.655	0.802
0.50	-0.110	0.660	0.793
1.00	-0.058	0.675	0.771
1.50	-0.045	0.678	0.766
2.00	-0.045	0.678	0.766
2.50	-0.047	0.678	0.767
3.75	-0.014	0.686	0.754

SIDEWALL, Z/C= -1.375

$\bar{X}$/C	C_P	P/PT	M
-3.75	0.019	0.695	0.740
-1.00	-0.035	0.681	0.762
-0.50	-0.022	0.684	0.756
0.00	-0.037	0.680	0.763
0.50	-0.035	0.681	0.762
1.00	-0.031	0.682	0.761
1.50	-0.018	0.685	0.755
2.00	-0.019	0.685	0.755
2.50	-0.010	0.687	0.752
3.75	-0.005	0.689	0.750

(b) $M_\infty = 0.749, \alpha = 1.99°, Re_{c,\infty} = 2.0 \times 10^6$.

Figure 13.– Continued.

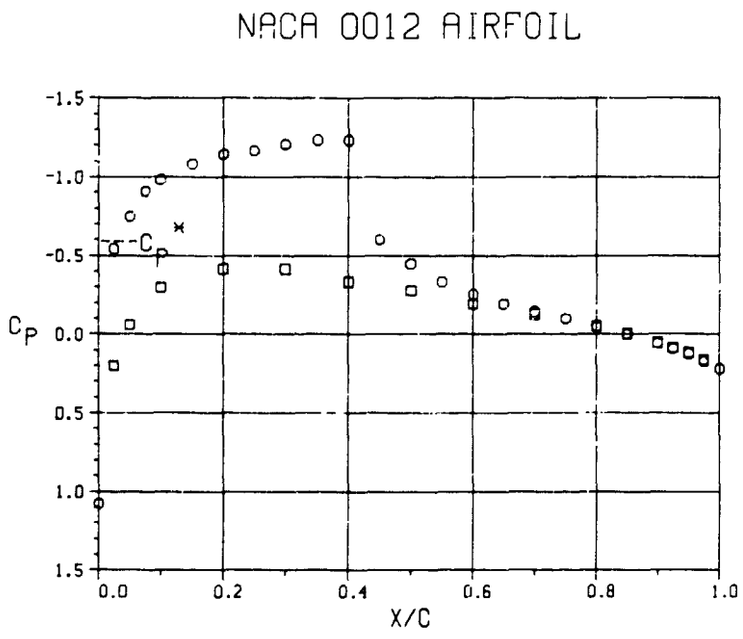

o - AIRFOIL UPPER SURFACE

X/C	C_P	P/PT	M
0.000	1.075	0.980	0.171
0.025	-0.543	0.543	0.980
0.050	-0.749	0.484	1.072
0.075	-0.909	0.441	1.148
0.100	-0.984	0.421	1.185
0.150	-1.083	0.394	1.235
0.200	-1.145	0.377	1.268
0.250	-1.168	0.371	1.280
0.300	-1.208	0.360	1.302
0.350	-1.235	0.352	1.318
0.400	-1.236	0.352	1.319
0.450	-0.602	0.524	1.006
0.500	-0.449	0.566	0.940
0.550	-0.334	0.597	0.891
0.600	-0.253	0.619	0.857
0.650	-0.194	0.635	0.832
0.700	-0.144	0.649	0.811
0.750	-0.101	0.660	0.793
0.800	-0.051	0.674	0.772
0.850	-0.002	0.687	0.752
0.900	0.055	0.703	0.728
0.925	0.088	0.712	0.714
0.950	0.122	0.721	0.700
0.975	0.172	0.735	0.679
1.000	0.219	0.747	0.659

□ - AIRFOIL LOWER SURFACE

X/C	C_P	P/PT	M
0.025	0.200	0.743	0.666
0.050	-0.061	0.671	0.776
0.100	-0.297	0.607	0.875
0.200	-0.416	0.576	0.924
0.300	-0.415	0.575	0.925
0.400	-0.334	0.598	0.890
0.500	-0.279	0.612	0.868
0.600	-0.195	0.636	0.831
0.700	-0.127	0.653	0.804
0.800	-0.051	0.675	0.771
0.850	-0.005	0.687	0.753
0.900	0.052	0.703	0.728
0.925	0.082	0.710	0.717
0.950	0.116	0.720	0.701
0.975	0.159	0.731	0.684

SIDEWALL, Z = 0

$\bar{X}$/C	C_P	P/PT	M
-3.75	0.044	0.700	0.732
-3.00	0.003	0.689	0.750
-1.25	0.044	0.700	0.732
1.25	0.017	0.693	0.743
3.75	0.008	0.690	0.747

SIDEWALL, Z/C = 1.375

$\bar{X}$/C	C_P	P/PT	M
-3.75	0.028	0.696	0.733
-2.50	-0.021	0.683	0.753
-2.00	-0.015	0.684	0.755
-1.50	-0.016	0.684	0.757
-1.00	-0.057	0.673	0.774
-0.50	-0.112	0.658	0.796
0.00	-0.084	0.666	0.785
0.50	-0.082	0.666	0.784
1.00	-0.035	0.679	0.765
1.50	-0.024	0.682	0.760
2.00	-0.026	0.682	0.761
2.50	-0.022	0.683	0.759
3.75	0.008	0.691	0.747

SIDEWALL, Z/C = -1.375

$\bar{X}$/C	C_P	P/PT	M
-3.75	0.033	0.697	0.736
-1.00	-0.016	0.684	0.757
-0.50	0.005	0.690	0.748
0.00	-0.013	0.685	0.756
0.50	-0.017	0.684	0.757
1.00	-0.015	0.685	0.756
1.50	0.002	0.689	0.749
2.00	0.003	0.689	0.749
2.50	0.014	0.692	0.744
3.75	0.017	0.693	0.743

(c) $M_\infty = 0.751$, $\alpha = 1.99°$, $Re_{c,\infty} = 3.9 \times 10^6$.

Figure 13.– Continued.

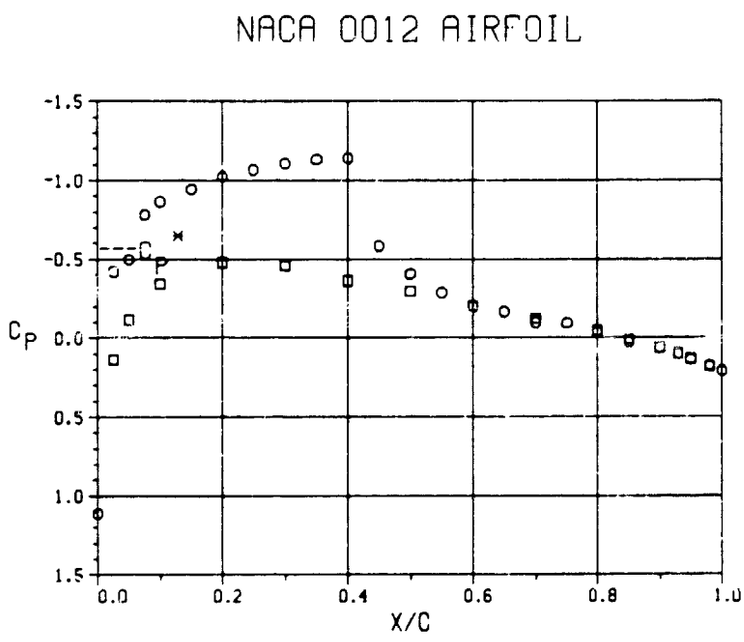

o - AIRFOIL UPPER SURFACE

X/C	C_P	P/PT	M
0.000	1.110	0.988	0.133
0.025	-0.422	0.562	0.945
0.050	-0.498	0.541	0.979
0.075	-0.781	0.463	1.110
0.100	-0.865	0.439	1.151
0.150	-0.944	0.417	1.191
0.200	-1.023	0.396	1.232
0.250	-1.067	0.383	1.255
0.300	-1.108	0.372	1.278
0.350	-1.133	0.365	1.292
0.400	-1.142	0.362	1.297
0.450	-0.582	0.518	1.017
0.500	-0.406	0.567	0.939
0.550	-0.288	0.599	0.887
0.600	-0.203	0.623	0.850
0.650	-0.168	0.633	0.835
0.700	-0.098	0.652	0.805
0.750	-0.094	0.654	0.804
0.800	-0.041	0.668	0.781
0.850	0.029	0.688	0.752
0.900	0.064	0.697	0.736
0.930	0.099	0.707	0.722
0.950	0.134	0.717	0.707
0.980	0.176	0.728	0.688
1.000	0.209	0.737	0.674

□ - AIRFOIL LOWER SURFACE

X/C	C_P	P/PT	M
0.025	0.135	0.719	0.703
0.050	-0.115	0.647	0.813
0.100	-0.343	0.584	0.911
0.200	-0.478	0.550	0.965
0.300	-0.459	0.552	0.962
0.400	-0.365	0.581	0.915
0.500	-0.296	0.597	0.890
0.600	-0.205	0.625	0.847
0.700	-0.125	0.645	0.817
0.800	-0.047	0.669	0.780
0.850	0.009	0.682	0.760
0.900	0.060	0.699	0.735
0.930	0.098	0.707	0.722
0.950	0.128	0.717	0.706
0.980	0.180	0.730	0.687

SIDEWALL, Z=0

$\bar{X}$/C	C_P	P/PT	M
-3.75	0.047	0.694	0.741
-3.00	0.006	0.681	0.762
-1.25	0.057	0.697	0.737
1.25	0.033	0.690	0.747
3.75	0.051	0.695	0.740

SIDEWALL, Z/C= 1.375

$\bar{X}$/C	C_P	P/PT	M
-3.75	0.028	0.690	0.747
-2.50	-0.013	0.679	0.765
-2.00	-0.010	0.680	0.763
-1.50	0.001	0.683	0.759
-1.00	-0.043	0.671	0.777
-0.50	-0.095	0.656	0.799
0.00	-0.029	0.675	0.772
0.50	-0.064	0.665	0.786
1.00	-0.030	0.674	0.772
1.50	0.010	0.685	0.755
2.00	-0.002	0.682	0.760
2.50	-0.002	0.682	0.760
3.75	0.023	0.689	0.749

SIDEWALL, Z/C=-1.375

$\bar{X}$/C	C_P	P/PT	M
-3.75	0.037	0.693	0.744
-1.00	-0.016	0.678	0.766
-0.50	0.135	0.720	0.702
0.00	-0.016	0.678	0.766
0.50	0.014	0.686	0.753
1.00	-0.020	0.677	0.768
1.50	0.005	0.684	0.757
2.00	-0.011	0.679	0.764
2.50	0.013	0.686	0.754
3.75	0.031	0.691	0.746

(d) $M_\infty = 0.759$, $\alpha = 2.05°$, $Re_{c,\infty} = 6.3 \times 10^6$.

Figure 13.– Continued.

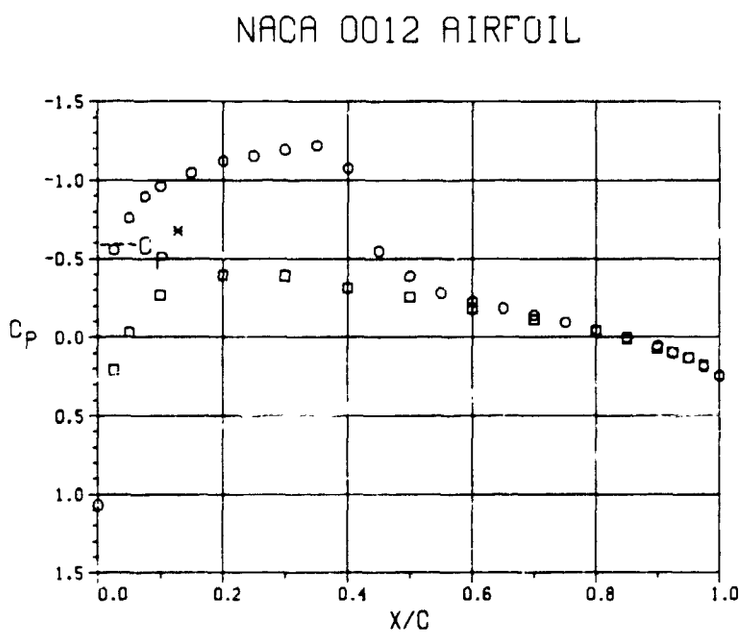

o - AIRFOIL UPPER SURFACE

X/C	C_P	P/PT	M
0.000	1.068	0.978	0.179
0.025	-0.557	0.537	0.986
0.050	-0.759	0.482	1.076
0.075	-0.896	0.445	1.141
0.100	-0.961	0.427	1.173
0.150	-1.047	0.404	1.216
0.200	-1.123	0.383	1.256
0.250	-1.153	0.375	1.271
0.300	-1.195	0.364	1.294
0.350	-1.222	0.356	1.309
0.400	-1.078	0.396	1.232
0.450	-0.547	0.540	0.982
0.500	-0.388	0.583	0.913
0.550	-0.283	0.611	0.869
0.600	-0.229	0.626	0.846
0.650	-0.185	0.638	0.828
0.700	-0.140	0.650	0.8[illegible]
0.750	-0.097	0.662	0.791
0.800	-0.045	0.676	0.769
0.850	0.005	0.689	0.749
0.900	0.056	0.703	0.727
0.925	0.097	0.714	0.710
0.950	0.130	0.723	0.696
0.975	0.185	0.738	0.673
1.000	0.244	0.754	0.648

□ - AIRFOIL LOWER SURFACE

X/C	C_P	P/PT	M
0.025	0.209	0.745	0.662
0.050	-0.032	0.679	0.764
0.100	-0.267	0.616	0.862
0.200	-0.394	0.582	0.915
0.300	-0.393	0.581	0.916
0.400	-0.316	0.603	0.881
0.500	-0.258	0.618	0.858
0.600	-0.181	0.640	0.825
0.700	-0.112	0.658	0.797
0.800	-0.041	0.678	0.767
0.850	0.007	0.690	0.748
0.900	0.068	0.707	0.721
0.925	0.096	0.714	0.710
0.950	0.131	0.724	0.695
0.975	0.177	0.736	0.676

SIDEWALL, Z = 0

$\bar{X}$/C	C_P	P/PT	M
-3.75	0.051	0.702	0.729
-3.00	0.007	0.690	0.748
-1.25	0.054	0.703	0.728
1.25	0.030	0.697	0.738
3.75	0.021	0.694	0.741

SIDEWALL, Z/C = 1.375

$\bar{X}$/C	C_P	P/PT	M
-3.75	0.031	0.697	0.7[illegible]7
-2.50	-0.008	0.686	0.753
-2.00	-0.013	0.685	0.755
-1.50	-0.012	0.685	0.755
-1.00	-0.023	0.682	0.760
-0.50	-0.041	0.677	0.767
0.00	-0.021	0.683	0.759
0.50	-0.037	0.679	0.765
1.00	-0.003	0.688	0.751
1.50	0.021	0.694	0.741
2.00	0.119	0.721	0.700
2.50	-0.006	0.687	0.752
3.75	0.025	0.695	0.739

SIDEWALL, Z/C = -1.375

$\bar{X}$/C	C_P	P/PT	M
-3.75	0.040	0.700	0.733
-1.00	0.010	0.691	0.746
-0.50	0.014	0.692	0.744
0.00	0.002	0.689	0.749
0.50	0.007	0.691	0.747
1.00	0.008	0.691	0.746
1.50	0.015	0.693	0.744
2.00	0.011	0.692	0.745
2.50	0.027	0.696	0.738
3.75	0.031	0.697	0.737

(e) $M_\infty = 0.751, \alpha = 1.99°, Re_{c,\infty} = 7.9 \times 10^6$.

Figure 13.– Continued.

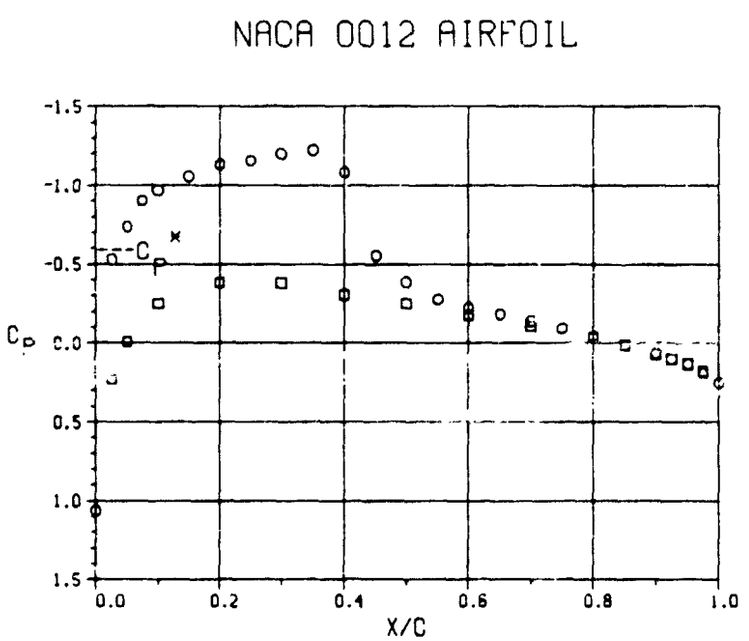

o - AIRFOIL UPPER SURFACE

X/C	C_p	P/PT	M
0.000	1.060	0.976	0.187
0.025	-0.532	0.543	0.976
0.050	-0.739	0.487	1.068
0.075	-0.904	0.442	1.146
0.100	-0.970	0.424	1.178
0.150	-1.057	0.400	1.222
0.200	-1.133	0.380	1.263
0.250	-1.158	0.373	1.276
0.300	-1.200	0.362	1.299
0.350	-1.224	0.355	1.312
0.400	-1.086	0.393	1.237
0.450	-0.553	0.537	0.985
0.500	-0.388	0.582	[illegible]
0.550	-0.279	0.612	0.868
0.600	-0.225	0.626	0.846
0.650	-0.184	0.638	0.828
0.700	-0.139	0.650	0.809
0.750	-0.094	0.662	0.791
0.800	-0.042	0.676	0.769
0.850	0.009	0.690	0.748
0.900	0.063	0.705	0.725
0.925	0.099	0.715	0.710
0.950	0.133	0.724	0.696
0.975	0.189	0.739	0.672
1.000	0.249	0.755	0.646

□ - AIRFOIL LOWER SURFACE

X/C	C_p	P/PT	M
0.025	0.228	0.749	0.655
0.050	-0.009	0.685	0.755
0.100	-0.253	0.619	0.857
0.200	-0.384	0.583	0.912
0.300	-0.380	0.584	0.911
0.400	-0.306	0.604	0.880
0.500	-0.251	0.619	0.856
0.600	-0.175	0.640	0.824
0.700	-0.106	0.659	0.796
0.800	-0.035	0.678	0.766
0.850	0.012	0.691	0.747
0.900	0.070	0.707	0.722
0.925	0.098	0.714	0.710
0.950	0.133	0.724	0.695
0.975	0.179	0.736	0.676

SIDEWALL, Z = 0

$\bar{X}$/C	C_p	P/PT	M
-3.75	0.057	0.703	0.728
-3.00	0.010	0.690	0.747
-1.25	0.059	0.704	0.727
1.25	0.034	0.697	0.737
3.75	0.027	0.695	0.740

SIDEWALL, Z/C = 1.375

$\bar{X}$/C	C_p	P/PT	M
-3.75	0.035	0.697	0.736
-2.50	-0.014	0.684	0.757
-2.00	-0.012	0.685	0.756
-1.50	-0.008	0.685	0.755
-1.00	-0.048	0.675	0.771
-0.50	-0.096	0.662	0.791
0.00	-0.058	0.672	0.776
0.50	-0.071	0.669	0.781
1.00	-0.019	0.683	0.759
1.50	-0.001	0.688	0.752
2.00	-0.009	0.685	0.755
2.50	-0.003	0.687	0.752
3.75	0.027	0.695	0.740

SIDEWALL, Z/C = -1.375

$\bar{X}$/C	C_p	P/PT	M
-3.75	0.045	0.700	0.733
-1.00	-0.004	0.687	0.753
-0.50	0.019	0.693	0.743
0.00	0.004	0.689	0.750
0.50	-0.005	0.686	0.753
1.00	-0.004	0.687	0.753
1.50	0.020	0.693	0.743
2.00	0.014	0.692	0.745
2.50	0.031	0.696	0.739
3.75	0.036	0.697	0.736

(f) $M_\infty = 0.751, \alpha = 1.99°, Re_{c,\infty} = 9.5 \times 10^6$.

Figure 13.– Continued.

NACA 0012 AIRFOIL

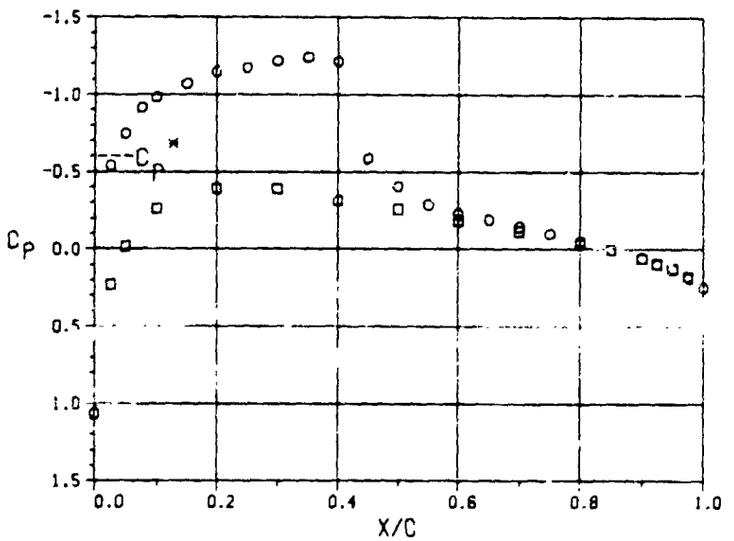

o - AIRFOIL UPPER SURFACE

X/C	C_p	P/PT	M
0.000	1.061	0.976	0.185
0.025	-0.539	0.544	0.975
0.050	-0.748	0.487	1.068
0.075	-0.916	0.442	1.147
0.100	-0.983	0.424	1.179
0.150	-1.072	0.400	1.224
0.200	1.148	0.379	1.264
0.250	-1.176	0.371	1.279
0.300	-1.219	0.360	1.302
0.350	-1.243	0.353	1.316
0.400	-1.215	0.361	1.300
0.450	-0.585	0.531	0.995
0.500	-0.408	0.579	0.919
[illegible]	-0.289	0.611	0.869
[illegible]	-0.232	0.627	0.845
[illegible]	[illegible]	0.638	0.827
0.700	-0.144	0.650	0.808
0.750	-0.100	0.662	0.790
0.800	-0.048	0.677	0.769
0.850	0.002	0.690	0.748
0.900	0.057	0.705	0.725
0.925	0.094	0.715	0.710
0.950	0.128	0.724	0.695
0.975	0.185	0.739	0.671
1.000	0.247	0.756	0.645

□ - AIRFOIL LOWER SURFACE

X/C	C_p	P/PT	M
0.025	0.231	0.753	0.650
0.050	-0.017	0.685	0.756
0.100	-0.263	0.618	0.858
0.200	-0.392	0.584	0.911
0.300	-0.390	0.584	0.911
0.400	-0.314	0.605	0.878
0.500	-0.261	0.619	0.857
0.600	-0.184	0.641	0.824
0.700	-0.115	0.658	0.796
0.800	-0.043	0.679	0.765
0.850	0.005	0.691	0.747
0.900	0.062	0.707	0.722
0.925	0.092	0.714	0.710
0.950	0.126	0.724	0.695
0.975	0.174	0.737	0.676

SIDEWALL, Z=0

$\bar{X}$/C	C_p	P/PT	M
-3.75	0.051	0.703	0.727
-3.00	0.003	0.690	0.747
-1.25	0.053	0.704	0.726
1.25	0.028	0.697	0.736
3.75	0.022	0.696	0.739

SIDEWALL, Z/C= 1.375

$\bar{X}$/C	C_p	P/PT	M
-3.75	0.029	0.698	0.736
-2.50	-0.022	0.684	0.757
-2.00	-0.021	0.684	0.756
-1.50	-0.019	0.685	0.756
-1.00	-0.059	0.674	0.772
-0.50	-0.104	0.662	0.791
0.00	-0.054	0.676	0.770
0.50	-0.080	0.668	0.781
1.00	-0.027	0.683	0.759
1.50	-0.012	0.687	0.753
2.00	-0.018	0.685	0.755
2.50	-0.009	0.688	0.751
3.75	0.020	0.696	0.739

SIDEWALL, Z/C=-1.375

$\bar{X}$/C	C_p	P/PT	M
-3.75	0.038	0.700	0.732
-1.00	-0.013	0.687	0.753
-0.50	0.012	0.693	0.742
0.00	-0.003	0.689	0.749
0.50	-0.012	0.687	0.753
1.00	-0.012	0.687	0.752
1.50	0.013	0.694	0.742
2.00	0.008	0.692	0.744
2.50	0.023	0.696	0.736
3.75	0.028	0.698	0.736

(g) $M_\infty = 0.749$, $\alpha = 2.00°$, $Re_{c,\infty} = 11.7 \times 10^6$.

Figure 13.– Continued.

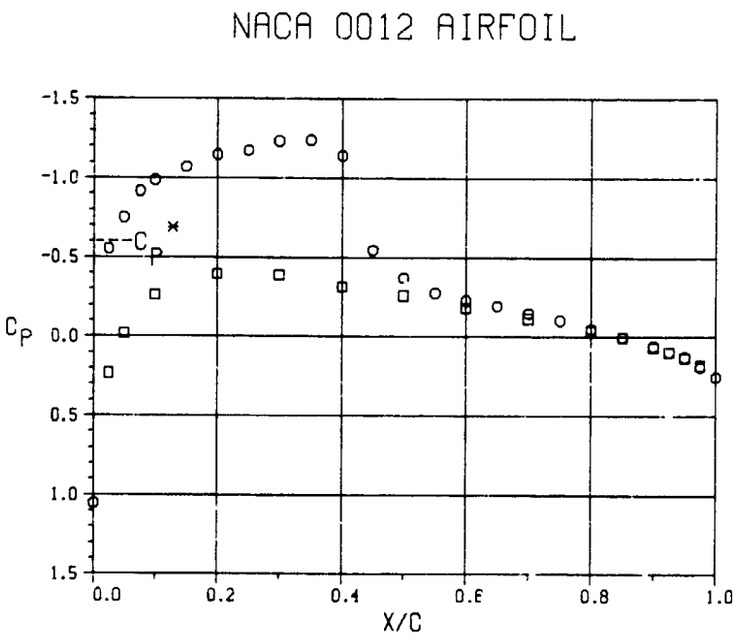

o - AIRFOIL UPPER SURFACE

X/C	C_P	P/PT	M
0.000	1.053	0.975	0.192
0.025	-0.554	0.541	0.980
0.050	-0.750	0.488	1.067
0.075	-0.917	0.443	1.144
0.100	-0.985	0.424	1.178
0.150	-1.070	0.402	1.220
0.200	-1.149	0.380	1.261
0.250	-1.174	0.374	1.274
0.300	-1.234	0.357	1.307
0.350	-1.239	0.356	1.310
0.400	-1.142	0.382	1.257
0.450	-0.546	0.543	0.976
0.500	-0.373	0.590	0.902
0.550	-0.276	0.616	0.862
0.600	-0.231	0.628	0.843
0.650	-0.195	0.638	0.828
0.700	-0.148	0.650	0.809
0.750	-0.103	0.663	0.790
0.800	-0.049	0.677	0.768
0.850	0.003	0.691	0.74
0.900	0.057	0.706	0.72
0.925	0.094	0.716	0.70
0.950	0.128	0.725	0.694
0.975	0.186	0.741	0.669
1.000	0.251	0.758	0.641

□ - AIRFOIL LOWER SURFACE

X/C	C_P	P/PT	M
0.025	0.232	0.752	0.651
0.050	-0.019	0.685	0.755
0.100	-0.201	0.619	0.857
0.200	-0.394	0.583	0.913
0.300	-0.390	0.585	0.910
0.400	-0.314	0.604	0.880
0.500	-0.259	0.620	0.855
0.600	-0.183	0.640	0.825
0.700	-0.114	0.659	0.795
0.800	-0.041	0.678	0.766
0.850	0.005	0.692	0.745
0.900	0.066	0.707	0.721
0.925	0.094	0.716	0.708
0.950	0.130	0.724	0.695
0.975	0.179	0.739	0.672

SIDEWALL, Z/C= 1.375

$\bar{X}$/C	C_P	P/PT	M
-3.75	0.033	0.698	0.736
-2.50	-0.022	0.683	0.758
-2.00	-0.021	0.683	0.758
-1.50	-0.021	0.683	0.758
-1.00	-0.024	0.682	0.759
-0.50	-0.040	0.678	0.766
0.00	-0.007	0.687	0.753
0.50	-0.041	0.678	0.766
1.00	-0.004	0.688	0.751
1.50	0.025	0.696	0.739
2.00	0.035	0.698	0.735
2.50	-0.005	0.688	0.751
3.75	0.027	0.696	0.738

SIDEWALL, Z/C= -1.375

$\bar{X}$/C	C_P	P/PT	M
-3.75	0.042	0.700	0.732
-1.00	0.007	0.691	0.746
-0.50	0.014	0.693	0.744
0.00	-0.002	0.688	0.750
0.50	0.007	0.691	0.746
1.00	0.004	0.690	0.748
1.50	0.017	0.693	0.742
2.00	0.010	0.692	0.745
2.50	0.026	0.696	0.739
3.75	0.032	0.698	0.736

SIDEWALL, Z/C= 0

$\bar{X}$/C	C_P	P/PT	M
-3.75	0.054	0.704	0.726
-3.00	0.005	0.692	0.745
-1.25	0.055	0.704	0.726
1.25	0.031	0.698	0.736
3.75	0.024	0.696	0.739

(h) $M_\infty = 0.747, \alpha = 2.01°, Re_{c,\infty} = 13.9 \times 10^6$.

Figure 13.– Concluded.

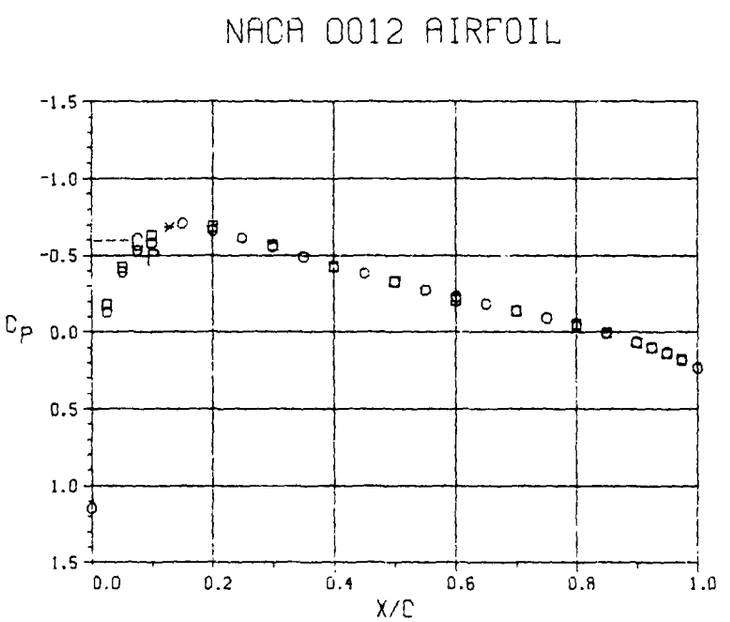

o - AIRFOIL UPPER SURFACE

X/C	C_P	P/PT	M
0.000	1.146	0.999	0.032
0.025	-0.130	0.654	0.803
0.050	-0.392	0.583	0.914
0.075	-0.535	0.544	0.975
0.100	-0.579	0.532	0.994
0.150	-0.711	0.496	1.053
0.200	-0.664	0.509	1.031
0.250	-0.613	0.523	1.009
0.300	-0.556	0.538	0.984
0.350	-0.489	0.556	0.955
0.400	-0.424	0.574	0.927
0.450	-0.382	0.585	0.909
0.500	-0.328	0.600	0.887
0.550	-0.274	0.615	0.864
0.600	-0.232	0.626	0.846
0.650	-0.185	0.639	0.826
0.700	-0.138	0.652	0.807
0.750	-0.092	0.664	0.788
0.800	-0.042	0.677	0.767
0.850	0.007	0.691	0.746
0.900	0.063	0.706	0.723
0.925	0.097	0.715	0.709
0.950	0.133	0.725	0.694
0.975	0.182	0.738	0.673
1.000	0.231	0.752	0.652

□ - AIRFOIL LOWER SURFACE

X/C	C_P	P/PT	M
0.025	-0.183	0.640	0.825
0.050	-0.422	0.575	0.926
0.100	-0.632	0.518	1.017
0.200	-0.688	0.503	1.041
0.300	-0.565	0.536	0.988
0.400	-0.428	0.574	0.927
0.500	-0.329	0.600	0.887
0.600	-0.208	0.633	0.835
0.700	-0.138	0.651	0.807
0.800	-0.051	0.676	0.770
0.850	0.005	0.690	0.748
0.900	0.067	0.707	0.721
0.925	0.100	0.716	0.708
0.950	0.134	0.726	0.693
0.975	0.177	0.737	0.675

SIDEWALL, Z = 0

$\bar{X}$/C	C_P	P/PT	M
-3.75	0.049	0.703	0.728
-3.00	0.004	0.690	0.748
-1.25	0.051	0.703	0.727
1.25	0.028	0.697	0.737
3.75	0.015	0.694	0.742

SIDEWALL, Z/C = 1.375

$\bar{X}$/C	C_P	P/PT	M
-3.75	0.037	0.700	0.733
-2.50	-0.001	0.690	0.748
-2.00	0.008	0.692	0.745
-1.50	0.014	0.694	0.742
-1.00	-0.017	0.685	0.755
-0.50	-0.033	0.681	0.762
0.00	-0.005	0.689	0.750
0.50	-0.018	0.685	0.755
1.00	0.028	0.698	0.736
1.50	0.001	0.690	0.748
2.00	-0.036	0.680	0.763
2.50	-0.020	0.684	0.756
3.75	0.032	0.698	0.735

SIDEWALL, Z/C = -1.375

$\bar{X}$/C	C_P	P/PT	M
-3.75	0.034	0.699	0.734
-1.00	-0.024	0.683	0.758
-0.50	-0.005	0.688	0.750
0.00	-0.030	0.682	0.760
0.50	-0.031	0.682	0.761
1.00	-0.012	0.687	0.753
1.50	0.002	0.690	0.747
2.00	-0.003	0.689	0.749
2.50	0.012	0.693	0.743
3.75	0.019	0.695	0.740

(a) $M_\infty = 0.753$, $\alpha = -0.02°$, $Re_{c,\infty} = 4.0 \times 10^6$.

Figure 14.– Airfoil and test-channel sidewall pressure measurements, Data Set 2 ($M_N = 0.75$, $\alpha_N = 0°$).

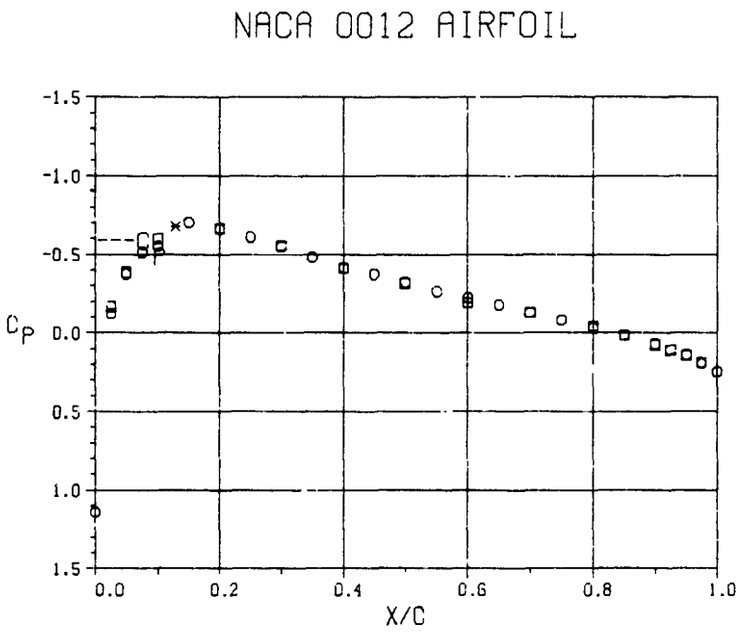

o - AIRFOIL UPPER SURFACE

X/C	C_P	P/PT	M
0.000	1.141	0.998	0.056
0.025	-0.124	0.655	0.802
0.050	-0.376	0.586	0.908
0.075	-0.513	0.549	0.966
0.100	-0.555	0.538	0.985
0.150	-0.703	0.497	1.051
0.200	-0.664	0.508	1.033
0.250	-0.611	0.523	1.009
0.300	-0.551	0.539	0.983
0.350	-0.484	0.557	0.954
0.400	-0.416	0.575	0.925
0.450	-0.375	0.586	0.908
0.500	-0.322	0.601	0.885
0.550	-0.266	0.616	0.862
0.600	-0.224	0.628	0.844
0.650	-0.179	0.640	0.825
0.700	-0.130	0.653	0.805
0.750	-0.084	0.665	0.786
0.800	-0.033	0.679	0.764
0.850	0.015	0.692	0.744
0.900	0.070	0.707	0.721
0.925	0.106	0.717	0.706
0.950	0.140	0.726	0.692
0.975	0.192	0.740	0.670
1.000	0.245	0.755	0.647

□ - AIRFOIL LOWER SURFACE

X/C	C_P	P/PT	M
0.025	-0.166	0.645	0.817
0.050	-0.387	0.583	0.913
0.100	-0.593	0.526	1.004
0.200	-0.665	0.510	1.030
0.300	-0.556	0.537	0.985
0.400	-0.411	0.578	0.920
0.500	-0.318	0.602	0.883
0.600	-0.194	0.637	0.829
0.700	-0.128	0.653	0.804
0.800	-0.043	0.678	0.766
0.850	0.013	0.692	0.745
0.900	0.076	0.710	0.717
0.925	0.109	0.718	0.705
0.950	0.143	0.728	0.689
0.975	0.189	0.739	0.671

SIDEWALL, Z=0

$\bar{X}$/C	C_P	P/PT	M
-3.75	0.052	0.703	0.728
-3.00	0.009	0.691	0.747
-1.25	0.059	0.705	0.725
1.25	0.037	0.699	0.734
3.75	0.024	0.696	0.739

SIDEWALL, Z/C= 1.375

$\bar{X}$/C	C_P	P/PT	M
-3.75	0.037	0.700	0.733
-2.50	0.000	0.690	0.748
-2.00	0.011	0.693	0.744
-1.50	0.022	0.695	0.739
-1.00	-0.009	0.687	0.752
-0.50	-0.026	0.683	0.759
0.00	0.007	0.692	0.745
0.50	-0.011	0.687	0.753
1.00	0.036	0.699	0.733
1.50	0.009	0.692	0.745
2.00	-0.027	0.682	0.760
2.50	-0.012	0.686	0.753
3.75	0.040	0.700	0.732

SIDEWALL, Z/C=-1.375

$\bar{X}$/C	C_P	P/PT	M
-3.75	0.039	0.700	0.732
-1.00	-0.015	0.685	0.755
-0.50	0.004	0.691	0.747
0.00	-0.017	0.685	0.755
0.50	-0.024	0.683	0.758
1.00	-0.005	0.688	0.750
1.50	0.011	0.693	0.744
2.00	0.005	0.691	0.746
2.50	0.020	0.695	0.740
3.75	0.028	0.697	0.737

(b) $M_\infty = 0.750, \alpha = -0.02°, Re_{c,\infty} = 6.0 \times 10^6$.

Figure 14.– Continued.

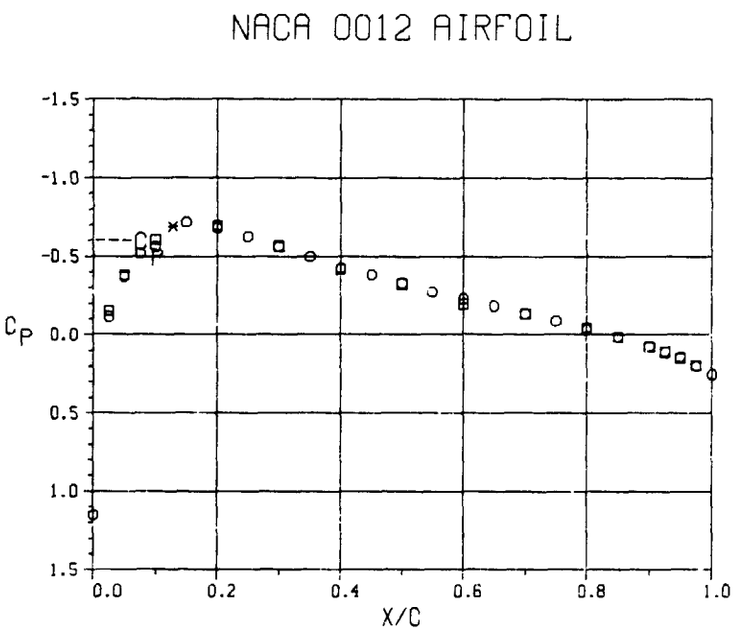

□ - AIRFOIL LOWER SURFACE

X/C	C_P	P/PT	M
0.025	-0.153	0.648	0.812
0.050	-0.384	0.586	0.908
0.100	-0.609	0.526	1.004
0.200	-0.695	0.502	1.013
0.300	-0.566	0.537	0.986
0.400	-0.419	0.577	0.923
0.500	-0.324	0.602	0.883
0.600	-0.195	0.637	0.829
0.700	-0.132	0.654	0.803
0.800	-0.042	0.679	0.765
0.850	0.013	0.694	0.742
0.900	0.079	0.711	0.715
0.925	0.109	0.719	0.702
0.950	0.147	0.729	0.687
0.975	0.193	0.742	0.667

SIDEWALL, Z=0

$\bar{X}$/C	C_P	P/PT	M
-3.75	0.049	0.704	0.726
-3.00	0.004	0.691	0.746
-1.25	0.061	0.707	0.721
1.25	0.038	0.701	0.731
3.75	0.025	0.697	0.736

○ - AIRFOIL UPPER SURFACE

X/C	C_P	P/PT	M
0.000	1.150	1.001	0.000
0.025	-0.115	0.659	0.796
0.050	-0.373	0.589	0.903
0.075	-0.520	0.549	0.966
0.100	-0.564	0.538	0.985
0.150	-0.717	0.496	1.053
0.200	-0.680	0.506	1.036
0.250	-0.626	0.521	1.012
0.300	-0.563	0.538	0.985
0.350	-0.497	0.556	0.956
0.400	-0.424	0.575	0.925
0.450	-0.383	0.586	0.907
0.500	-0.329	0.601	0.885
0.550	-0.272	0.616	0.861
0.600	-0.230	0.628	0.843
0.650	-0.185	0.640	0.824
0.700	-0.133	0.654	0.803
0.750	-0.088	0.666	0.784
0.800	-0.034	0.681	0.762
0.850	0.015	0.694	0.742
0.900	0.070	0.709	0.718
0.925	0.107	0.719	0.703
0.950	0.141	0.728	0.689
0.975	0.198	0.743	0.665
1.000	0.254	0.759	0.641

SIDEWALL, Z/C= 1.375

$\bar{X}$/C	C_P	P/PT	M
-3.75	0.032	0.699	0.734
-2.50	-0.005	0.689	0.749
-2.00	0.008	0.693	0.743
-1.50	0.021	0.696	0.738
-1.00	-0.010	0.688	0.751
-0.50	-0.027	0.684	0.758
0.00	0.010	0.693	0.743
0.50	-0.012	0.688	0.752
1.00	0.037	0.701	0.731
1.50	0.015	0.695	0.740
2.00	-0.028	0.683	0.758
2.50	-0.010	0.688	0.751
3.75	0.041	0.702	0.730

SIDEWALL, Z/C=-1.375

$\bar{X}$/C	C_P	P/PT	M
-3.75	0.038	0.701	0.731
-1.00	-0.018	0.686	0.754
-0.50	0.004	0.692	0.745
0.00	-0.020	0.685	0.755
0.50	-0.018	0.686	0.754
1.00	-0.006	0.689	0.749
1.50	0.012	0.694	0.742
2.00	0.005	0.692	0.745
2.50	0.021	0.696	0.738
3.75	0.029	0.699	0.734

(c) $M_\infty = 0.748$, $\alpha = -0.02°$, $Re_{c,\infty} = 7.8 \times 10^6$.

Figure 14.– Continued.

NACA 0012 AIRFOIL

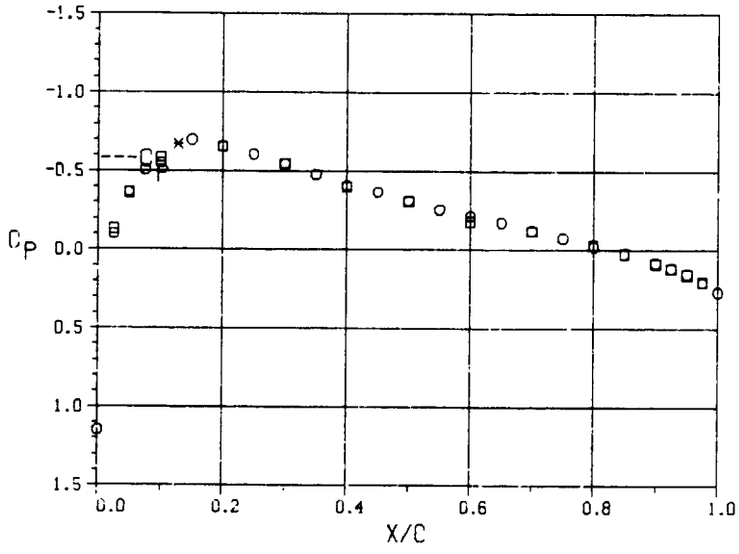

o - AIRFOIL UPPER SURFACE

X/C	C_P	P/P1	M
0.000	1.145	0.999	0.042
0.025	-0.101	0.660	0.794
0.050	-0.365	0.588	0.905
0.075	-0.509	0.549	0.967
0.100	-0.551	0.537	0.986
0.150	-0.699	0.497	1.052
0.200	-0.655	0.509	1.032
0.250	-0.605	0.522	1.010
0.300	-0.544	0.539	0.983
0.350	-0.478	0.557	0.954
0.400	-0.407	0.576	0.924
0.450	-0.367	0.587	0.906
0.500	-0.315	0.601	0.884
0.550	-0.258	0.617	0.860
0.600	-0.217	0.628	0.843
0.650	-0.172	0.640	0.824
0.700	-0.121	0.654	0.803
0.750	-0.075	0.667	0.784
0.800	-0.023	0.681	0.762
0.850	0.026	0.694	0.741
0.900	0.080	0.709	0.719
0.925	0.116	0.719	0.704
0.950	0.150	0.728	0.689
0.975	0.206	0.743	0.665
1.000	0.265	0.759	0.640

□ - AIRFOIL LOWER SURFACE

X/C	C_P	P/PT	M
0.025	-0.133	0.651	0.808
0.050	-0.364	0.588	0.905
0.100	-0.586	0.528	1.001
0.200	-0.655	0.509	1.031
0.300	-0.544	0.539	0.983
0.400	-0.399	0.579	0.920
0.500	-0.307	0.603	0.881
0.600	-0.180	0.639	0.827
0.700	-0.118	0.655	0.802
0.800	-0.031	0.679	0.765
0.850	0.023	0.693	0.743
0.900	0.088	0.711	0.715
0.925	0.119	0.719	0.702
0.950	0.156	0.730	0.686
0.975	0.203	0.742	0.667

SIDEWALL, Z=0

$\bar{X}$/C	C_P	P/PT	M
-3.75	0.061	0.704	0.727
-3.00	0.014	0.691	0.746
-1.25	0.072	0.707	0.722
1.25	0.050	0.701	0.731
3.75	0.037	0.697	0.737

SIDEWALL, Z/C= 1.375

$\bar{X}$/C	C_P	P/PT	M
-3.75	0.045	0.699	0.733
-2.50	0.006	0.689	0.750
-2.00	0.019	0.692	0.744
-1.50	0.032	0.696	0.739
-1.00	0.002	0.688	0.752
-0.50	-0.016	0.683	0.759
0.00	0.024	0.694	0.742
0.50	0.000	0.687	0.752
1.00	0.050	0.701	0.731
1.50	0.029	0.695	0.740
2.00	-0.016	0.683	0.759
2.50	0.001	0.688	0.752
3.75	0.053	0.702	0.730

SIDEWALL, Z/C=-1.375

$\bar{X}$/C	C_P	P/PT	M
-3.75	0.049	0.701	0.732
-1.00	-0.004	0.686	0.754
-0.50	0.016	0.692	0.745
0.00	-0.007	0.685	0.755
0.50	-0.008	0.685	0.756
1.00	0.006	0.689	0.750
1.50	0.024	0.694	0.742
2.00	0.016	0.692	0.745
2.50	0.032	0.696	0.739
3.75	0.041	0.698	0.735

(d) $M_\infty = 0.752, \alpha = -0.02°, Re_{c,\infty} = 9.4 \times 10^6$.

Figure 14.– Continued.

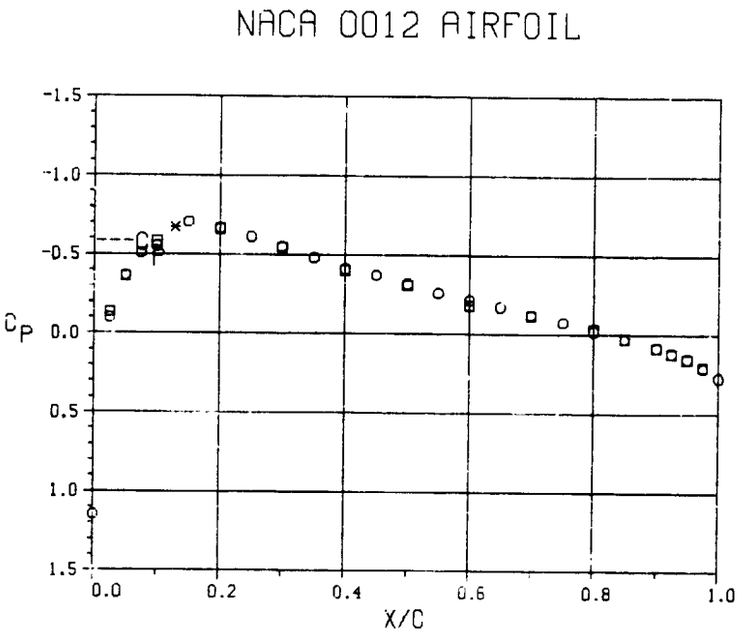

□ - AIRFOIL LOWER SURFACE

X/C	C_P	P/PT	M
0.025	-0.134	0.651	0.808
0.050	-0.360	0.589	0.904
0.100	-0.584	0.528	1.001
0.200	-0.663	0.507	1.035
0.300	-0.546	0.538	0.984
0.400	-0.403	0.578	0.921
0.500	-0.308	0.603	0.882
0.600	-0.183	0.638	0.828
0.700	-0.120	0.654	0.803
0.800	-0.035	0.678	0.766
0.850	0.022	0.693	0.743
0.900	0.085	0.710	0.716
0.925	0.120	0.719	0.702
0.950	0.154	0.729	0.687
0.975	0.203	0.742	0.667

SIDEWALL, Z=0

$\bar{X}$/C	C_P	P/PT	M
-3.75	0.060	0.704	0.727
-3.00	0.013	0.690	0.747
-1.25	0.071	0.707	0.722
1.25	0.048	0.701	0.732
3.75	0.036	0.697	0.737

o - AIRFOIL UPPER SURFACE

X/C	C_P	P/PT	M
0.000	1.146	0.999	0.037
0.025	-0.100	0.660	0.795
0.050	-0.365	0.587	0.906
0.075	-0.510	0.548	0.969
0.100	-0.554	0.536	0.988
0.150	-0.707	0.494	1.056
0.200	-0.668	0.505	1.038
0.250	-0.612	0.520	1.013
0.300	-0.549	0.537	0.986
0.350	-0.480	0.556	0.955
0.400	-0.410	0.575	0.925
0.450	-0.371	0.586	0.909
0.500	-0.318	0.600	0.886
0.550	-0.261	0.615	0.862
0.600	-0.217	0.626	0.844
0.650	-0.174	0.639	0.825
0.700	-0.122	0.653	0.804
0.750	-0.077	0.666	0.785
0.800	-0.023	0.681	0.762
0.850	0.027	0.694	0.742
0.900	0.082	0.709	0.718
0.925	0.116	0.719	0.704
0.950	0.151	0.729	0.689
0.975	0.210	0.744	0.664
1.000	0.272	0.761	0.637

SIDEWALL, Z/C= 1.375

$\bar{X}$/C	C_P	P/PT	M
-3.75	0.041	0.699	0.734
-2.50	0.000	0.688	0.751
-2.00	0.011	0.691	0.747
-1.50	0.025	0.694	0.741
-1.00	-0.004	0.687	0.753
-0.50	-0.020	0.682	0.760
0.00	0.022	0.694	0.742
0.50	-0.005	0.685	0.754
1.00	0.044	0.700	0.733
1.50	0.023	0.694	0.742
2.00	-0.022	0.682	0.761
2.50	-0.002	0.687	0.752
3.75	0.048	0.701	0.731

SIDEWALL, Z/C=-1.375

$\bar{X}$/C	C_P	P/PT	M
-3.75	0.047	0.701	0.731
-1.00	-0.009	0.685	0.755
-0.50	0.013	0.691	0.746
0.00	-0.011	0.685	0.756
0.50	-0.014	0.684	0.757
1.00	0.000	0.688	0.751
1.50	0.021	0.693	0.743
2.00	0.009	0.690	0.748
2.50	0.026	0.695	0.740
3.75	0.037	0.698	0.736

(e) $M_\infty = 0.753$, $\alpha = -0.02°$, $Re_{c,\infty} = 12.2 \times 10^6$.

Figure 14.– Concluded.

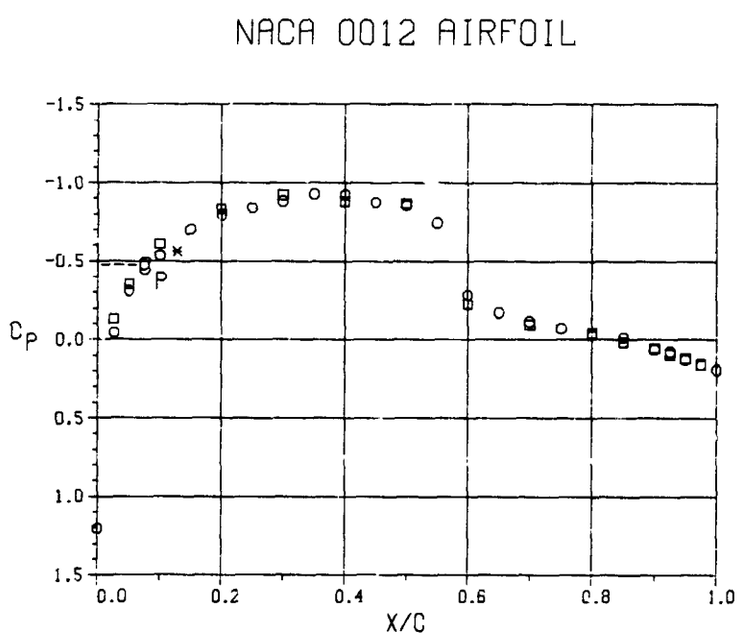

□ - AIRFOIL LOWER SURFACE

X/C	C_P	P/PT	M
0.025	-0.129	0.629	0.841
0.050	-0.356	0.562	0.946
0.100	-0.608	0.489	1.064
0.200	-0.833	0.427	1.173
0.300	-0.924	0.399	1.226
0.400	-0.879	0.414	1.197
0.500	-0.867	0.415	1.195
0.600	-0.229	0.600	0.886
0.700	-0.095	0.637	0.829
0.800	-0.044	0.654	0.804
0.850	0.013	0.668	0.781
0.900	0.056	0.682	0.760
0.925	0.092	0.691	0.746
0.950	0.118	0.700	0.733
0.975	0.156	0.710	0.717

SIDEWALL, Z=0

$\bar{X}$/C	C_P	P/PT	M
-3.75	0.038	0.677	0.768
-3.00	-0.009	0.662	0.791
-1.25	0.035	0.676	0.770
1.25	-0.011	0.662	0.790
3.75	-0.031	0.657	0.799

○ - AIRFOIL UPPER SURFACE

X/C	C_P	P/PT	M
0.000	1.203	1.011	0.000
0.025	-0.044	0.652	0.806
0.050	-0.311	0.575	0.925
0.075	-0.475	0.528	1.001
0.100	-0.534	0.511	1.029
0.150	-0.701	0.463	1.110
0.200	-0.797	0.435	1.158
0.250	-0.840	0.423	1.181
0.300	-0.883	0.410	1.204
0.350	-0.929	0.397	1.229
0.400	-0.926	0.398	1.227
0.450	-0.876	0.412	1.200
0.500	-0.857	0.418	1.190
0.550	-0.745	0.450	1.132
0.600	-0.287	0.582	0.914
0.650	-0.172	0.615	0.863
0.700	-0.115	0.631	0.838
0.750	-0.072	0.644	0.819
0.800	-0.031	0.656	0.801
0.850	-0.015	0.660	0.794
0.900	0.061	0.682	0.760
0.925	0.076	0.686	0.753
0.950	0.125	0.701	0.731
0.975	0.159	0.710	0.717
1.000	0.191	0.720	0.702

SIDEWALL, Z/C= 1.375

$\bar{X}$/C	C_P	P/PT	M
-3.75	0.032	0.675	0.770
-2.50	-0.007	0.664	0.787
-2.00	0.003	0.667	0.783
-1.50	0.001	0.667	0.784
-1.00	-0.041	0.655	0.802
-0.50	-0.104	0.637	0.830
0.00	-0.100	0.638	0.828
0.50	-0.078	0.644	0.819
1.00	-0.053	0.651	0.807
1.50	-0.042	0.654	0.803
2.00	-0.038	0.655	0.801
2.50	-0.043	0.654	0.803
3.75	-0.026	0.659	0.795

SIDEWALL, Z/C=-1.375

$\bar{X}$/C	C_P	P/PT	M
-3.75	0.018	0.672	0.776
-1.00	-0.041	0.655	0.802
-0.50	-0.061	0.649	0.811
0.00	-0.132	0.628	0.842
0.50	-0.054	0.651	0.808
1.00	-0.052	0.651	0.807
1.50	-0.040	0.655	0.802
2.00	-0.050	0.652	0.806
2.50	0.038	0.656	0.801
3.75	0.029	0.658	0.797

(a) $M_\infty = 0.787$, $\alpha = -0.10°$, $Re_{c,\infty} = 1.0 \times 10^6$.

Figure 15.– Airfoil and test channel sidewall pressure measurements, Data Set 3 ($M_N = 0.80$, $\alpha_N = 0°$).

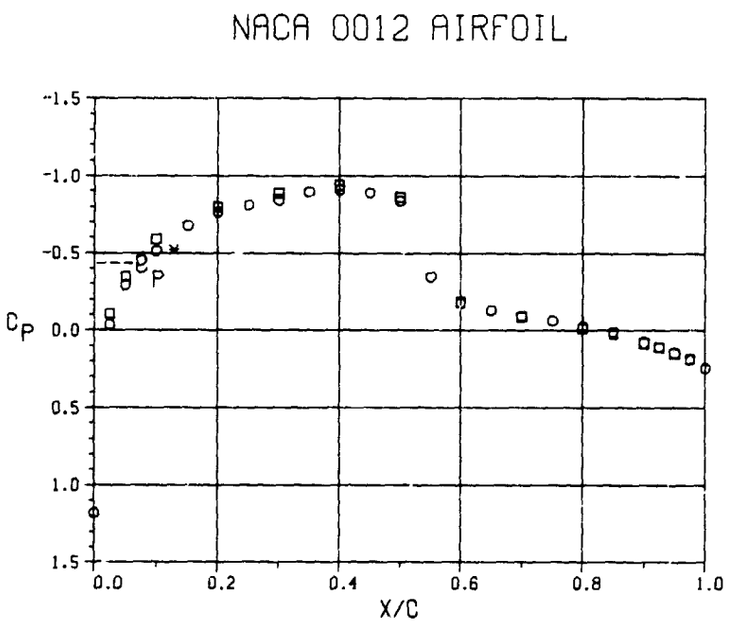

o - AIRFOIL UPPER SURFACE

X/C	C_P	P/PT	M
0.000	1.180	1.003	0.000
0.025	-0.036	0.645	0.817
0.050	-0.293	0.569	0.934
0.075	-0.455	0.522	1.011
0.100	-0.515	0.504	1.040
0.150	-0.678	0.456	1.121
0.200	-0.765	0.430	1.167
0.250	-0.811	0.417	1.191
0.300	-0.849	0.406	1.212
0.350	-0.898	0.392	1.239
0.400	-0.911	0.388	1.247
0.450	-0.892	0.393	1.236
0.500	-0.839	0.409	1.206
0.550	-0.350	0.553	0.961
0.600	-0.179	0.603	0.882
0.650	-0.130	0.618	0.859
0.700	-0.095	0.628	0.844
0.750	-0.065	0.637	0.830
0.800	-0.026	0.648	0.812
0.850	0.009	0.658	0.797
0.900	0.075	0.678	0.767
0.925	0.106	0.687	0.753
0.950	0.144	0.698	0.735
0.975	0.188	0.711	0.715
1.000	0.240	0.726	0.692

□ - AIRFOIL LOWER SURFACE

X/C	C_P	P/PT	M
0.025	-0.107	0.625	0.847
0.050	-0.349	0.553	0.960
0.100	-0.592	0.481	1.078
0.200	-0.799	0.422	1.182
0.300	-0.891	0.393	1.236
0.400	-0.941	0.381	1.260
0.500	-0.863	0.402	1.220
0.600	-0.185	0.602	0.883
0.700	-0.088	0.630	0.840
0.800	-0.015	0.652	0.806
0.850	0.017	0.661	0.793
0.900	0.081	0.681	0.762
0.925	0.106	0.687	0.753
0.950	0.148	0.700	0.732
0.975	0.183	0.709	0.718

SIDEWALL, Z/C= 1.375

$\bar{X}$/C	C_P	P/PT	M
-3.75	0.043	0.669	0.780
-2.50	-0.001	0.656	0.799
-2.00	0.020	0.663	0.790
-1.50	0.026	0.664	0.787
-1.00	-0.015	0.652	0.805
-0.50	-0.080	0.633	0.835
0.00	-0.066	0.638	0.828
0.50	-0.053	0.641	0.823
1.00	-0.024	0.650	0.810
1.50	-0.012	0.653	0.804
2.00	-0.006	0.655	0.802
2.50	-0.013	0.653	0.805
3.75	0.007	0.659	0.796

SIDEWALL, Z/C= 0

$\bar{X}$/C	C_P	P/PT	M
-3.75	0.047	0.670	0.778
-3.00	-0.001	0.655	0.801
-1.25	0.057	0.673	0.774
1.25	0.016	0.661	0.792
3.75	0.000	0.656	0.800

SIDEWALL, Z/C= -1.375

$\bar{X}$/C	C_P	P/PT	M
-3.75	0.036	0.667	0.783
-1.00	-0.017	0.652	0.806
-0.50	-0.034	0.647	0.814
0.00	-0.101	0.627	0.844
0.50	-0.023	0.650	0.809
1.00	-0.032	0.648	0.813
1.50	-0.013	0.653	0.805
2.00	-0.015	0.653	0.805
2.50	-0.012	0.653	0.804
3.75	0.004	0.658	0.797

(b) $M_\infty = 0.801, \alpha = -0.10°, Re_{c,\infty} = 2.0 \times 10^6$.

Figure 15.– Continued.

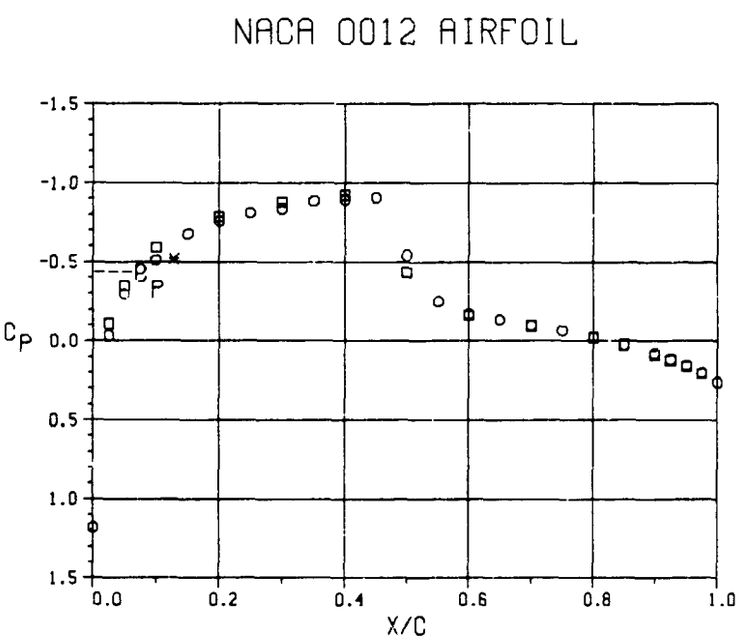

o - AIRFOIL UPPER SURFACE

X/C	C_P	P/PT	M
0.000	1.180	1.003	0.000
0.025	-0.034	0.645	0.817
0.050	-0.296	0.568	0.937
0.075	-0.456	0.521	1.012
0.100	-0.512	0.504	1.039
0.150	-0.678	0.455	1.122
0.200	-0.760	0.431	1.165
0.250	-0.809	0.417	1.192
0.300	-0.837	0.409	1.207
0.350	-0.886	0.394	1.234
0.400	-0.895	0.392	1.239
0.450	-0.907	0.388	1.246
0.500	-0.543	0.495	1.054
0.550	-0.250	0.581	0.915
0.600	-0.169	0.605	0.878
0.650	-0.135	0.616	0.862
0.700	-0.100	0.626	0.847
0.750	-0.067	0.635	0.832
0.800	-0.025	0.648	0.813
0.850	0.024	0.662	0.791
0.900	0.079	0.679	0.765
0.925	0.116	0.689	0.749
0.950	0.152	0.700	0.732
0.975	0.199	0.714	0.711
1.000	0.260	0.732	0.683

□ - AIRFOIL LOWER SURFACE

X/C	C_P	P/PT	M
0.025	-0.110	0.622	0.852
0.050	-0.349	0.552	0.961
0.100	-0.591	0.481	1.078
0.200	-0.789	0.422	1.182
0.300	-0.879	0.396	1.230
0.400	-0.922	0.383	1.256
0.500	-0.434	0.527	1.001
0.600	-0.166	0.606	0.877
0.700	-0.099	0.626	0.846
0.800	-0.023	0.648	0.812
0.850	0.022	0.662	0.791
0.900	0.089	0.681	0.762
0.925	0.121	0.691	0.747
0.950	0.159	0.702	0.730
0.975	0.205	0.715	0.709

SIDEWALL, Z = 0

$\bar{X}$/C	C_P	P/PT	M
-3.75	0.050	0.670	0.779
-3.00	0.004	0.656	0.799
-1.25	0.063	0.674	0.773
1.25	0.028	0.663	0.789
3.75	0.013	0.659	0.795

SIDEWALL, Z/C = 1.375

$\bar{X}$/C	C_P	P/PT	M
-3.75	0.042	0.667	0.783
-2.50	0.000	0.655	0.802
-2.00	0.018	0.660	0.793
-1.50	0.032	0.664	0.787
-1.00	-0.012	0.651	0.807
-0.50	-0.070	0.634	0.833
0.00	-0.043	0.642	0.821
0.50	-0.039	0.643	0.820
1.00	-0.012	0.651	0.807
1.50	-0.001	0.655	0.802
2.00	0.005	0.656	0.799
2.50	0.000	0.655	0.801
3.75	0.022	0.662	0.792

SIDEWALL, Z/C = -1.375

$\bar{X}$/C	C_P	P/PT	M
-3.75	0.036	0.666	0.785
-1.00	-0.017	0.650	0.809
-0.50	-0.019	0.649	0.810
0.00	-0.082	0.631	0.839
0.50	-0.004	0.654	0.803
1.00	-0.019	0.649	0.810
1.50	-0.002	0.654	0.803
2.00	0.000	0.655	0.802
2.50	0.001	0.655	0.801
3.75	0.016	0.660	0.794

(c) $M_\infty = 0.801$, $\alpha = -0.10°$, $Re_{c,\infty} = 4.0 \times 10^6$.

Figure 15.– Continued.

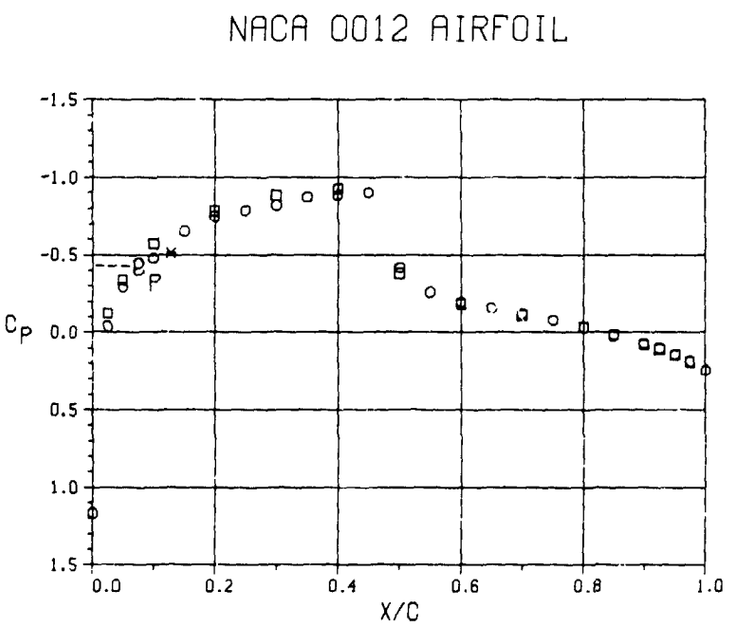

o - AIRFOIL UPPER SURFACE

X/C	C_P	P/PT	M
0.000	1.165	0.998	0.055
0.025	-0.041	0.642	0.822
0.050	-0.292	0.567	0.937
0.075	-0.444	0.523	1.009
0.100	-0.480	0.512	1.027
0.150	-0.651	0.462	1.112
0.200	-0.749	0.433	1.163
0.250	-0.788	0.421	1.184
0.300	-0.819	0.412	1.201
0.350	-0.874	0.396	1.231
0.400	-0.886	0.392	1.238
0.450	-0.901	0.388	1.247
0.500	-0.419	0.530	0.997
0.550	-0.260	0.577	0.922
0.600	-0.194	0.597	0.892
0.650	-0.157	0.607	0.875
0.700	-0.119	0.619	0.858
0.750	-0.080	0.630	0.839
0.800	-0.035	0.644	0.819
0.850	0.023	0.661	0.793
0.900	0.071	0.675	0.771
0.925	0.104	0.685	0.756
0.950	0.142	0.696	0.739
0.975	0.185	0.709	0.719
1.000	0.247	0.727	0.691

□ - AIRFOIL LOWER SURFACE

X/C	C_P	P/PT	M
0.025	-0.125	0.617	0.860
0.050	-0.339	0.554	0.959
0.100	-0.574	0.484	1.073
0.200	-0.784	0.422	1.182
0.300	-0.883	0.393	1.236
0.400	-0.926	0.380	1.261
0.500	-0.380	0.542	0.978
0.600	-0.186	0.599	0.888
0.700	-0.109	0.622	0.853
0.800	-0.034	0.644	0.819
0.850	0.014	0.658	0.797
0.900	0.078	0.677	0.768
0.925	0.110	0.686	0.754
0.950	0.147	0.697	0.737
0.975	0.191	0.710	0.716

SIDEWALL, Z = 0

$\bar{X}$/C	C_P	P/PT	M
-3.75	0.047	0.668	0.782
-3.00	0.007	0.656	0.800
-1.25	0.055	0.670	0.778
1.25	0.025	0.661	0.792
3.75	0.009	0.656	0.799

SIDEWALL, Z/C = 1.375

$\bar{X}$/C	C_P	P/PT	M
-3.75	0.037	0.665	0.786
-2.50	-0.005	0.652	0.806
-2.00	0.010	0.657	0.799
-1.50	0.023	0.661	0.793
-1.00	-0.018	0.648	0.812
-0.50	-0.075	0.632	0.837
0.00	-0.030	0.645	0.817
0.50	-0.043	0.641	0.823
1.00	-0.016	0.649	0.810
1.50	-0.007	0.652	0.806
2.00	0.000	0.654	0.804
2.50	-0.005	0.652	0.806
3.75	0.018	0.659	0.795

SIDEWALL, Z/C = -1.375

$\bar{X}$/C	C_P	P/PT	M
-3.75	0.033	0.664	0.788
-1.00	-0.019	0.648	0.812
-0.50	-0.021	0.648	0.813
0.00	-0.078	0.631	0.839
0.50	-0.008	0.652	0.807
1.00	-0.025	0.646	0.815
1.50	-0.008	0.651	0.807
2.00	-0.007	0.652	0.806
2.50	-0.003	0.653	0.805
3.75	0.011	0.657	0.798

(d) $M_\infty = 0.803$, $\alpha = -0.10°$, $Re_{c,\infty} = 6.5 \times 10^6$.

Figure 15.– Continued.

NACA 0012 AIRFOIL

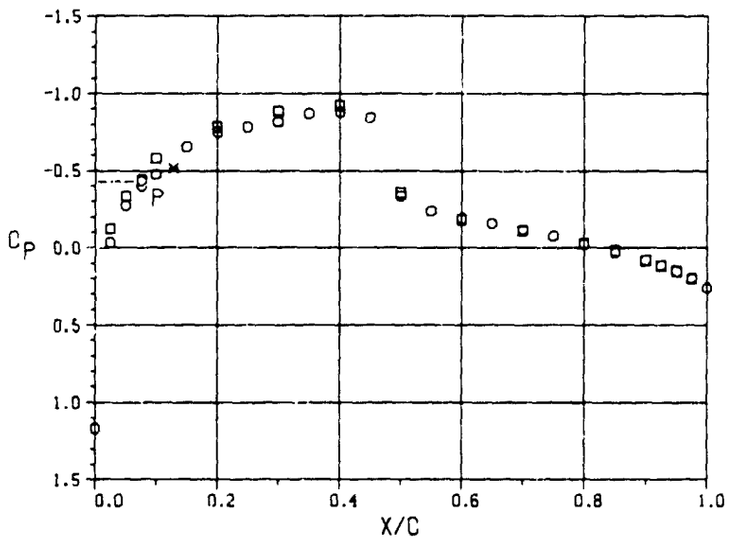

o - AIRFOIL UPPER SURFACE

X/C	C_P	P/PT	M
0.000	1.166	0.998	0.048
0.025	-0.034	0.644	0.818
0.050	-0.276	0.573	0.928
0.075	-0.434	0.526	1.003
0.100	-0.475	0.514	1.023
0.150	-0.654	0.461	1.112
0.200	-0.750	0.433	1.162
0.250	-0.784	0.423	1.180
0.300	-0.816	0.414	1.197
0.350	-0.870	0.398	1.227
0.400	-0.880	0.395	1.233
0.450	-0.846	0.405	1.214
0.500	-0.338	0.555	0.957
0.550	-0.239	0.584	0.912
0.600	-0.191	0.593	0.889
0.650	-0.158	0.608	0.874
0.700	-0.119	0.619	0.856
0.750	-0.076	0.632	0.837
0.800	-0.029	0.646	0.816
0.850	0.031	0.664	0.788
0.900	0.078	0.678	0.767
0.925	0.113	0.688	0.751
0.950	0.149	0.696	0.735
0.975	0.193	0.711	0.715
1.000	0.258	0.731	0.685

□ - AIRFOIL LOWER SURFACE

X/C	C_P	P/PT	M
0.025	-0.123	0.618	0.858
0.050	-0.338	0.555	0.957
0.100	-0.579	0.484	1.074
0.200	-0.786	0.423	1.181
0.300	-0.884	0.394	1.235
0.400	-0.923	0.382	1.258
0.500	-0.358	0.549	0.967
0.600	-0.186	0.600	0.887
0.700	-0.111	0.622	0.853
0.800	-0.033	0.645	0.817
0.850	0.018	0.660	0.794
0.900	0.081	0.679	0.765
0.925	0.116	0.689	0.750
0.950	0.151	0.699	0.734
0.975	0.198	0.713	0.713

SIDEWALL, Z=0

$\bar{X}$/C	C_P	P/PT	M
-3.75	0.050	0.669	0.781
-3.00	0.007	0.657	0.799
-1.25	0.060	0.672	0.776
1.25	0.032	0.663	0.789
3.75	0.016	0.659	0.796

SIDEWALL, Z/C= 1.375

$\bar{X}$/C	C_P	P/PT	M
-3.75	0.040	0.666	0.785
-2.50	-0.004	0.653	0.805
-2.00	0.010	0.657	0.799
-1.50	0.025	0.661	0.792
-1.00	-0.016	0.649	0.810
-0.50	-0.065	0.635	0.833
0.00	-0.014	0.650	0.809
0.50	-0.034	0.644	0.818
1.00	-0.006	0.652	0.806
1.50	0.003	0.655	0.802
2.00	0.003	0.655	0.802
2.50	-0.001	0.654	0.804
3.75	0.024	0.661	0.792

SIDEWALL, Z/C=-1.375

$\bar{X}$/C	C_P	P/PT	M
-3.75	0.038	0.665	0.786
-1.00	-0.017	0.649	0.811
-0.50	-0.015	0.650	0.810
0.00	-0.072	0.633	0.836
0.50	-0.001	0.654	0.803
1.00	-0.020	0.648	0.812
1.50	-0.004	0.653	0.805
2.00	-0.004	0.653	0.805
2.50	0.000	0.654	0.803
3.75	0.018	0.660	0.795

(e) $M_\infty = 0.802, \alpha = -0.10°, Re_{c,\infty} = 8.3\times10^6$.

Figure 15.– Continued.

NACA 0012 AIRFOIL

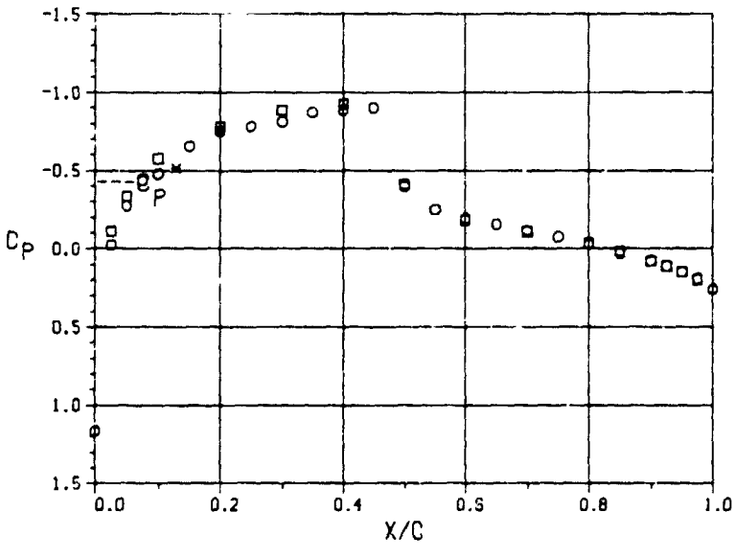

o - AIRFOIL UPPER SURFACE

X/C	C_P	P/PT	M
0.000	1.163	0.998	0.060
0.025	-0.026	0.647	0.814
0.050	-0.277	0.572	0.929
0.075	-0.435	0.526	1.004
0.100	-0.479	0.513	1.025
0.150	-0.655	0.461	1.113
0.200	-0.752	0.432	1.163
0.250	-0.783	0.423	1.180
0.300	-0.814	0.414	1.197
0.350	-0.873	0.397	1.229
0.400	-0.886	0.393	1.237
0.450	-0.900	0.389	1.244
0.500	-0.401	0.536	0.987
0.550	-0.251	0.580	0.917
0.600	-0.191	0.598	0.889
0.650	-0.156	0.608	0.873
0.700	-0.118	0.620	0.856
0.750	-0.076	0.632	0.837
0.800	-0.030	0.645	0.816
0.850	0.028	0.663	0.790
0.900	0.075	0.677	0.768
0.925	0.109	0.687	0.753
0.950	0.147	0.698	0.736
0.975	0.190	0.710	0.716
1.000	0.257	0.730	0.685

□ - AIRFOIL LOWER SURFACE

X/C	C_P	P/PT	M
0.025	-0.112	0.621	0.854
0.050	-0.336	0.555	0.957
0.100	-0.578	0.484	1.074
0.200	-0.783	0.423	1.181
0.300	-0.885	0.393	1.236
0.400	-0.925	0.381	1.260
0.500	-0.413	0.533	0.993
0.600	-0.184	0.600	0.887
0.700	-0.111	0.622	0.853
0.800	-0.035	0.644	0.819
0.850	0.014	0.658	0.796
0.900	0.079	0.677	0.767
0.925	0.110	0.687	0.753
0.950	0.148	0.698	0.736
0.975	0.196	0.712	0.714

SIDEWALL, Z/C= 1.375

$\bar{X}$/C	C_P	P/PT	M
-3.75	0.037	0.665	0.786
-2.50	-0.007	0.652	0.806
-2.00	0.006	0.656	0.800
-1.50	0.022	0.661	0.793
-1.00	-0.022	0.648	0.813
-0.50	-0.073	0.633	0.826
0.00	-0.021	0.648	0.812
0.50	-0.041	0.642	0.821
1.00	-0.011	0.651	0.808
1.50	-0.003	0.653	0.804
2.00	-0.003	0.653	0.804
2.50	-0.006	0.652	0.806
3.75	0.020	0.660	0.794

SIDEWALL, Z/C= 0

$\bar{X}$/C	C_P	P/PT	M
-3.75	0.048	0.668	0.781
-3.00	0.004	0.656	0.801
-1.25	0.057	0.671	0.777
1.25	0.027	0.662	0.790
3.75	0.011	0.658	0.798

SIDEWALL, Z/C= -1.375

$\bar{X}$/C	C_P	P/PT	M
-3.75	0.033	0.664	0.788
-1.00	-0.020	0.648	0.812
-0.50	-0.019	0.649	0.811
0.00	-0.080	0.631	0.839
0.50	-0.006	0.652	0.805
1.00	-0.027	0.646	0.815
1.50	-0.010	0.651	0.807
2.00	-0.009	0.652	0.807
2.50	-0.004	0.653	0.805
3.75	0.014	0.658	0.797

(l) $M_\infty = 0.803$, $\alpha = -0.10°$, $Re_{c,\infty} = 10.0 \times 10^6$.

Figure 15.– Continued.

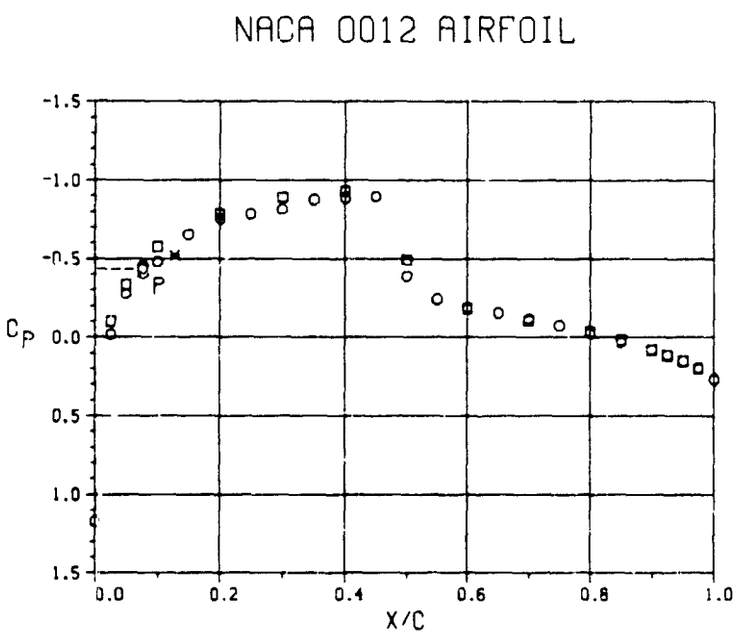

o - AIRFOIL UPPER SURFACE

X/C	C_P	P/PT	M
0.000	1.171	1.000	0.004
0.025	-0.020	0.649	0.811
0.050	-0.278	0.573	0.928
0.075	-0.436	0.527	1.003
0.100	-0.481	0.514	1.024
0.150	-0.656	0.462	1.111
0.200	-0.754	0.433	1.162
0.250	-0.784	0.424	1.178
0.300	-0.816	0.415	1.195
0.350	-0.877	0.397	1.229
0.400	-0.889	0.393	1.236
0.450	-0.897	0.391	1.240
0.500	-0.391	0.540	0.981
0.550	-0.242	0.584	0.912
0.600	-0.186	0.600	0.886
0.650	-0.155	0.609	0.872
0.700	-0.117	0.621	0.854
0.750	-0.075	0.633	0.835
0.800	-0.028	0.647	0.814
0.850	0.031	0.664	0.787
0.900	0.078	0.678	0.766
0.925	0.112	0.688	0.751
0.950	0.150	0.699	0.733
0.975	0.194	0.712	0.713
1.000	0.265	0.733	0.681

□ - AIRFOIL LOWER SURFACE

X/C	C_P	P/PT	M
0.025	-0.103	0.625	0.848
0.050	-0.334	0.557	0.954
0.100	-0.578	0.485	1.072
0.200	-0.786	0.424	1.179
0.300	-0.891	0.393	1.237
0.400	-0.933	0.380	1.261
0.500	-0.494	0.510	1.031
0.600	-0.184	0.601	0.885
0.700	-0.105	0.624	0.849
0.800	-0.034	0.645	0.817
0.850	0.017	0.660	0.794
0.900	0.080	0.679	0.765
0.925	0.115	0.689	0.750
0.950	0.150	0.699	0.733
0.975	0.200	0.714	0.711

SIDEWALL, Z=0

$\bar{X}$/C	C_P	P/PT	M
-3.75	0.050	0.670	0.779
-3.00	0.004	0.656	0.800
-1.25	0.062	0.673	0.774
1.25	0.031	0.664	0.788
3.75	0.013	0.659	0.795

SIDEWALL, Z/C= 1.375

$\bar{X}$/C	C_P	P/PT	M
-3.75	0.033	0.666	0.784
-2.50	-0.007	0.653	0.804
-2.00	0.006	0.657	0.799
-1.50	0.022	0.662	0.791
-1.00	-0.021	0.649	0.811
-0.50	-0.073	0.634	0.834
0.00	-0.014	0.651	0.808
0.50	-0.038	0.644	0.819
1.00	-0.009	0.652	0.805
1.50	-0.001	0.655	0.802
2.00	-0.002	0.654	0.802
2.50	-0.006	0.653	0.804
3.75	0.022	0.661	0.792

SIDEWALL, Z/C=-1.375

$\bar{X}$/C	C_P	P/PT	M
-3.75	0.035	0.665	0.786
-1.00	-0.021	0.649	0.811
-0.50	-0.020	0.649	0.810
0.00	-0.083	0.631	0.839
0.50	-0.005	0.654	0.804
1.00	-0.027	0.647	0.814
1.50	-0.008	0.653	0.805
2.00	-0.011	0.652	0.806
2.50	-0.004	0.654	0.803
3.75	0.017	0.660	0.794

(g) $M_\infty = 0.801$, $\alpha = -0.08°$, $Re_{c,\infty} = 12.1 \times 10^6$.

Figure 15.– Concluded.

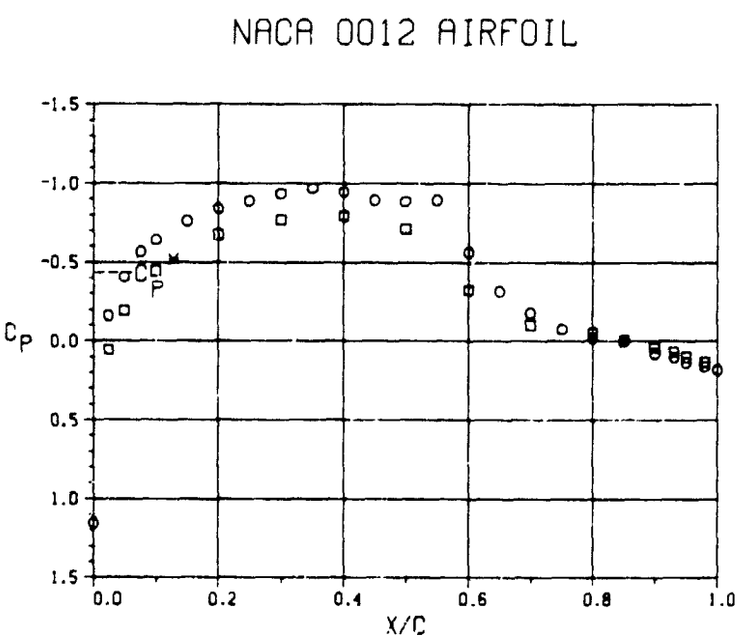

o - AIRFOIL UPPER SURFACE

X/C	C_P	P/PT	M
0.000	1.155	0.995	0.083
0.025	-0.162	0.608	0.875
0.050	-0.407	0.535	0.989
0.075	-0.565	0.489	1.065
0.100	-0.642	0.466	1.104
0.150	-0.762	0.431	1.166
0.200	-0.841	0.408	1.209
0.250	-0.888	0.394	1.235
0.300	-0.937	0.379	1.263
0.350	-0.971	0.369	1.283
0.400	-0.950	0.376	1.271
0.450	-0.895	0.392	1.239
0.500	-0.886	0.394	1.234
0.550	-0.893	0.392	1.238
0.600	-0.565	0.489	1.065
0.650	-0.316	0.562	0.946
0.700	-0.178	0.603	0.882
0.750	-0.076	0.633	0.836
0.800	-0.020	0.649	0.810
0.850	0.003	0.656	0.800
0.900	0.076	0.678	0.767
0.930	0.100	0.685	0.756
0.950	0.132	0.694	0.741
0.980	0.159	0.702	0.729
1.000	0.179	0.708	0.720

□ - AIRFOIL LOWER SURFACE

X/C	C_P	P/PT	M
0.025	0.054	0.672	0.776
0.050	-0.195	0.598	0.890
0.100	-0.443	0.525	1.006
0.200	-0.675	0.458	1.118
0.300	-0.770	0.428	1.170
0.400	-0.793	0.423	1.180
0.500	-0.714	0.445	1.141
0.600	-0.325	0.561	0.948
0.700	-0.103	0.625	0.848
0.800	-0.053	0.641	0.824
0.850	-0.010	0.652	0.806
0.900	0.037	0.667	0.783
0.930	0.065	0.674	0.772
0.950	0.099	0.685	0.755
0.980	0.128	0.693	0.743

SIDEWALL, Z = 0

$\bar{X}$/C	C_P	P/PT	M
-3.75	0.054	0.672	0.776
-3.00	-0.020	0.649	0.810
-1.25	0.053	0.672	0.776
1.25	0.010	0.659	0.796
3.75	-0.001	0.655	0.801

SIDEWALL, Z/C = 1.375

$\bar{X}$/C	C_P	P/PT	M
-3.75	0.061	0.674	0.772
-2.50	0.012	0.660	0.794
-2.00	0.020	0.662	0.790
-1.50	0.024	0.663	0.789
-1.00	-0.014	0.652	0.806
-0.50	-0.092	0.629	0.841
0.00	-0.093	0.629	0.842
0.50	-0.088	0.630	0.839
1.00	-0.050	0.642	0.822
1.50	-0.031	0.647	0.813
2.00	-0.019	0.651	0.808
2.50	-0.020	0.651	0.808
3.75	-0.004	0.655	0.801

SIDEWALL, Z/C = -1.375

$\bar{X}$/C	C_P	P/PT	M
-3.75	0.041	0.668	0.781
-1.00	-0.028	0.648	0.812
-0.50	-0.032	0.647	0.814
0.00	-0.111	0.624	0.850
0.50	-0.026	0.649	0.811
1.00	-0.045	0.643	0.820
1.50	-0.021	0.650	0.809
2.00	-0.020	0.650	0.809
2.50	-0.011	0.653	0.804
3.75	-0.006	0.655	0.802

(a) $M_\infty = 0.801$, $\alpha = 0.95°$, $Re_{c,\infty} = 1.0 \times 10^6$.

Figure 16.– Airfoil and test channel sidewall pressure measurements, Data Set 4 ($M_N = 0.80$, $\alpha_N = 1°$).

NACA 0012 AIRFOIL

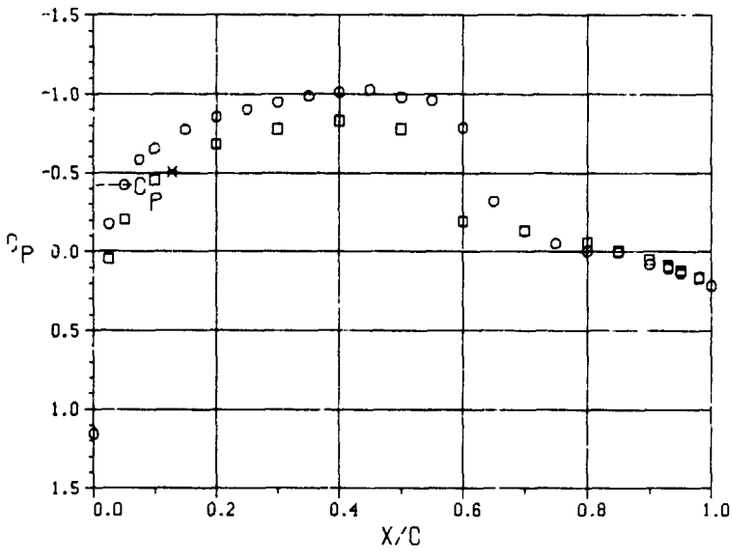

o - AIRFOIL UPPER SURFACE

X/C	C_P	P/PT	M
0.000	1.154	0.995	0.088
0.025	-0.177	0.600	0.886
0.050	-0.423	0.527	1.002
0.075	-0.587	0.479	1.083
0.100	-0.655	0.459	1.117
0.150	-0.774	0.423	1.180
0.200	-0.856	0.399	1.225
0.250	-0.904	0.385	1.253
0.300	-0.951	0.371	1.280
0.350	-0.989	0.360	1.303
0.400	-1.012	0.353	1.317
0.450	-1.026	0.349	1.325
0.500	-0.980	0.362	1.297
0.550	-0.961	0.368	1.285
0.600	-0.788	0.419	1.187
0.650	-0.321	0.557	0.953
0.700	-0.134	0.613	0.866
0.750	-0.053	0.637	0.830
0.800	-0.006	0.651	0.808
0.850	0.002	0.653	0.804
0.900	0.078	0.676	0.770
0.930	0.104	0.683	0.758
0.950	0.134	0.692	0.744
0.980	0.168	0.702	0.729
1.000	0.214	0.716	0.708

□ - AIRFOIL LOWER SURFACE

X/C	C_P	P/PT	M
0.025	0.044	0.666	0.784
0.050	-0.205	0.592	0.899
0.100	-0.457	0.517	1.018
0.200	-0.683	0.451	1.130
0.300	-0.780	0.422	1.183
0.400	-0.830	0.408	1.209
0.500	-0.778	0.422	1.182
0.600	-0.192	0.596	0.892
0.700	-0.135	0.612	0.867
0.800	-0.060	0.636	0.832
0.850	-0.007	0.651	0.808
0.900	0.050	0.668	0.782
0.930	0.086	0.678	0.766
0.950	0.120	0.689	0.750
0.980	0.162	0.700	0.732

SIDEWALL, Z = 0

$\bar{X}$/C	C_P	P/PT	M
-3.75	0.049	0.667	0.782
-3.00	-0.002	0.652	0.806
-1.25	0.045	0.666	0.784
1.25	0.009	0.656	0.800
3.75	-0.009	0.650	0.809

SIDEWALL, Z/C = 1.375

$\bar{X}$/C	C_P	P/PT	M
-3.75	0.048	0.667	0.783
-2.50	0.002	0.654	0.803
-2.00	0.010	0.656	0.800
-1.50	0.010	0.656	0.799
-1.00	-0.030	0.644	0.818
-0.50	-0.106	0.622	0.852
0.00	-0.105	0.622	0.852
0.50	-0.107	0.622	0.853
1.00	-0.061	0.635	0.832
1.50	-0.038	0.642	0.821
2.00	-0.025	0.646	0.816
2.50	-0.028	0.645	0.817
3.75	-0.005	0.652	0.806

SIDEWALL, Z/C = -1.375

$\bar{X}$/C	C_P	P/PT	M
-3.75	0.034	0.663	0.789
-1.00	-0.034	0.643	0.820
-0.50	-0.042	0.641	0.823
0.00	-0.108	0.621	0.853
0.50	-0.031	0.644	0.818
1.00	-0.044	0.640	0.824
1.50	-0.027	0.645	0.816
2.00	-0.023	0.647	0.815
2.50	-0.014	0.649	0.810
3.75	-0.004	0.652	0.806

(b) $M_\infty = 0.805$, $\alpha = 0.97°$, $Re_{c,\infty} = 2.0 \times 10^6$.

Figure 16.– Continued.

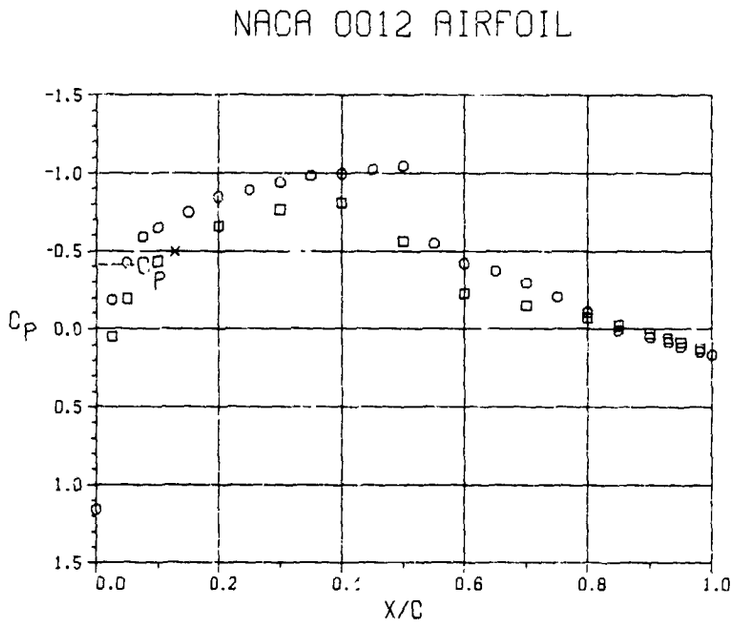

o - AIRFOIL UPPER SURFACE

X/C	C_p	P/PT	M
0.000	1.156	0.995	0.088
0.025	-0.186	0.595	0.894
0.050	-0.427	0.524	1.008
0.075	-0.592	0.474	1.089
0.100	-0.650	0.457	1.119
0.150	-0.749	0.428	1.172
0.200	-0.849	0.398	1.227
0.250	-0.891	0.385	1.251
0.300	-0.942	0.370	1.281
0.350	-0.983	0.358	1.306
0.400	-0.999	0.353	1.316
0.450	-1.024	0.346	1.331
0.500	-1.045	0.339	1.345
0.550	-0.549	0.487	1.068
0.600	-0.422	0.525	1.005
0.650	-0.372	0.540	0.981
0.700	-0.297	0.562	0.946
0.750	-0.207	0.589	0.903
0.800	-0.110	0.618	0.859
0.850	0.010	0.654	0.804
0.900	0.052	0.666	0.785
0.930	0.084	0.675	0.770
0.950	0.114	0.684	0.756
0.980	0.144	0.693	0.743
1.000	0.164	0.699	0.734

□ - AIRFOIL LOWER SURFACE

X/C	C_p	P/PT	M
0.025	0.050	0.666	0.785
0.050	-0.195	0.592	0.898
0.100	-0.433	0.522	1.011
0.200	-0.662	0.454	1.125
0.300	-0.707	0.422	1.182
0.400	-0.812	0.409	1.206
0.500	-0.564	0.483	1.076
0.600	-0.226	0.584	0.912
0.700	-0.152	0.605	0.878
0.800	-0.071	0.630	0.840
0.850	-0.023	0.644	0.819
0.900	0.029	0 660	0.794
0.930	0.059	0.668	0.781
0.950	0.084	0.676	0.769
0.980	0.124	0.688	0.751

SIDEWALL, Z=0

$\bar{X}$/C	C_p	P/PT	M
-3.75	0.052	0.666	0.784
-3.00	0.010	0.654	0.804
-1.25	0.049	0.666	0.785
1.25	0.018	0.656	0.800
3.75	0.001	0.651	0.807

SIDEWALL, Z/C= 1.375

$\bar{X}$/C	C_p	P/PT	M
-3.75	0.036	0.662	0.791
-2.50	-0.001	0.651	0.808
-2.00	0.007	0.653	0.805
-1.50	0.014	0.655	0.801
-1.00	-0.029	0.643	0.821
-0.50	-0.105	0.620	0.856
0.00	-0.092	0.624	0.850
0.50	-0.102	0.621	0.854
1.00	-0.047	0.637	0.829
1.50	-0.031	0.642	0.822
2.00	-0.016	0.646	0.815
2.50	-0.019	0.645	0.816
3.75	0.008	0.653	0.805

SIDEWALL, Z/C=-1.375

$\bar{X}$/C	C_p	P/PT	M
-3.75	0.033	0.661	0.793
-1.00	-0.028	0.643	0.820
-0.50	-0.030	0.642	0.821
0.00	-0.094	0.623	0.851
0.50	-0.019	0.645	0.816
1.00	-0.035	0.641	0.823
1.50	-0.018	0.646	0.816
2.00	-0.019	0.645	0.816
2.50	-0.008	0.649	0.811
3.75	0.009	0.654	0.804

(c) $M_\infty = 0.808$, $\alpha = 0.97°$, $Re_{c,\infty} = 4.1 \times 10^6$.

Figure 16.– Continued.

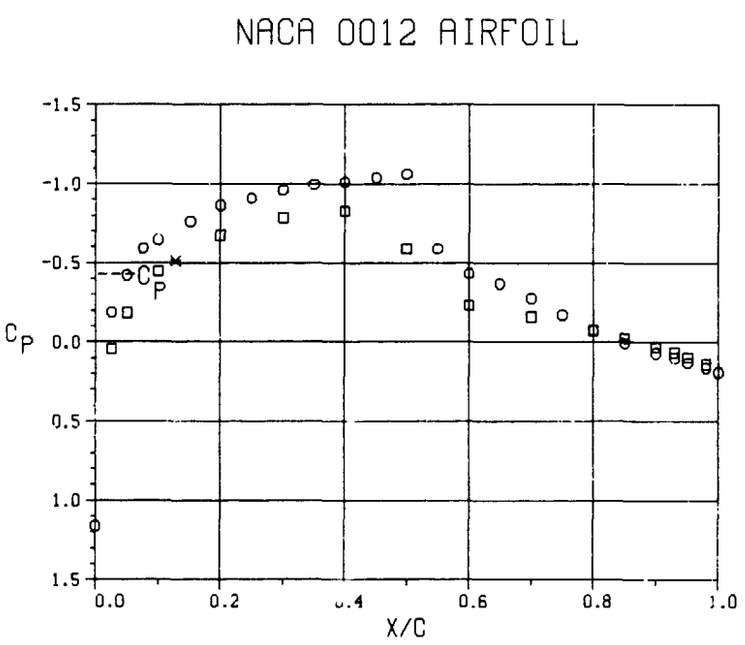

□ - AIRFOIL LOWER SURFACE

X/C	C_P	P/PT	M
0.025	0.043	0.666	0.784
0.050	-0.186	0.599	0.888
0.100	-0.446	0.522	1.011
0.200	-0.676	0.454	1.125
0.300	-0.784	0.422	1.183
0.400	-0.827	0.409	1.206
0.500	-0.591	0.479	1.082
0.600	-0.234	0.584	0.911
0.700	-0.162	0.606	0.878
0.800	-0.075	0.631	0.838
0.850	-0.025	0.646	0.815
0.900	0.033	0.663	0.789
0.930	0.063	0.672	0.775
0.950	0.095	0.682	0.761
0.980	0.138	0.695	0.741

SIDEWALL, Z=0

$\bar{X}$/C	C_P	P/PT	M
-3.75	0.044	0.667	0.784
-3.00	0.004	0.655	0.802
-1.25	0.046	0.667	0.783
1.25	0.015	0.658	0.797
3.75	-0.002	0.653	0.805

○ - AIRFOIL UPPER SURFACE

X/C	C_P	P/PT	M
0.000	1.160	0.996	0.073
0.025	-0.189	0.598	0.890
0.050	-0.421	0.529	0.999
0.075	-0.593	0.478	1.083
0.100	0.647	0.462	1.110
0.150	-0.762	0.428	1.171
0.200	-0.866	0.398	1.228
0.250	-0.907	0.385	1.251
0.300	-0.960	0.370	1.282
0.350	-0.996	0.359	1.304
0.400	-1.013	0.354	1.314
0.450	-1.039	0.347	1.330
0.500	-1.063	0.339	1.345
0.550	-0.590	0.479	1.081
0.600	-0.434	0.525	1.005
0.650	-0.369	0.545	0.974
0.700	-0.277	0.572	0.931
0.750	-0.173	0.602	0.883
0.800	-0.074	0.632	0.837
0.850	0.008	0.656	0.800
0.900	0.069	0.674	0.772
0.930	0.099	0.683	0.759
0.950	0.129	0.692	0.745
0.980	0.160	0.701	0.731
1.000	0.191	0.710	0.717

SIDEWALL, Z/C= 1.375

$\bar{X}$/C	C_P	P/PT	M
-3.75	0.030	0.662	0.790
-2.50	-0.010	0.650	0.809
-2.00	-0.003	0.653	0.805
-1.50	0.010	0.657	0.799
-1.00	-0.033	0.644	0.819
-0.50	-0.110	0.621	0.854
0.00	-0.089	0.627	0.844
0.50	-0.104	0.623	0.851
1.00	-0.052	0.638	0.828
1.50	-0.031	0.644	0.818
2.00	-0.020	0.647	0.813
2.50	-0.022	0.647	0.814
3.75	0.004	0.655	0.802

SIDEWALL, Z/C=-1.375

$\bar{X}$/C	C_P	P/PT	M
-3.75	0.026	0.661	0.792
-1.00	-0.035	0.643	0.820
-0.50	-0.036	0.643	0.820
0.00	-0.103	0.623	0.851
0.50	-0.025	0.646	0.815
1.00	-0.044	0.641	0.824
1.50	-0.024	0.646	0.815
2.00	-0.024	0.646	0.815
2.50	-0.011	0.650	0.809
3.75	0.004	0.655	0.802

(d) $M_\infty = 0.804$, $\alpha = 0.96°$, $Re_{c,\infty} = 6.1 \times 10^6$.

Figure 16.– Continued.

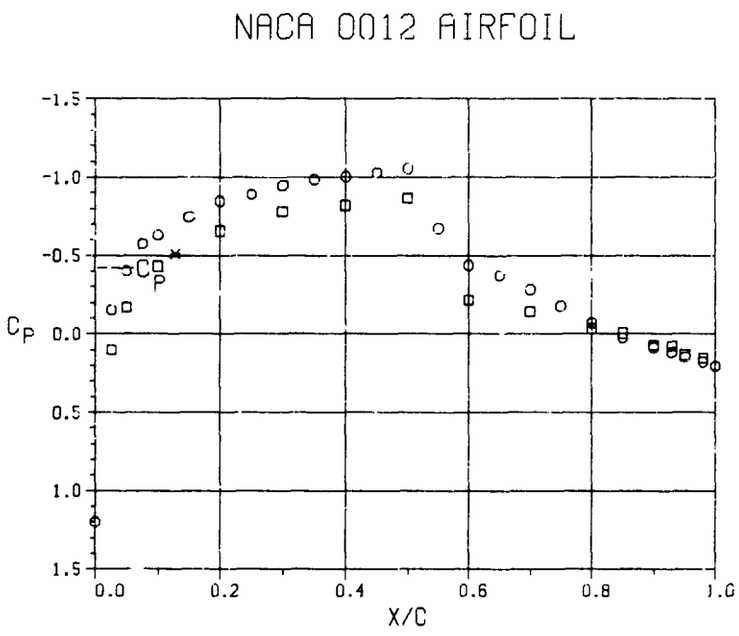

o - AIRFOIL UPPER SURFACE

X/C	C_P	P/PT	M
0.000	1.198	1.000	0.000
0.025	-0.154	0.607	0.875
0.050	-0.403	0.534	0.991
0.075	-0.575	0.483	1.075
0.100	-0.631	0.466	1.103
0.150	-0.747	0.432	1.164
0.200	-0.849	0.402	1.220
0.250	-0.890	0.390	1.243
0.300	-0.949	0.372	1.277
0.350	-0.986	0.361	1.299
0.400	-1.004	0.356	1.310
0.450	-1.030	0.348	1.326
0.500	-1.056	0.340	1.343
0.550	-0.675	0.453	1.126
0.600	-0.437	0.524	1.008
0.650	-0.372	0.543	0.976
0.700	-0.282	0.569	0.934
0.750	-0.178	0.600	0.886
0.800	-0.074	0.631	0.838
0.850	0.025	0.661	0.793
0.900	0.086	0.679	0.765
0.930	0.118	0.688	0.751
0.950	0.148	0.697	0.737
0.980	0.178	0.706	0.724
1.000	0.204	0.713	0.712

□ - AIRFOIL LOWER SURFACE

X/C	C_P	P/PT	M
0.025	0.101	0.684	0.758
0.050	-0.169	0.603	0.882
0.100	-0.432	0.525	1.005
0.200	-0.657	0.460	1.115
0.300	-0.783	0.421	1.183
0.400	-0.819	0.412	1.201
0.500	-0.869	0.396	1.231
0.600	-0.216	0.590	0.902
0.700	-0.140	0.612	0.868
0.800	-0.034	0.644	0.819
0.850	-0.007	0.651	0.808
0.900	0.072	0.675	0.771
0.930	0.077	0.676	0.770
0.950	0.132	0.693	0.744
0.980	0.152	0.698	0.736

SIDEWALL, Z=0

$\bar{X}$/C	C_P	P/PT	M
-3.75	0.087	0.679	0.764
-3.00	0.025	0.661	0.793
-1.25	0.087	0.679	0.764
1.25	0.054	0.670	0.779
3.75	0.037	0.664	0.787

SIDEWALL, Z/C= 1.375

$\bar{X}$/C	C_P	P/PT	M
-3.75	0.082	0.678	0.766
-2.50	0.042	0.666	0.784
-2.00	0.050	0.669	0.781
-1.50	0.060	0.672	0.776
-1.00	0.016	0.659	0.796
-0.50	-0.064	0.635	0.832
0.00	-0.043	0.641	0.823
0.50	-0.059	0.637	0.830
1.00	-0.004	0.653	0.805
1.50	0.020	0.660	0.794
2.00	0.028	0.662	0.790
2.50	0.025	0.661	0.792
3.75	0.053	0.670	0.779

SIDEWALL, Z/C=-1.375

$\bar{X}$/C	C_P	P/PT	M
-3.75	0.076	0.676	0.769
-1.00	0.017	0.659	0.795
-0.50	0.010	0.657	0.798
0.00	-0.067	0.634	0.833
0.50	0.028	0.662	0.790
1.00	0.006	0.656	0.800
1.50	0.027	0.662	0.791
2.00	0.022	0.661	0.793
2.50	0.041	0.666	0.784
3.75	0.058	0.671	0.777

(e) $M_\infty = 0.805, \alpha = 1.00°, Re_{c,\infty} = 8.3 \times 10^6$.

Figure 16.– Continued.

NACA 0012 AIRFOIL

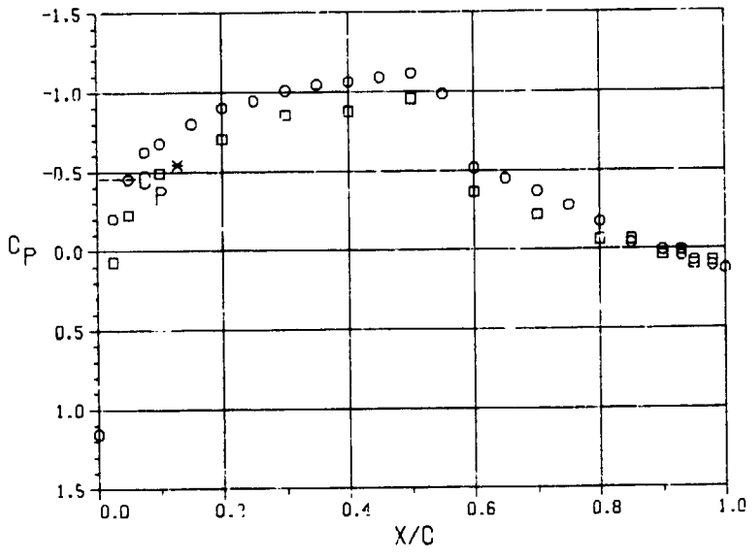

o - AIRFOIL UPPER SURFACE

X/C	C_P	P/PT	M
0.000	1.154	0.996	0.074
0.025	-0.203	0.601	0.884
0.050	-0.454	0.528	1.000
0.075	-0.626	0.478	1.083
0.100	-0.681	0.462	1.110
0.150	-0.802	0.427	1.173
0.200	-0.904	0.398	1.228
0.250	-0.947	0.385	1.252
0.300	-1.009	0.367	1.288
0.350	-1.046	0.356	1.310
0.400	-1.064	0.351	1.320
0.450	-1.091	0.343	1.337
0.500	-1.117	0.335	1.353
0.550	-0.988	0.373	1.275
0.600	-0.519	0.510	1.031
0.650	-0.450	0.529	0.998
0.700	-0.370	0.553	0.961
0.750	-0.279	0.579	0.919
0.800	-0.177	0.609	0.872
0.850	-0.041	0.649	0.811
0.900	0.005	0.662	0.791
0.930	0.042	0.673	0.775
0.950	0.072	0.681	0.761
0.980	0.104	0.691	0.747
1.000	0.125	0.697	0.737

□ - AIRFOIL LOWER SURFACE

X/C	C_P	P/PT	M
0.025	0.068	0.680	0.763
0.050	-0.229	0.594	0.896
0.100	-0.493	0.517	1.018
0.200	-0.707	0.454	1.125
0.300	-0.858	0.411	1.203
0.400	-0.876	0.405	1.214
0.500	-0.957	0.382	1.258
0.600	-0.367	0.553	0.960
0.700	-0.222	0.596	0.893
0.800	-0.063	0.642	0.822
0.850	-0.063	0.642	0.821
0.900	0.038	0.671	0.777
0.930	0.010	0.663	0.789
0.950	0.096	0.688	0.751
0.980	0.075	0.682	0.759

SIDEWALL, Z=0

$\bar{X}$/C	C_P	P/PT	M
-3.75	0.038	0.671	0.777
-3.00	-0.122	0.625	0.848
-1.25	0.041	0.672	0.776
1.25	0.002	0.661	0.793
3.75	-0.016	0.655	0.801

SIDEWALL, Z/C= 1.375

$\bar{X}$/C	C_P	P/PT	M
-3.75	0.045	0.673	0.774
-2.50	0.005	0.661	0.792
-2.00	0.013	0.664	0.788
-1.50	0.025	0.667	0.783
-1.00	-0.022	0.653	0.804
-0.50	-0.103	0.630	0.840
0.00	-0.090	0.634	0.835
0.50	-0.101	0.630	0.839
1.00	-0.045	0.647	0.814
1.50	-0.023	0.653	0.805
2.00	-0.013	0.656	0.800
2.50	-0.016	0.655	0.801
3.75	0.013	0.663	0.789

SIDEWALL, Z/C=-1.375

$\bar{X}$/C	C_P	P/PT	M
-3.75	0.036	0.670	0.778
-1.00	-0.022	0.653	0.804
-0.50	-0.031	0.651	0.808
0.00	-0.119	0.625	0.848
0.50	-0.013	0.656	0.800
1.00	-0.032	0.650	0.809
1.50	-0.013	0.656	0.800
2.00	-0.018	0.654	0.802
2.50	0.001	0.660	0.794
3.75	0.019	0.665	0.786

(f) $M_\infty = 0.793$, $\alpha = 1.00°$, $Re_{c,\infty} = 10.3 \times 10^6$.

Figure 16.– Concluded.

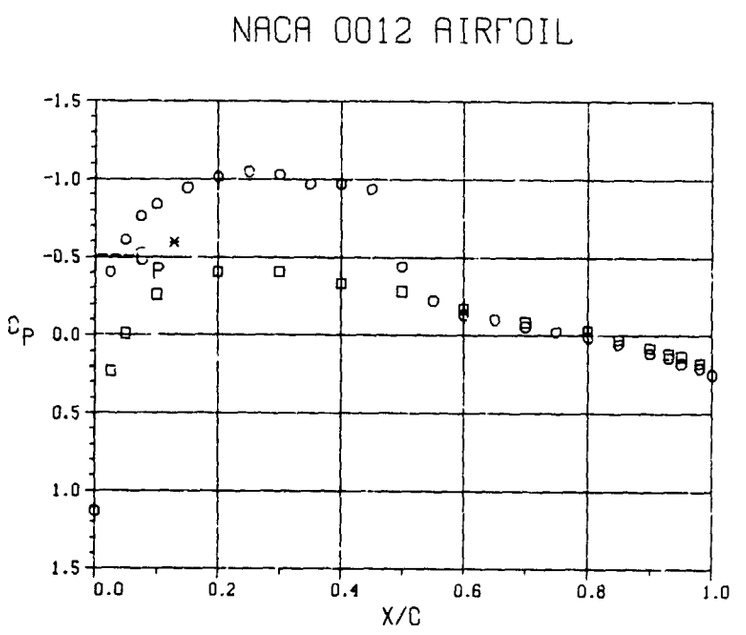

o - AIRFOIL UPPER SURFACE

X/C	C_P	P/PT	M
0.000	1.128	0.991	0.115
0.025	-0.405	0.556	0.956
0.050	-0.613	0.497	1.052
0.075	-0.763	0.454	1.124
0.100	-0.838	0.433	1.162
0.150	-0.947	0.402	1.219
0.200	-1.014	0.383	1.256
0.250	-1.050	0.373	1.276
0.300	-1.031	0.378	1.266
0.350	-0.971	0.395	1.232
0.400	-0.972	0.395	1.233
0.450	-0.938	0.404	1.215
0.500	-0.443	0.545	0.973
0.550	-0.226	0.607	0.876
0.600	-0.132	0.633	0.835
0.650	-0.105	0.641	0.823
0.700	-0.058	0.654	0.803
0.750	-0.027	0.663	0.789
0.800	0.012	0.674	0.772
0.850	0.054	0.686	0.754
0.900	0.113	0.703	0.728
0.930	0.141	0.711	0.716
0.950	0.180	0.722	0.699
0.980	0.208	0.730	0.686
1.000	0.248	0.741	0.668

□ - AIRFOIL LOWER SURFACE

X/C	C_P	P/PT	M
0.025	0.230	0.737	0.675
0.050	-0.012	0.667	0.783
0.100	-0.259	0.597	0.891
0.200	-0.406	0.557	0.953
0.300	-0.407	0.555	0.957
0.400	-0.330	0.579	0.920
0.500	-0.283	0.590	0.901
0.600	-0.172	0.623	0.850
0.700	-0.087	0.646	0.816
0.800	-0.030	0.664	0.788
0.850	0.025	0.678	0.767
0.900	0.076	0.694	0.742
0.930	0.115	0.703	0.727
0.950	0.132	0.709	0.718
0.980	0.177	0.721	0.700

SIDEWALL, Z/C= 1.375

$\bar{X}$/C	C_P	P/PT	M
-3.75	0.084	0.696	0.738
-2.50	0.046	0.685	0.755
-2.00	0.049	0.686	0.754
-1.50	0.043	0.684	0.756
-1.00	0.008	0.675	0.772
-0.50	-0.058	0.656	0.800
0.00	-0.047	0.659	0.796
0.50	-0.037	0.662	0.791
1.00	-0.020	0.666	0.784
1.50	0.008	0.674	0.772
2.00	0.019	0.678	0.767
2.50	0.017	0.677	0.768
3.75	0.036	0.683	0.759

SIDEWALL, Z=0

$\bar{X}$/C	C_P	P/PT	M
-3.75	0.087	0.696	0.738
-3.00	0.031	0.680	0.764
-1.25	0.086	0.696	0.739
1.25	0.069	0.691	0.746
3.75	0.043	0.684	0.757

SIDEWALL, Z/C=-1.375

$\bar{X}$/C	C_P	P/PT	M
-3.75	0.081	0.695	0.740
-1.00	0.029	0.680	0.763
-0.50	0.032	0.681	0.761
0.00	0.010	0.675	0.771
0.50	0.030	0.681	0.762
1.00	0.021	0.678	0.766
1.50	0.025	0.679	0.764
2.00	0.028	0.680	0.763
2.50	0.044	0.685	0.756
3.75	0.037	0.683	0.759

(a) $M_\infty = 0.775$, $\alpha = 2.03°$, $Re_{c,\infty} = 1.0 \times 10^6$.

Figure 17.– Airfoil and test channel sidewall pressure measurements, Data Set 5 ($M_N = 0.775$, $\alpha_N = 2°$).

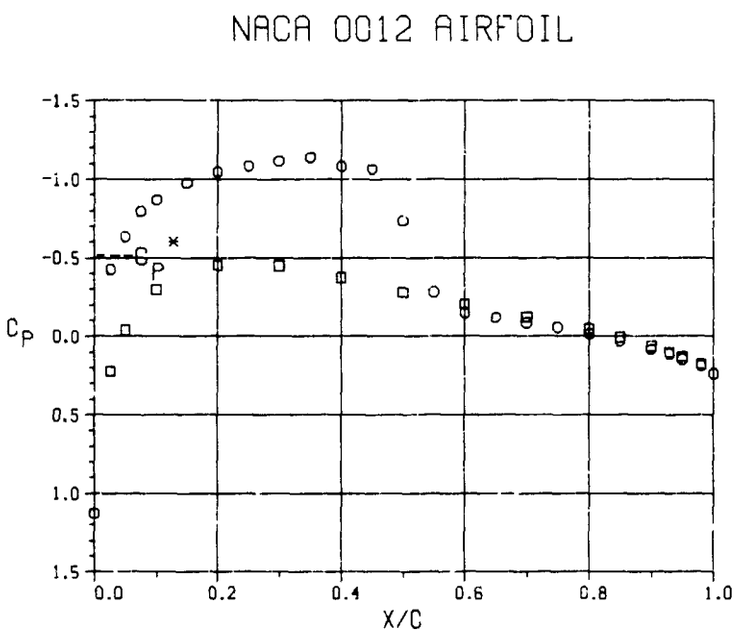

o - AIRFOIL UPPER SURFACE

X/C	C_P	P/PT	M
0.000	1.127	0.991	0.114
0.025	-0.428	0.551	0.964
0.050	-0.634	0.492	1.059
0.075	-0.795	0.447	1.137
0.100	-0.869	0.426	1.175
0.150	-0.977	0.395	1.232
0.200	-1.047	0.376	1.271
0.250	-1.085	0.365	1.292
0.300	-1.118	0.356	1.311
0.350	-1.140	0.349	1.324
0.400	-1.084	0.365	1.291
0.450	-1.066	0.370	1.281
0.500	-0.734	0.464	1.107
0.550	-0.282	0.592	0.899
0.600	-0.149	0.630	0.840
0.650	-0.118	0.638	0.827
0.700	-0.085	0.648	0.813
0.750	-0.057	0.656	0.800
0.800	-0.015	0.668	0.782
0.850	0.030	0.680	0.763
0.900	0.082	0.695	0.740
0.930	0.110	0.703	0.728
0.950	0.145	0.713	0.712
0.980	0.184	0.724	0.695
1.000	0.235	0.738	0.673

□ - AIRFOIL LOWER SURFACE

X/C	C_P	P/PT	M
0.025	0.221	0.735	0.678
0.050	-0.040	0.661	0.793
0.100	-0.296	0.588	0.905
0.200	-0.453	0.545	0.974
0.300	-0.449	0.545	0.973
0.400	-0.375	0.567	0.939
0.500	-0.278	0.593	0.897
0.600	-0.205	0.615	0.864
0.700	-0.126	0.636	0.830
0.800	-0.046	0.659	0.795
0.850	0.007	0.674	0.773
0.900	0.063	0.690	0.748
0.930	0.100	0.700	0.732
0.950	0.131	0.710	0.718
0.980	0.176	0.722	0.699

SIDEWALL, Z/C= 1.375

$\bar{X}$/C	C_P	P/PT	M
-3.75	0.070	0.692	0.744
-2.50	0.026	0.680	0.763
-2.00	0.025	0.680	0.764
-1.50	0.022	0.679	0.765
-1.00	-0.018	0.667	0.783
-0.50	-0.087	0.648	0.812
0.00	-0.076	0.651	0.808
0.50	-0.066	0.654	0.803
1.00	-0.034	0.663	0.789
1.50	-0.012	0.669	0.780
2.00	0.006	0.674	0.772
2.50	0.005	0.674	0.773
3.75	0.028	0.681	0.762

SIDEWALL, Z/C= 0

$\bar{X}$/C	C_P	P/PT	M
-3.75	0.082	0.695	0.739
-3.00	0.017	0.677	0.768
-1.25	0.068	0.692	0.745
1.25	0.046	0.685	0.755
3.75	0.025	0.679	0.764

SIDEWALL, Z/C= -1.375

$\bar{X}$/C	C_P	P/PT	M
-3.75	0.071	0.693	0.744
-1.00	0.006	0.674	0.772
-0.50	0.015	0.677	0.768
0.00	-0.007	0.671	0.778
0.50	0.011	0.676	0.770
1.00	-0.005	0.671	0.777
1.50	0.017	0.677	0.767
2.00	0.018	0.678	0.767
2.50	0.024	0.679	0.764
3.75	0.035	0.682	0.759

(b) $M_\infty = 0.774, \alpha = 2.03^\circ, Re_{c,\infty} = 1.9 \times 10^6$.

Figure 17.– Continued.

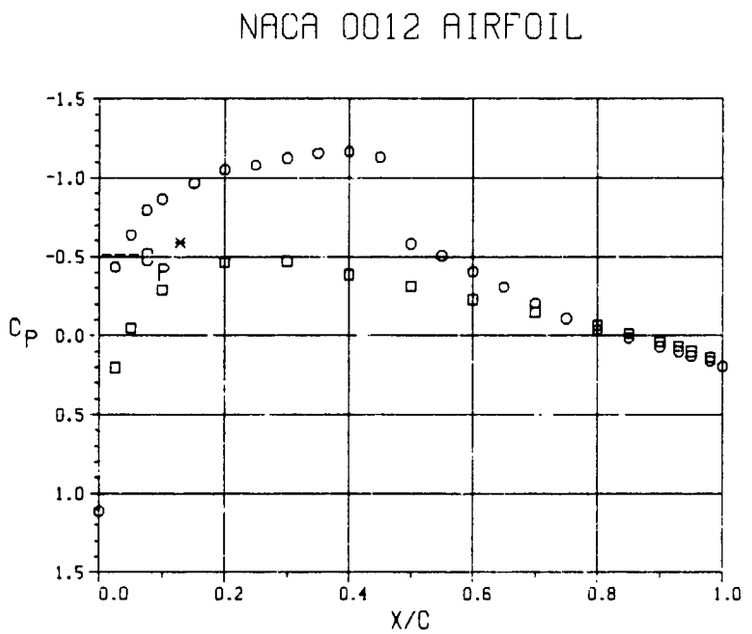

□ - AIRFOIL LOWER SURFACE

X/C	C_P	P/PT	M
0.025	0.203	0.728	0.689
0.050	-0.046	0.656	0.800
0.100	-0.291	0.587	0.907
0.200	-0.466	0.538	0.985
0.300	-0.473	0.535	0.989
0.400	-0.386	0.561	0.948
0.500	-0.314	0.580	0.917
0.600	-0.231	0.605	0.879
0.700	-0.151	0.627	0.845
0.800	-0.067	0.651	0.807
0.850	-0.016	0.665	0.786
0.900	0.038	0.681	0.762
0.930	0.065	0.688	0.750
0.950	0.098	0.698	0.735
0.980	0.136	0.709	0.719

SIDEWALL, Z=0

$\bar{X}$/C	C_P	P/PT	M
-3.75	0.061	0.688	0.752
-3.00	0.009	0.672	0.775
-1.25	0.054	0.685	0.755
1.25	0.025	0.677	0.768
3.75	0.010	0.673	0.774

○ - AIRFOIL UPPER SURFACE

X/C	C_P	P/PT	M
0.000	1.110	0.985	0.145
0.025	-0.134	0.546	0.971
0.050	-0.639	0.488	1.068
0.075	-0.797	0.443	1.144
0.100	-0.866	0.423	1.180
0.150	-0.966	0.395	1.233
0.200	-1.052	0.370	1.281
0.250	-1.081	0.362	1.297
0.300	-1.124	0.350	1.323
0.350	-1.158	0.340	1.343
0.400	-1.167	0.338	1.348
0.450	-1.131	0.348	1.327
0.500	-0.584	0.504	1.040
0.550	-0.508	0.525	1.005
0.600	-0.407	0.554	0.959
0.650	-0.310	0.582	0.915
0.700	-0.204	0.612	0.868
0.750	-0.110	0.639	0.827
0.800	-0.036	0.659	0.795
0.850	0.015	0.674	0.772
0.900	0.070	0.690	0.749
0.930	0.099	0.698	0.736
0.950	0.126	0.706	0.724
0.980	0.160	0.715	0.709
1.000	0.193	0.725	0.694

SIDEWALL, Z/C= 1.375

$\bar{X}$/C	C_P	P/PT	M
-3.75	0.046	0.683	0.758
-2.50	0.003	0.671	0.777
-2.00	0.004	0.671	0.776
-1.50	0.009	0.673	0.774
-1.00	-0.036	0.660	0.794
-0.50	-0.109	0.639	0.826
0.00	-0.104	0.641	0.824
0.50	-0.094	0.644	0.819
1.00	-0.053	0.655	0.801
1.50	-0.032	0.661	0.792
2.00	-0.009	0.668	0.782
2.50	-0.009	0.668	0.782
3.75	0.012	0.674	0.773

SIDEWALL, Z/C=-1.375

$\bar{X}$/C	C_P	P/PT	M
-3.75	0.042	0.682	0.760
-1.00	-0.010	0.667	0.783
-0.50	0.000	0.670	0.778
0.00	-0.023	0.664	0.788
0.50	-0.011	0.667	0.783
1.00	-0.023	0.664	0.788
1.50	-0.005	0.669	0.780
2.00	-0.006	0.669	0.781
2.50	0.005	0.672	0.776
3.75	0.021	0.676	0.769

(c) $M_\infty = 0.777$, $\alpha = 2.03°$, $Re_{c,\infty} = 3.9 \times 10^6$.

Figure 17.– Continued.

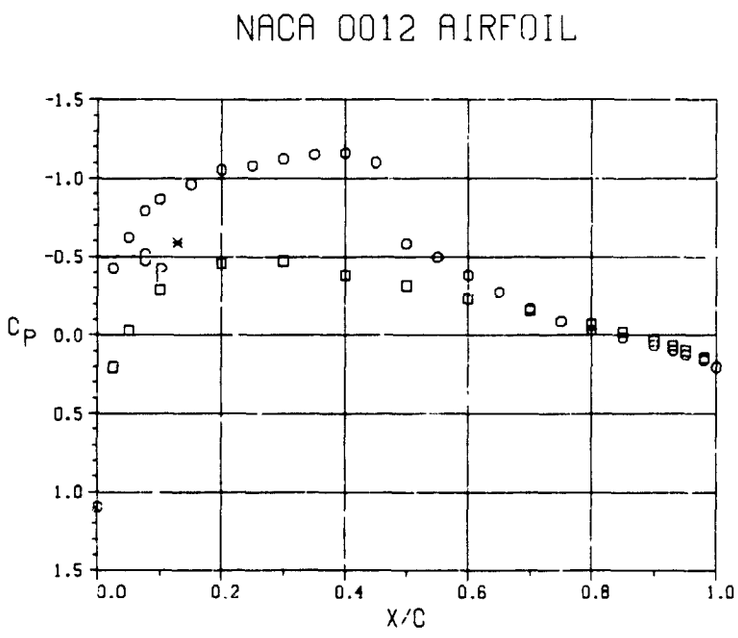

□ - AIRFOIL LOWER SURFACE

X/C	C_P	P/PT	M
0.025	0.201	0.727	0.690
0.050	-0.033	0.660	0.794
0.100	-0.293	0.586	0.909
0.200	-0.460	0.539	0.983
0.300	-0.474	0.534	0.991
0.400	-0.384	0.561	0.948
0.500	-0.318	0.579	0.920
0.600	-0.235	0.603	0.882
0.700	-0.158	0.624	0.849
0.800	-0.070	0.650	0.809
0.850	-0.020	0.663	0.789
0.900	0.035	0.680	0.764
0.930	0.066	0.688	0.751
0.950	0.099	0.698	0.736
0.980	0.144	0.710	0.717

SIDEWALL, Z = 0

$\bar{X}$/C	C_P	P/PT	M
-3.75	0.049	0.683	0.758
-3.00	0.009	0.672	0.776
-1.25	0.050	0.684	0.757
1.25	0.024	0.676	0.769
3.75	0.008	0.672	0.776

○ - AIRFOIL UPPER SURFACE

X/C	C_P	P/PT	M
0.000	1.093	0.980	0.168
0.025	-0.429	0.547	0.970
0.050	-0.625	0.491	1.061
0.075	-0.794	0.443	1.145
0.100	-0.869	0.422	1.183
0.150	-0.963	0.395	1.233
0.200	-1.056	0.368	1.285
0.250	-1.082	0.361	1.300
0.300	-1.125	0.349	1.325
0.350	-1.152	0.341	1.341
0.400	-1.162	0.338	1.348
0.450	-1.103	0.355	1.312
0.500	-0.586	0.502	1.043
0.550	-0.498	0.527	1.002
0.600	-0.384	0.560	0.949
0.650	-0.276	0.591	0.901
0.700	-0.170	0.621	0.854
0.750	-0.089	0.644	0.819
0.800	-0.033	0.660	0.794
0.850	0.014	0.673	0.774
0.900	0.064	0.688	0.752
0.930	0.094	0.696	0.739
0.950	0.123	0.704	0.726
0.980	0.157	0.714	0.711
1.000	0.202	0.727	0.691

SIDEWALL, Z/C = 1.375

$\bar{X}$/C	C_P	P/PT	M
-3.75	0.030	0.678	0.766
-2.50	-0.011	0.666	0.784
-2.00	-0.007	0.668	0.782
-1.50	0.003	0.671	0.778
-1.00	-0.042	0.658	0.797
-0.50	-0.112	0.638	0.828
0.00	-0.095	0.643	0.821
0.50	-0.095	0.643	0.821
1.00	-0.054	0.654	0.802
1.50	-0.035	0.660	0.794
2.00	-0.014	0.666	0.785
2.50	-0.011	0.667	0.784
3.75	0.011	0.673	0.774

SIDEWALL, Z/C = -1.375

$\bar{X}$/C	C_P	P/PT	M
-3.75	0.031	0.678	0.766
-1.00	-0.015	0.665	0.786
-0.50	-0.002	0.660	0.780
0.00	-0.026	0.662	0.790
0.50	-0.006	0.668	0.781
1.00	-0.028	0.662	0.791
1.50	-0.007	0.668	0.782
2.00	-0.009	0.667	0.783
2.50	0.003	0.671	0.777
3.75	0.019	0.675	0.771

(d) $M_\infty = 0.778, \alpha = 2.03°, Re_{c,\infty} = 6.0 \times 10^6$.

Figure 17.– Continued.

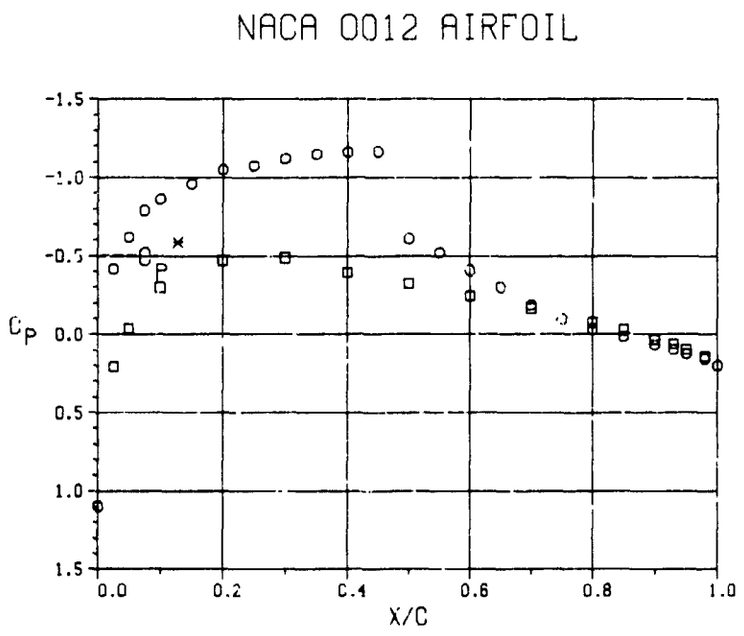

o - AIRFOIL UPPER SURFACE

X/C	C_P	P/PT	M
0.000	1.097	0.982	0.163
0.025	-0.418	0.550	0.965
0.050	-0.620	0.492	1.060
0.075	-0.791	0.444	1.143
0.100	-0.863	0.423	1.181
0.150	-0.961	0.395	1.233
0.200	-1.052	0.369	1.283
0.250	-1.077	0.362	1.298
0.300	-1.122	0.349	1.324
0.350	-1.151	0.341	1.342
0.400	-1.163	0.337	1.349
0.450	-1.166	0.336	1.351
0.500	-0.612	0.495	1.056
0.550	-0.521	0.520	1.013
0.600	-0.411	0.552	0.962
0.650	-0.300	0.583	0.912
0.700	-0.188	0.615	0.863
0.750	-0.099	0.641	0.824
0.800	-0.035	0.659	0.795
0.850	0.014	0.673	0.774
0.900	0.066	0.688	0.751
0.930	0.095	0.696	0.739
0.950	0.123	0.704	0.726
0.980	0.156	0.714	0.711
1.000	0.199	0.726	0.693

□ - AIRFOIL LOWER SURFACE

X/C	C_P	P/PT	M
0.025	0.204	0.727	0.690
0.050	-0.039	0.658	0.797
0.100	-0.301	0.583	0.913
0.200	-0.473	0.534	0.990
0.300	-0.491	0.529	0.999
0.400	-0.398	0.557	0.954
0.500	-0.327	0.576	0.924
0.600	-0.244	0.600	0.887
0.700	-0.167	0.621	0.853
0.800	-0.077	0.647	0.813
0.850	-0.028	0.661	0.792
0.900	0.030	0.678	0.767
0.930	0.059	0.686	0.754
0.950	0.094	0.696	0.736
0.980	0.140	0.709	0.719

SIDEWALL, Z=0

$\bar{X}$/C	C_P	P/PT	M
-3.75	0.050	0.683	0.758
-3.00	0.007	0.671	0.777
-1.25	0.051	0.684	0.758
1.25	0.023	0.676	0.770
3.75	0.008	0.672	0.776

SIDEWALL, Z/C= 1.375

$\bar{X}$/C	C_P	P/PT	M
-3.75	0.031	0.678	0.766
-2.50	-0.011	0.666	0.785
-2.00	-0.009	0.667	0.784
-1.50	0.002	0.670	0.779
-1.00	-0.042	0.657	0.798
-0.50	-0.113	0.637	0.829
0.00	-0.083	0.646	0.816
0.50	-0.099	0.641	0.823
1.00	-0.052	0.654	0.802
1.50	-0.036	0.659	0.796
2.00	-0.017	0.664	0.787
2.50	-0.014	0.665	0.786
3.75	0.010	0.672	0.776

SIDEWALL, Z/C= -1.375

$\bar{X}$/C	C_P	P/PT	M
-3.75	0.033	0.679	0.765
-1.00	-0.015	0.665	0.786
-0.50	-0.002	0.669	0.781
0.00	-0.029	0.661	0.792
0.50	-0.005	0.668	0.782
1.00	-0.031	0.660	0.793
1.50	-0.008	0.667	0.783
2.00	-0.011	0.666	0.785
2.50	0.002	0.670	0.779
3.75	0.020	0.675	0.771

(e) $M_\infty = 0.778$, $\alpha = 2.03°$, $Re_{c,\infty} = 7.8 \times 10^6$.

Figure 17.– Continued.

NACA 0012 AIRFOIL

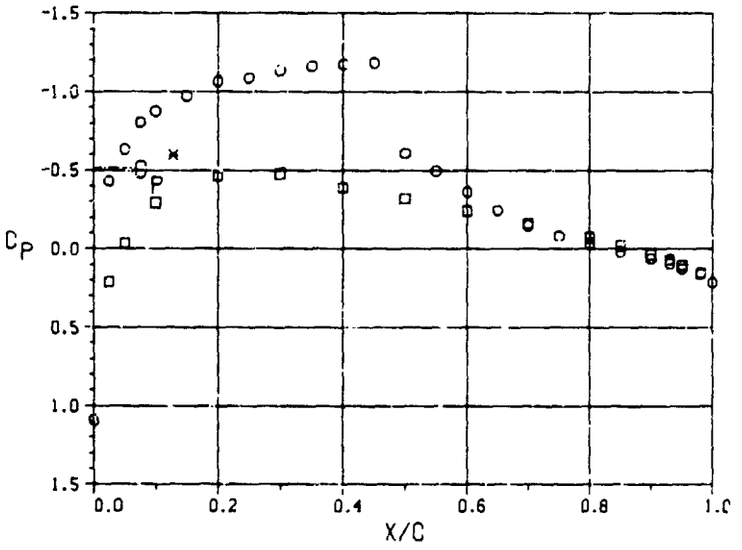

□ - AIRFOIL LOWER SURFACE

X/C	C_P	P/PT	M
0.025	0.212	0.731	0.684
0.050	-0.036	0.661	0.793
0.100	-0.295	0.587	0.906
0.200	-0.466	0.539	0.982
0.300	-0.478	0.536	0.980
0.400	-0.390	0.561	0.948
0.500	-0.320	0.580	0.917
0.600	-0.242	0.603	0.882
0.700	-0.164	0.625	0.848
0.800	-0.074	0.650	0.809
0.850	-0.023	0.665	0.787
0.900	0.034	0.681	0.762
0.930	0.065	0.690	0.748
0.950	0.101	0.700	0.733
0.980	0.151	0.714	0.711

SIDEWALL, Z=0

X/C	C_P	P/PT	M
-3.75	0.048	0.685	0.755
-3.00	0.009	0.674	0.773
-1.25	0.051	0.686	0.754
1.25	0.024	0.678	0.766
3.75	0.009	0.674	0.773

○ - AIRFOIL UPPER SURFACE

X/C	C_P	P/PT	M
0.000	1.090	0.980	0.169
0.025	-0.431	0.549	0.967
0.050	-0.634	0.491	1.061
0.075	-0.805	0.443	1.145
0.100	-0.878	0.422	1.182
0.150	-0.975	0.395	1.233
0.200	-1.067	0.369	1.284
0.250	-1.089	0.362	1.297
0.300	-1.136	0.349	1.325
0.350	-1.164	0.341	1.341
0.400	-1.174	0.338	1.347
0.450	-1.182	0.336	1.352
0.500	-0.608	0.499	1.049
0.550	-0.497	0.530	0.997
0.600	-0.364	0.568	0.937
0.650	-0.246	0.601	0.884
0.700	-0.149	0.629	0.842
0.750	-0.082	0.648	0.813
0.800	-0.034	0.662	0.792
0.850	0.016	0.676	0.770
0.900	0.061	0.688	0.750
0.930	0.092	0.697	0.737
0.950	0.123	0.706	0.723
0.980	0.160	0.716	0.707
1.000	0.212	0.731	0.684

SIDEWALL, Z/C= 1.375

X/C	C_P	P/PT	M
-3.75	0.027	0.679	0.765
-2.50	-0.014	0.668	0.782
-2.00	-0.012	0.668	0.782
-1.50	-0.001	0.671	0.777
-1.00	-0.045	0.659	0.796
-0.50	-0.116	0.638	0.827
0.00	-0.074	0.651	0.808
0.50	-0.098	0.644	0.819
1.00	-0.051	0.657	0.799
1.50	-0.032	0.662	0.790
2.00	-0.019	0.666	0.785
2.50	-0.015	0.667	0.783
3.75	0.011	0.674	0.772

SIDEWALL, Z/C=-1.375

X/C	C_P	P/PT	M
-3.75	0.031	0.680	0.763
-1.00	-0.017	0.667	0.784
-0.50	-0.001	0.671	0.777
0.00	-0.027	0.664	0.788
0.50	-0.002	0.671	0.777
1.00	-0.033	0.662	0.791
1.50	-0.008	0.669	0.780
2.00	-0.013	0.668	0.782
2.50	0.001	0.672	0.776
3.75	0.020	0.677	0.768

(f) $M_\infty = 0.775$, $\alpha = 2.05°$, $Re_{c,\infty} = 9.9 \times 10^6$.

Figure 17.– Concluded.

NACA 0012 AIRFOIL

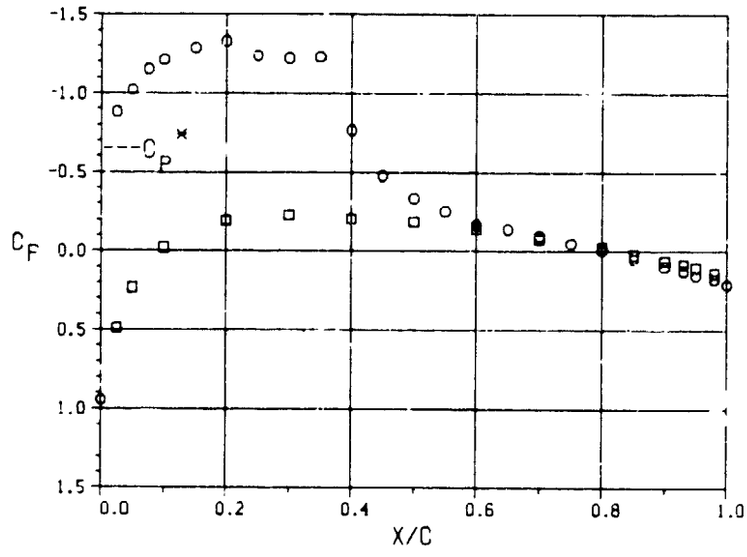

o - AIRFOIL UPPER SURFACE

X/C	C_P	P/PT	M
0.000	0.943	0.947	0.279
0.025	-0.882	0.466	1.104
0.050	-1.023	0.429	1.170
0.075	-1.155	0.394	1.235
0.100	-1.214	0.378	1.265
0.150	-1.287	0.359	1.304
0.200	-1.330	0.347	1.329
0.250	-1.239	0.372	1.278
0.300	-1.223	0.376	1.270
0.350	-1.230	0.374	1.274
0.400	-0.767	0.496	1.053
0.450	-0.478	0.572	0.929
0.500	-0.336	0.610	0.871
0.550	-0.254	0.632	0.837
0.600	-0.169	0.654	0.803
0.650	-0.138	0.662	0.791
0.700	-0.097	0.673	0.774
0.750	-0.050	0.685	0.755
0.800	-0.007	0.697	0.737
0.850	0.048	0.711	0.715
0.900	0.096	0.724	0.695
0.930	0.124	0.731	0.684
0.950	0.151	0.739	0.673
0.980	0.177	0.745	0.662
1.000	0.210	0.754	0.648

□ - AIRFOIL LOWER SURFACE

X/C	C_P	P/PT	M
0.025	0.489	0.828	0.526
0.050	0.231	0.759	0.640
0.100	-0.022	0.693	0.744
0.200	-0.193	0.649	0.811
0.300	-0.227	0.639	0.827
0.400	-0.206	0.645	0.817
0.500	-0.188	0.649	0.811
0.600	-0.140	0.663	0.790
0.700	-0.077	0.678	0.766
0.800	-0.027	0.692	0.744
0.850	0.024	0.705	0.725
0.900	0.059	0.715	0.709
0.930	0.085	0.721	0.700
0.950	0.104	0.727	0.691
0.980	0.139	0.735	0.678

SIDEWALL, Z/C = 1.375

$\bar{X}$/C	C_P	P/PT	M
-3.75	0.079	0.720	0.701
-2.50	0.047	0.712	0.714
-2.00	0.044	0.711	0.715
-1.50	0.031	0.708	0.721
-1.00	-0.005	0.698	0.735
-0.50	-0.073	0.680	0.763
0.00	-0.012	0.696	0.738
0.50	-0.047	0.687	0.752
1.00	-0.041	0.689	0.750
1.50	0.008	0.701	0.730
2.00	0.027	0.707	0.722
2.50	0.010	0.702	0.729
3.75	0.044	0.711	0.715

SIDEWALL, Z/C = 0

$\bar{X}$/C	C_P	P/PT	M
-3.75	0.095	0.724	0.695
-3.00	0.011	0.702	0.730
-1.25	0.093	0.724	0.696
1.25	0.041	0.710	0.717
3.75	0.050	0.712	0.714

SIDEWALL, Z/C = -1.375

$\bar{X}$/C	C_P	P/PT	M
-3.75	0.089	0.723	0.697
-1.00	0.042	0.711	0.716
-0.50	0.052	0.713	0.712
0.00	0.032	0.708	0.720
0.50	0.039	0.710	0.717
1.00	0.027	0.707	0.722
1.50	0.032	0.708	0.720
2.00	0.026	0.706	0.723
2.50	0.046	0.712	0.714
3.75	0.066	0.717	0.707

(a) $M_\infty = 0.734$, $\alpha = 4.04°$, $Re_{c,\infty} = 1.0 \times 10^6$.

Figure 18.– Airfoil and test channel sidewall pressure measurements, Data Set 6 ($M_N = 0.725$, $\alpha_N = 4°$).

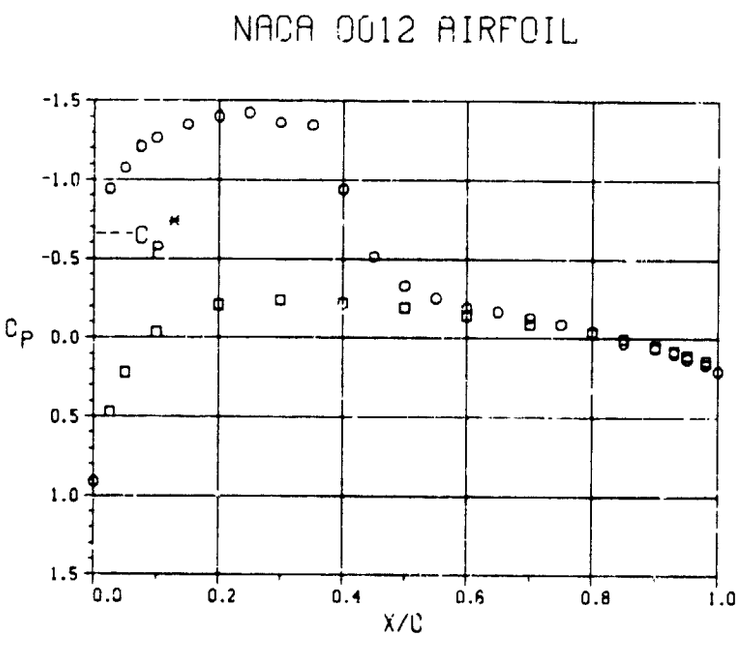

o - AIRFOIL UPPER SURFACE

X/C	C_p	P/PT	M
0.000	0.910	0.939	0.301
0.025	-0.943	0.452	1.128
0.050	-1.075	0.418	1.190
0.075	-1.211	0.382	1.259
0.100	-1.266	0.367	1.287
0.150	-1.352	0.345	1.333
0.200	-1.401	0.332	1.361
0.250	-1.424	0.326	1.375
0.300	-1.363	0.342	1.340
0.350	-1.348	0.346	1.331
0.400	-0.944	0.452	1.129
0.450	-0.516	0.564	0.942
0.500	-0.332	0.613	0.866
0.550	-0.253	0.634	0.834
0.600	-0.193	0.649	0.810
0.650	-0.168	0.656	0.800
0.700	-0.130	0.666	0.785
0.750	-0.090	0.676	0.769
0.800	-0.040	0.689	0.749
0.850	0.028	0.707	0.721
0.900	0.062	0.716	0.707
0.930	0.093	0.725	0.694
0.950	0.127	0.733	0.681
0.980	0.165	0.743	0.665
1.000	0.206	0.754	0.648

□ - AIRFOIL LOWER SURFACE

X/C	C_p	P/PT	M
0.025	0.472	0.824	0.533
0.050	0.220	0.758	0.642
0.100	-0.035	0.691	0.746
0.200	-0.208	0.646	0.815
0.300	-0.240	0.637	0.830
0.400	-0.222	0.643	0.821
0.500	-0.194	0.649	0.811
0.600	-0.141	0.664	0.788
0.700	-0.090	0.676	0.769
0.800	-0.038	0.691	0.747
0.850	0.004	0.701	0.731
0.900	0.052	0.714	0.710
0.930	0.078	0.721	0.701
0.950	0.107	0.729	0.688
0.980	0.141	0.737	0.675

SIDEWALL, Z = 0

$\bar{X}$/C	C_p	P/PT	M
-3.75	0.075	0.720	0.701
-3.00	0.013	0.703	0.727
-1.25	0.077	0.721	0.701
1.25	0.044	0.712	0.714
3.75	0.032	0.709	0.719

SIDEWALL, Z/C = 1.375

$\bar{X}$/C	C_p	P/PT	M
-3.75	0.056	0.716	0.708
-2.50	0.010	0.703	0.727
-2.00	0.013	0.704	0.726
-1.50	0.008	0.703	0.728
-1.00	-0.036	0.691	0.746
-0.50	-0.103	0.674	0.773
0.00	-0.037	0.691	0.746
0.50	-0.078	0.680	0.763
1.00	-0.057	0.686	0.754
1.50	-0.024	0.695	0.741
2.00	0.000	0.701	0.731
2.50	0.002	0.701	0.730
3.75	0.026	0.706	0.720

SIDEWALL, Z/C = -1.375

$\bar{X}$/C	C_p	P/PT	M
-3.75	0.069	0.719	0.703
-1.00	0.027	0.708	0.720
-0.50	0.031	0.709	0.719
0.00	0.019	0.706	0.724
0.50	0.024	0.707	0.721
1.00	0.008	0.703	0.728
1.50	0.023	0.707	0.722
2.00	0.020	0.706	0.723
2.50	0.030	0.709	0.719
3.75	0.055	0.715	0.709

(b) $M_\infty = 0.732, \alpha = 4.06°, Re_{c,\infty} = 1.9 \times 10^6$.

Figure 18.– Continued.

NACA 0012 AIRFOIL

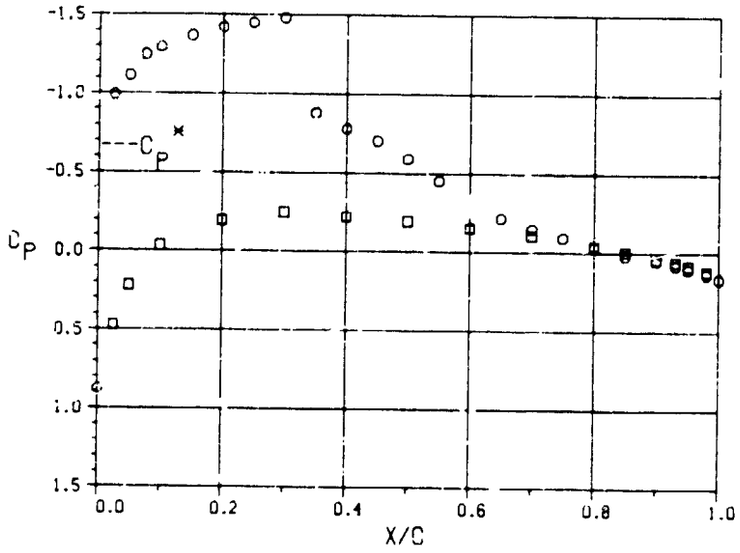

o - AIRFOIL UPPER SURFACE

X/C	C_P	P/PT	M
0.000	0.879	0.932	0.319
0.025	-0.992	0.443	1.144
0.050	-1.112	0.412	1.201
0.075	-1.247	0.377	1.268
0.100	-1.293	0.365	1.293
0.150	-1.367	0.345	1.332
0.200	-1.423	0.331	1.363
0.250	-1.450	0.324	1.379
0.300	-1.481	0.316	1.397
0.350	-0.880	0.473	1.093
0.400	-0.781	0.498	1.049
0.450	-0.705	0.518	1.016
0.500	-0.591	0.548	0.968
0.550	-0.453	0.584	0.911
0.600	-0.304	0.623	0.851
0.650	-0.216	0.646	0.816
0.700	-0.148	0.664	0.788
0.750	-0.095	0.677	0.767
0.800	-0.042	0.691	0.746
0.850	0.018	0.707	0.722
0.900	0.050	0.715	0.709
0.930	0.077	0.722	0.698
0.950	0.102	0.729	0.688
0.980	0.133	0.737	0.675
1.000	0.162	0.745	0.663

□ - AIRFOIL LOWER SURFACE

X/C	C_P	P/PT	M
0.025	0.472	0.826	0.530
0.050	0.218	0.759	0.640
0.100	-0.036	0.693	0.743
0.200	-0.195	0.651	0.807
0.300	-0.248	0.638	0.828
0.400	-0.221	0.644	0.818
0.500	-0.197	0.651	0.808
0.600	-0.151	0.663	0.790
0.700	-0.106	0.675	0.771
0.800	-0.045	0.691	0.747
0.850	-0.009	0.700	0.732
0.900	0.037	0.712	0.714
0.930	0.056	0.717	0.706
0.950	0.082	0.724	0.696
0.980	0.116	0.733	0.682

SIDEWALL, Z = 0

$\bar{X}$/C	C_P	P/PT	M
-3.75	0.058	0.717	0.705
-3.00	0.013	0.706	0.724
-1.25	0.062	0.719	0.704
1.25	0.028	0.710	0.718
3.75	0.016	0.706	0.723

SIDEWALL, Z/C = 1.375

$\bar{X}$/C	C_P	P/PT	M
-3.75	0.038	0.710	0.714
-2.50	-0.008	0.700	0.732
-2.00	-0.006	0.701	0.731
-1.50	-0.003	0.701	0.730
-1.00	-0.054	0.688	0.751
-0.50	-0.125	0.669	0.779
0.00	-0.049	0.689	0.749
0.50	-0.098	0.677	0.768
1.00	-0.069	0.684	0.757
1.50	-0.040	0.692	0.745
2.00	-0.013	0.699	0.734
2.50	-0.009	0.700	0.733
3.75	0.016	0.706	0.723

SIDEWALL, Z/C = -1.375

$\bar{X}$/C	C_P	P/PT	M
-3.75	0.047	0.714	0.710
-1.00	0.012	0.705	0.724
-0.50	0.022	0.708	0.720
0.00	0.014	0.706	0.723
0.50	0.014	0.706	0.723
1.00	-0.001	0.702	0.729
1.50	0.011	0.705	0.725
2.00	0.002	0.703	0.728
2.50	0.017	0.707	0.722
3.75	0.041	0.713	0.713

(c) $M_\infty = 0.729$, $\alpha = 3.93°$, $Re_{c,\infty} = 3.9 \times 10^6$.

Figure 13.– Continued.

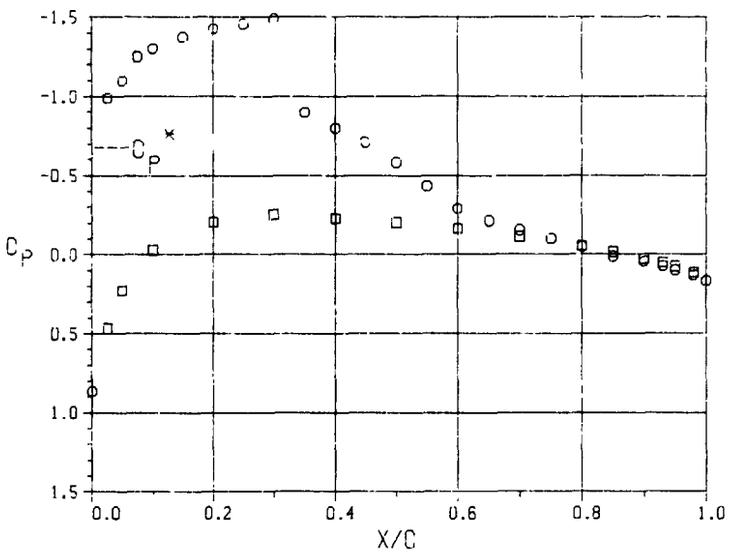

o - AIRFOIL UPPER SURFACE

X/C	C_p	P/PT	M
0.000	0.863	0.928	0.328
0.025	-0.990	0.446	1.140
0.050	-1.098	0.418	1.190
0.075	-1.253	0.377	1.267
0.100	-1.302	0.364	1.293
0.150	-1.375	0.345	1.332
0.200	-1.429	0.331	1.362
0.250	-1.456	0.324	1.377
0.300	-1.490	0.316	1.397
0.350	-0.899	0.470	1.098
0.400	-0.800	0.495	1.055
0.450	-0.710	0.519	1.016
0.500	-0.582	0.552	0.962
0.550	-0.432	0.591	0.900
0.600	-0.292	0.627	0.844
0.650	-0.214	0.648	0.813
0.700	-0.155	0.663	0.789
0.730	-0.101	0.677	0.767
0.800	-0.052	0.690	0.748
0.850	0.012	0.707	0.722
0.900	0.042	0.714	0.710
0.930	0.071	0.722	0.698
0.950	0.098	0.729	0.687
0.980	0.129	0.737	0.675
1.000	0.164	0.746	0.661

□ - AIRFOIL LOWER SURFACE

X/C	C_p	P/PT	M
0.025	0.466	0.826	0.531
0.050	0.229	0.763	0.634
0.100	-0.029	0.696	0.739
0.200	-0.204	0.652	0.807
0.300	-0.253	0.638	0.828
0.400	-0.227	0.646	0.816
0.500	-0.203	0.651	0.808
0.600	-0.164	0.662	0.791
0.700	-0.116	0.673	0.774
0.800	-0.054	0.690	0.747
0.850	-0.018	0.699	0.734
0.900	0.025	0.711	0.715
0.930	0.048	0.716	0.708
0.950	0.075	0.724	0.695
0.980	0.114	0.733	0.681

SIDEWALL, Z=0

$\bar{X}$/C	C_p	P/PT	M
-3.75	0.050	0.717	0.706
-3.00	0.010	0.706	0.723
-1.25	0.057	0.718	0.705
1.25	0.021	0.709	0.718
3.75	0.010	0.706	0.722

SIDEWALL, Z/C= 1.375

$\bar{X}$/C	C_p	P/PT	M
-3.75	0.025	0.711	0.716
-2.50	-0.020	0.699	0.734
-2.00	-0.021	0.699	0.734
-1.50	-0.015	0.701	0.732
-1.00	-0.066	0.687	0.752
-0.50	-0.135	0.669	0.780
0.00	-0.052	0.691	0.747
0.50	-0.107	0.677	0.768
1.00	-0.076	0.685	0.756
1.50	-0.053	0.691	0.747
2.00	-0.024	0.698	0.735
2.50	-0.018	0.700	0.733
3.75	0.008	0.706	0.723

SIDEWALL, Z/C=-1.375

$\bar{X}$/C	C_p	P/PT	M
-3.75	0.036	0.714	0.711
-1.00	0.000	0.704	0.725
-0.50	0.012	0.707	0.721
0.00	0.006	0.706	0.723
0.50	0.009	0.707	0.722
1.00	-0.017	0.700	0.732
1.50	0.001	0.705	0.725
2.00	-0.007	0.702	0.729
2.50	0.007	0.706	0.723
3.75	0.031	0.712	0.713

(d) $M_\infty = 0.727, \alpha = 4.04°, Re_{c,\infty} = 6.1 \times 10^6$.

Figure 18.– Continued.

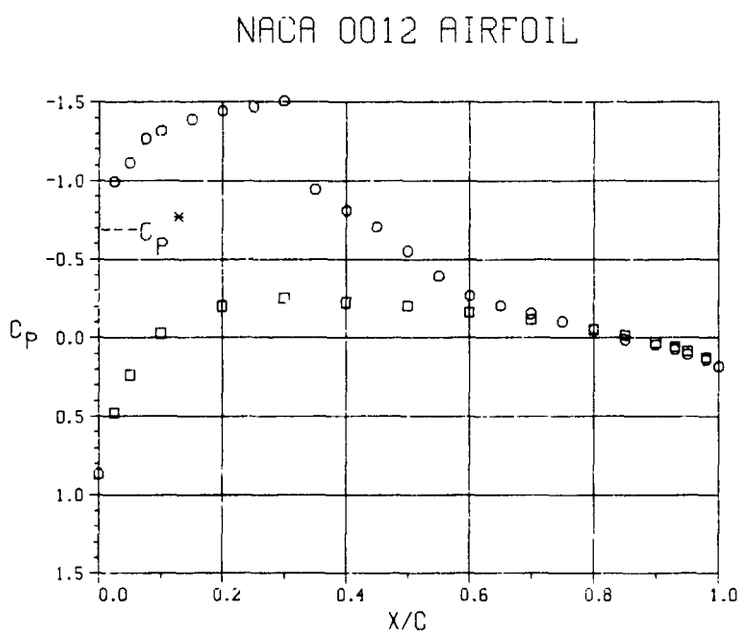

o - AIRFOIL UPPER SURFACE

X/C	C_P	P/PT	M
0.000	0.865	0.929	0.326
0.025	-0.994	0.447	1.136
0.050	-1.113	0.417	1.192
0.075	-1.270	0.376	1.270
0.100	-1.319	0.363	1.295
0.150	-1.390	0.345	1.333
0.200	-1.444	0.331	1.363
0.250	-1.470	0.324	1.378
0.300	-1.508	0.314	1.399
0.350	-0.946	0.460	1.115
0.400	-0.812	0.495	1.055
0.450	-0.706	0.522	1.010
0.500	-0.554	0.561	0.947
0.550	-0.394	0.603	0.882
0.600	-0.269	0.635	0.832
0.650	-0.204	0.652	0.806
0.700	-0.156	0.665	0.787
0.750	-0.104	0.678	0.766
0.800	-0.056	0.691	0.747
0.850	0.012	0.708	0.720
0.900	0.043	0.716	0.707
0.930	0.074	0.724	0.695
0.950	0.103	0.732	0.683
0.980	0.138	0.741	0.669
1.000	0.182	0.752	0.651

□ - AIRFOIL LOWER SURFACE

X/C	C_P	P/PT	M
0.025	0.475	0.828	0.525
0.050	0.236	0.766	0.629
0.100	-0.029	0.698	0.736
0.200	-0.202	0.653	0.804
0.300	-0.255	0.639	0.826
0.400	-0.226	0.647	0.813
0.500	-0.205	0.652	0.806
0.600	-0.164	0.663	0.789
0.700	-0.118	0.674	0.772
0.800	-0.053	0.692	0.745
0.850	-0.015	0.701	0.731
0.900	0.028	0.713	0.712
0.930	0.054	0.719	0.703
0.950	0.082	0.727	0.691
0.980	0.125	0.737	0.674

SIDEWALL, Z=0

$\bar{X}$/C	C_P	P/PT	M
-3.75	0.053	0.718	0.704
-3.00	0.011	0.708	0.720
-1.25	0.053	0.718	0.704
1.25	0.027	0.711	0.715
3.75	0.011	0.707	0.721

SIDEWALL, Z/C= 1.375

$\bar{X}$/C	C_P	P/PT	M
-3.75	0.027	0.712	0.714
-2.50	-0.017	0.700	0.732
-2.00	-0.019	0.700	0.733
-1.50	-0.011	0.702	0.730
-1.00	-0.064	0.688	0.751
-0.50	-0.134	0.670	0.779
0.00	-0.049	0.692	0.745
0.50	-0.107	0.677	0.768
1.00	-0.074	0.685	0.755
1.50	-0.046	0.693	0.744
2.00	-0.023	0.699	0.735
2.50	-0.016	0.700	0.732
3.75	0.009	0.707	0.722

SIDEWALL, Z/C=-1.375

$\bar{X}$/C	C_P	P/PT	M
-3.75	0.039	0.715	0.710
-1.00	0.002	0.705	0.724
-0.50	0.014	0.708	0.720
0.00	0.007	0.706	0.723
0.50	0.010	0.707	0.721
1.00	-0.015	0.701	0.731
1.50	0.004	0.706	0.724
2.00	-0.009	0.702	0.729
2.50	0.008	0.707	0.722
3.75	0.034	0.713	0.712

(e) $M_\infty = 0.725, \alpha = 4.04°, Re_{c,\infty} = 7.9 \times 10^6$.

Figure 18.-- Continued.

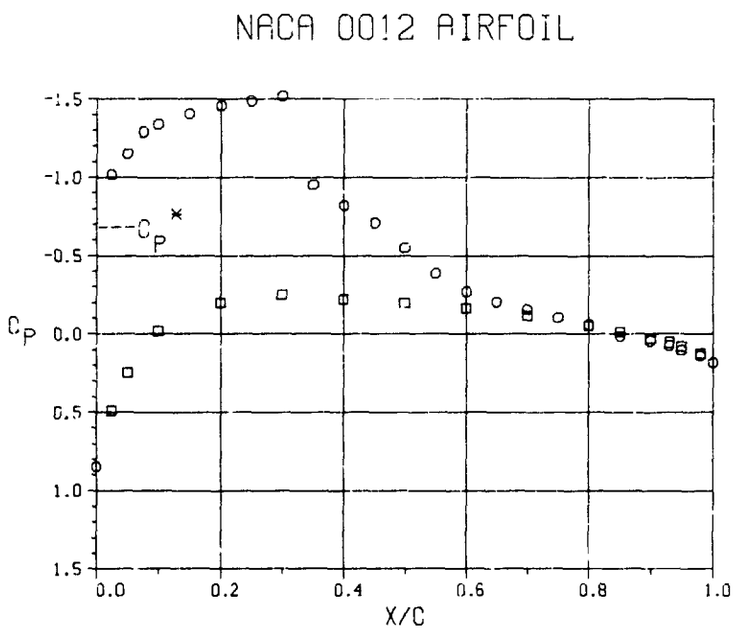

o - AIRFOIL UPPER SURFACE

X/C	C_P	P/PT	M
0.000	0.847	0.924	0.337
0.025	-1.017	0.440	1.150
0.050	-1.153	0.405	1.214
0.075	-1.291	0.369	1.284
0.100	-1.341	0.356	1.310
0.150	-1.409	0.338	1.347
0.200	-1.462	0.325	1.377
0.250	-1.489	0.318	1.393
0.300	-1.522	0.309	1.412
0.350	-0.955	0.456	1.121
0.400	-0.823	0.490	1.063
0.450	-0.711	0.520	1.014
0.500	-0.550	0.561	0.947
0.550	-0.388	0.603	0.881
0.600	-0.270	0.634	0.834
0.650	-0.206	0.651	0.808
0.700	-0.157	0.663	0.789
0.750	-0.107	0.676	0.769
0.800	-0.058	0.689	0.749
0.850	0.014	0.708	0.720
0.900	0.041	0.715	0.710
0.930	0.072	0.723	0.697
0.950	0.101	0.730	0.685
0.980	0.136	0.740	0.671
1.000	0.181	0.751	0.652

□ - AIRFOIL LOWER SURFACE

X/C	C_P	P/PT	M
0.025	0.486	0.830	0.522
0.050	0.244	0.768	0.627
0.100	-0.021	0.699	0.734
0.200	-0.198	0.653	0.805
0.300	-0.251	0.639	0.826
0.400	-0.224	0.646	0.815
0.500	-0.200	0.652	0.806
0.600	-0.165	0.661	0.792
0.700	-0.118	0.674	0.773
0.800	-0.054	0.690	0.748
0.850	-0.016	0.700	0.732
0.900	0.026	0.711	0.716
0.930	0.051	0.718	0.705
0.950	0.079	0.725	0.694
0.980	0.125	0.737	0.675

SIDEWALL, Z=0

$\bar{X}$/C	C_P	P/PT	M
-3.75	0.050	0.717	0.706
-3.00	0.011	0.707	0.721
-1.25	0.052	0.718	0.705
1.25	0.023	0.710	0.717
3.75	0.010	0.707	0.722

SIDEWALL, Z/C= 1.375

$\bar{X}$/C	C_P	P/PT	M
-3.75	0.022	0.710	0.717
-2.50	-0.020	0.699	0.734
-2.00	-0.023	0.698	0.735
-1.50	-0.016	0.700	0.732
-1.00	-0.069	0.686	0.753
-0.50	-0.140	0.668	0.782
0.00	-0.048	0.692	0.745
0.50	-0.110	0.676	0.770
1.00	-0.074	0.685	0.755
1.50	-0.049	0.692	0.745
2.00	-0.028	0.697	0.737
2.50	-0.019	0.699	0.733
3.75	0.007	0.706	0.723

SIDEWALL, Z/C=-1.375

$\bar{X}$/C	C_P	P/PT	M
-3.75	0.034	0.713	0.712
-1.00	-0.001	0.704	0.726
-0.50	0.013	0.708	0.721
0.00	0.006	0.706	0.723
0.50	0.009	0.707	0.722
1.00	-0.019	0.699	0.734
1.50	0.002	0.705	0.725
2.00	-0.011	0.701	0.730
2.50	0.005	0.705	0.724
3.75	0.031	0.712	0.713

(f) $M_\infty = 0.726, \alpha = 3.91°, Re_{c,\infty} = 9.3 \times 10^6$.

Figure 18.– Concluded.

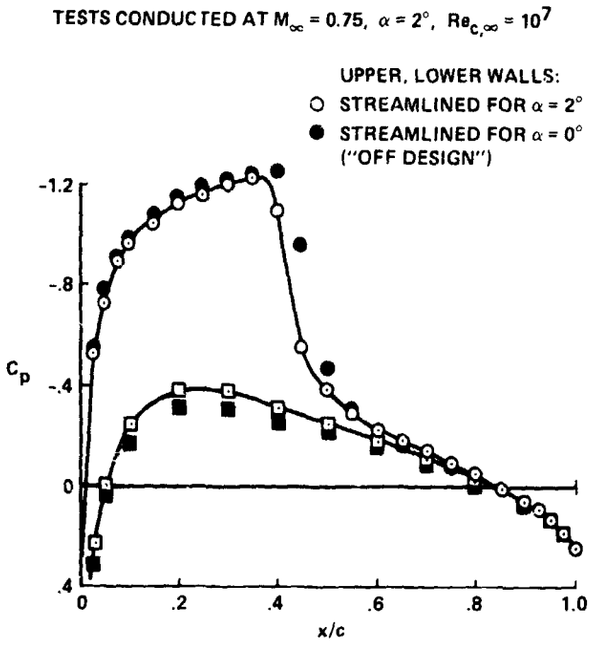

(a) "Off design" in angle of attack.

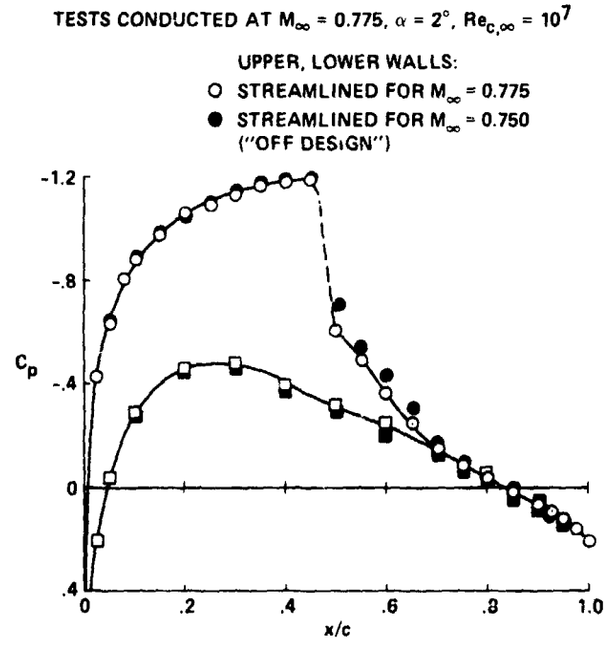

(b) "Off design" in Mach number.

Figure 19.– Effects of off design wall contouring on airfoil pressure coefficient.

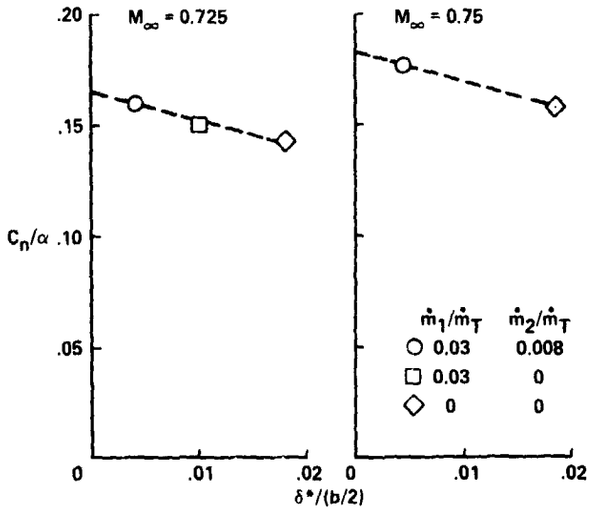

Figure 20.– Effect of sidewall boundary-layer displacement thickness on normal force coefficient.

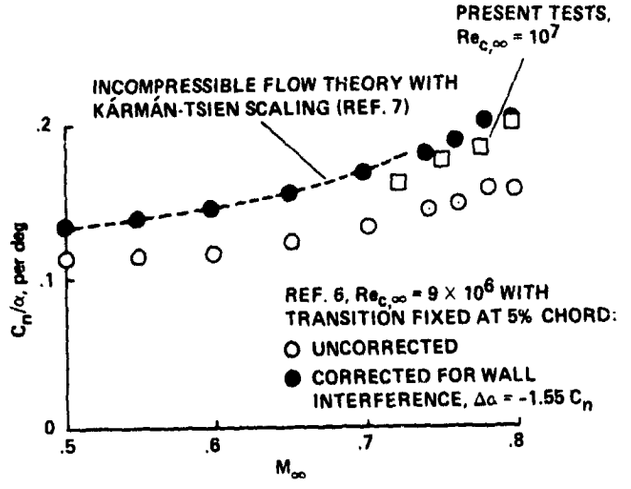

Figure 21.– Comparison of present test results with measurements and estimates from references 6 and 7.

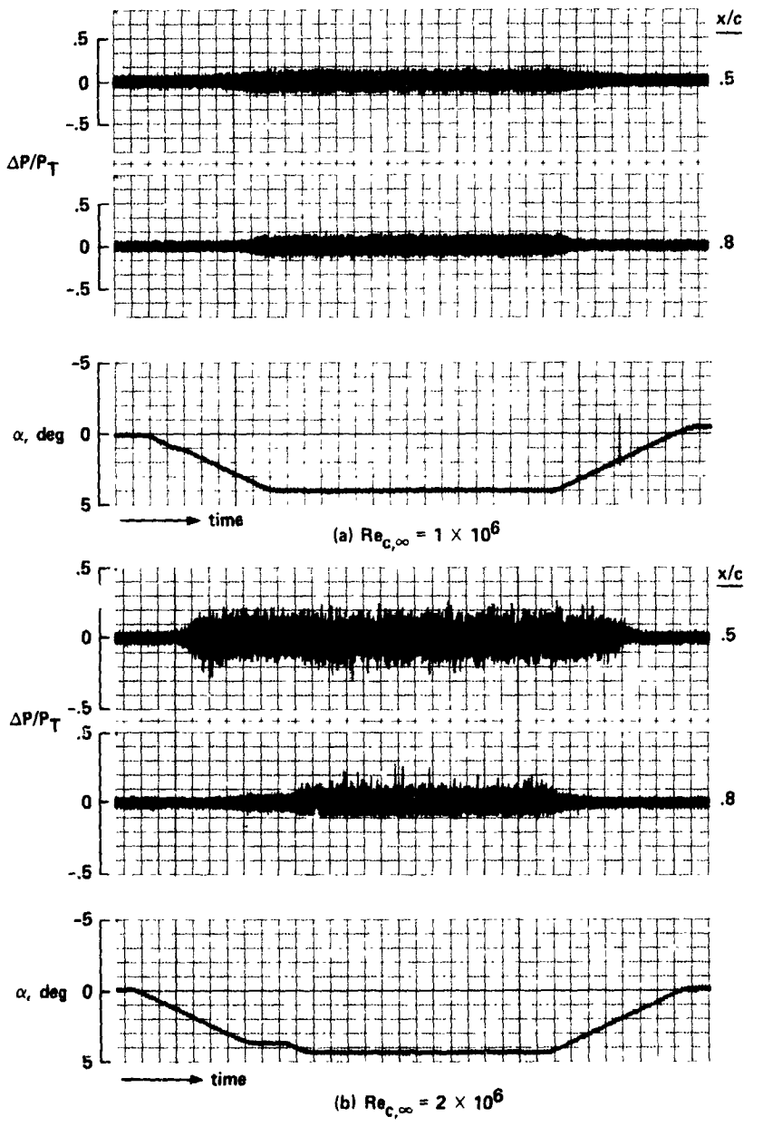

Figure 22.– Envelopes of pressure deviations from the mean, Data Set 5 ($M_N = 0.775$, $\alpha_N = 2°$).

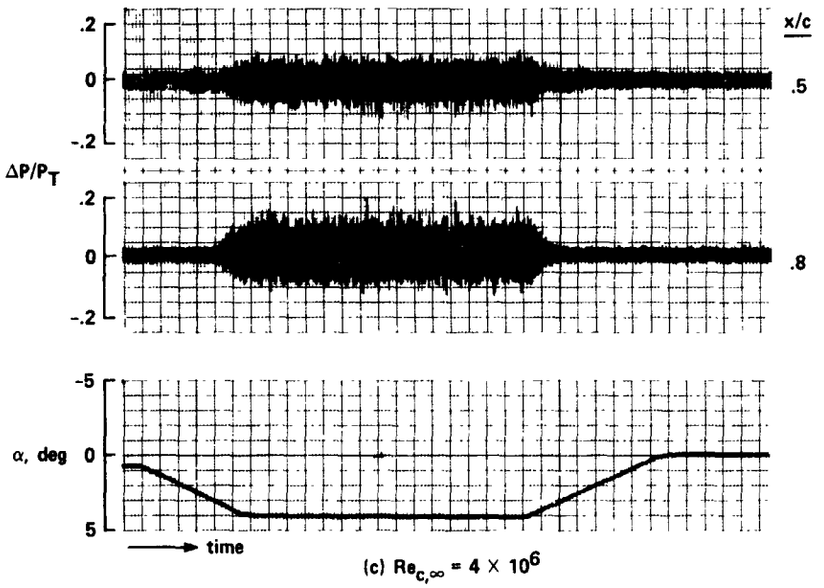

(c) $Re_{c,\infty} = 4 \times 10^6$

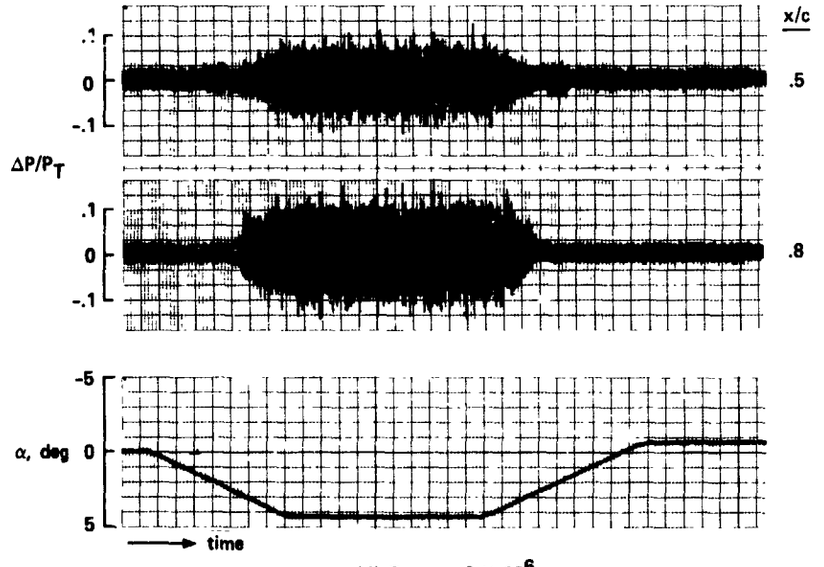

(d) $Re_{c,\infty} = 6 \times 10^6$

Figure 22.– Continued.

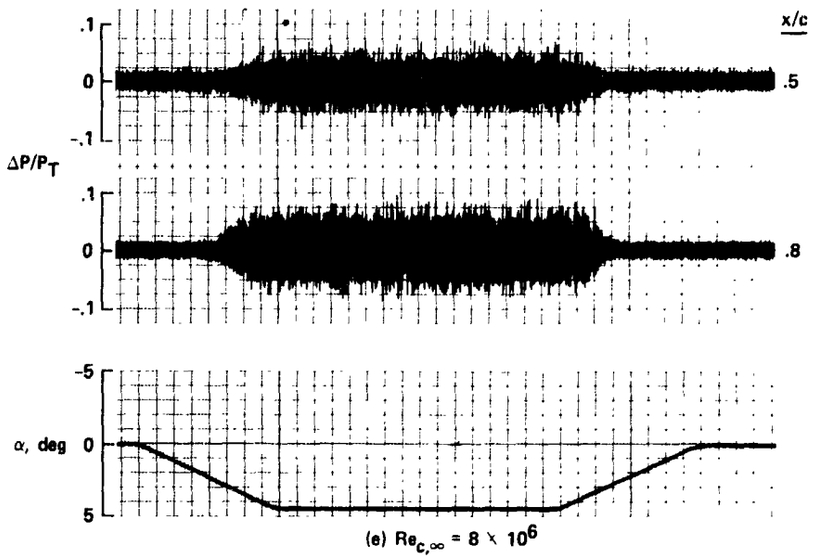

(e) $Re_{c,\infty} = 8 \times 10^6$

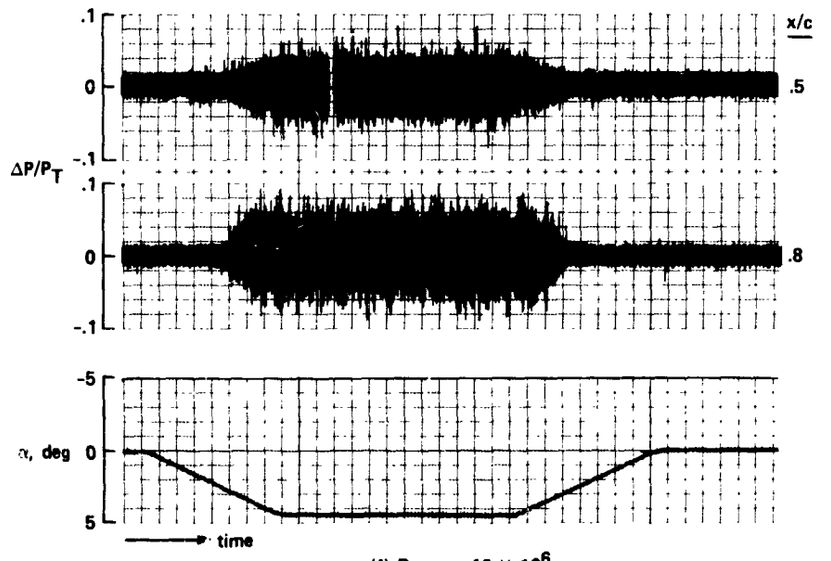

(f) $Re_{c,\infty} = 10 \times 10^6$

Figure 22.– Concluded.

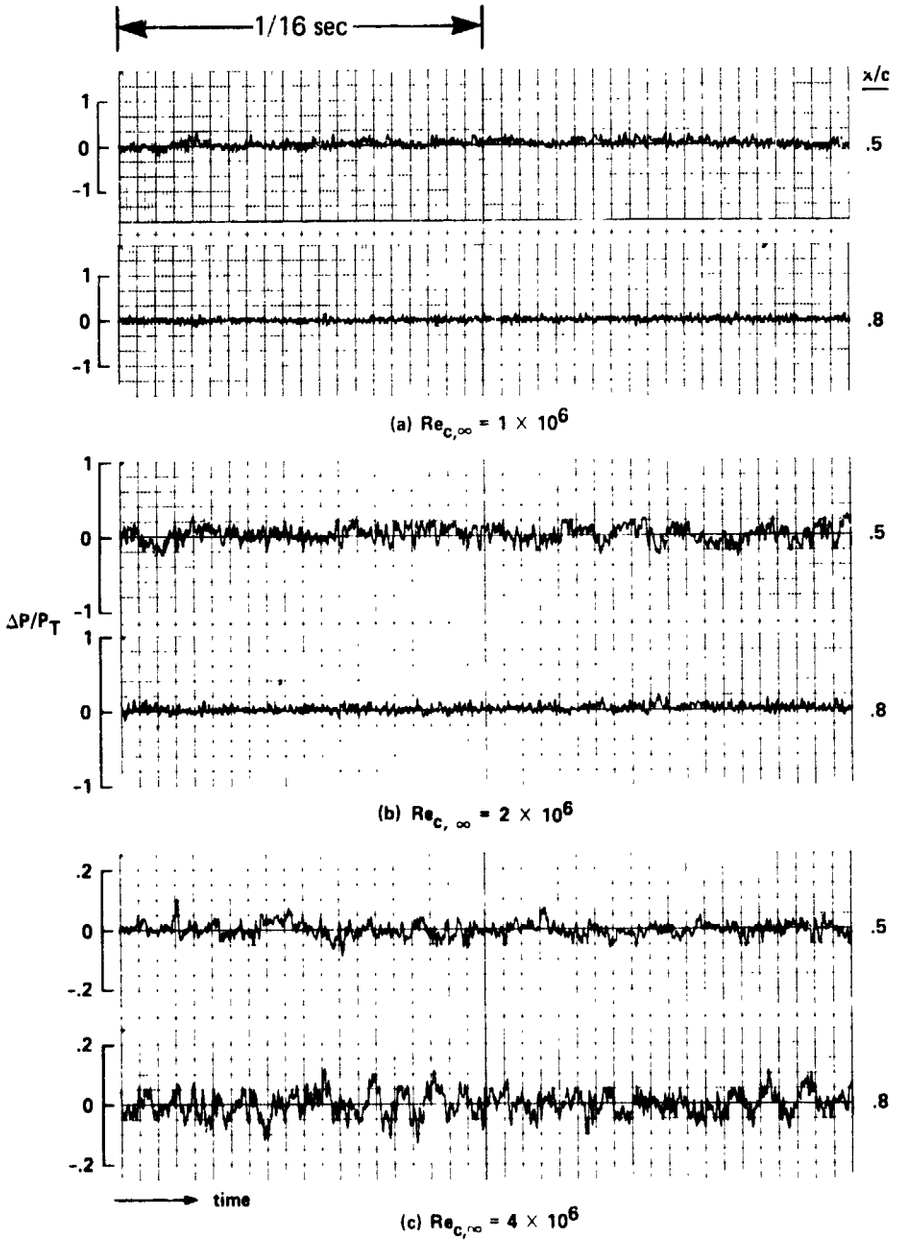

Figure 23.– Wave forms at $\alpha = 4°$, Data Set 5 ($M_N = 0.775$, $\alpha_N = 2°$).

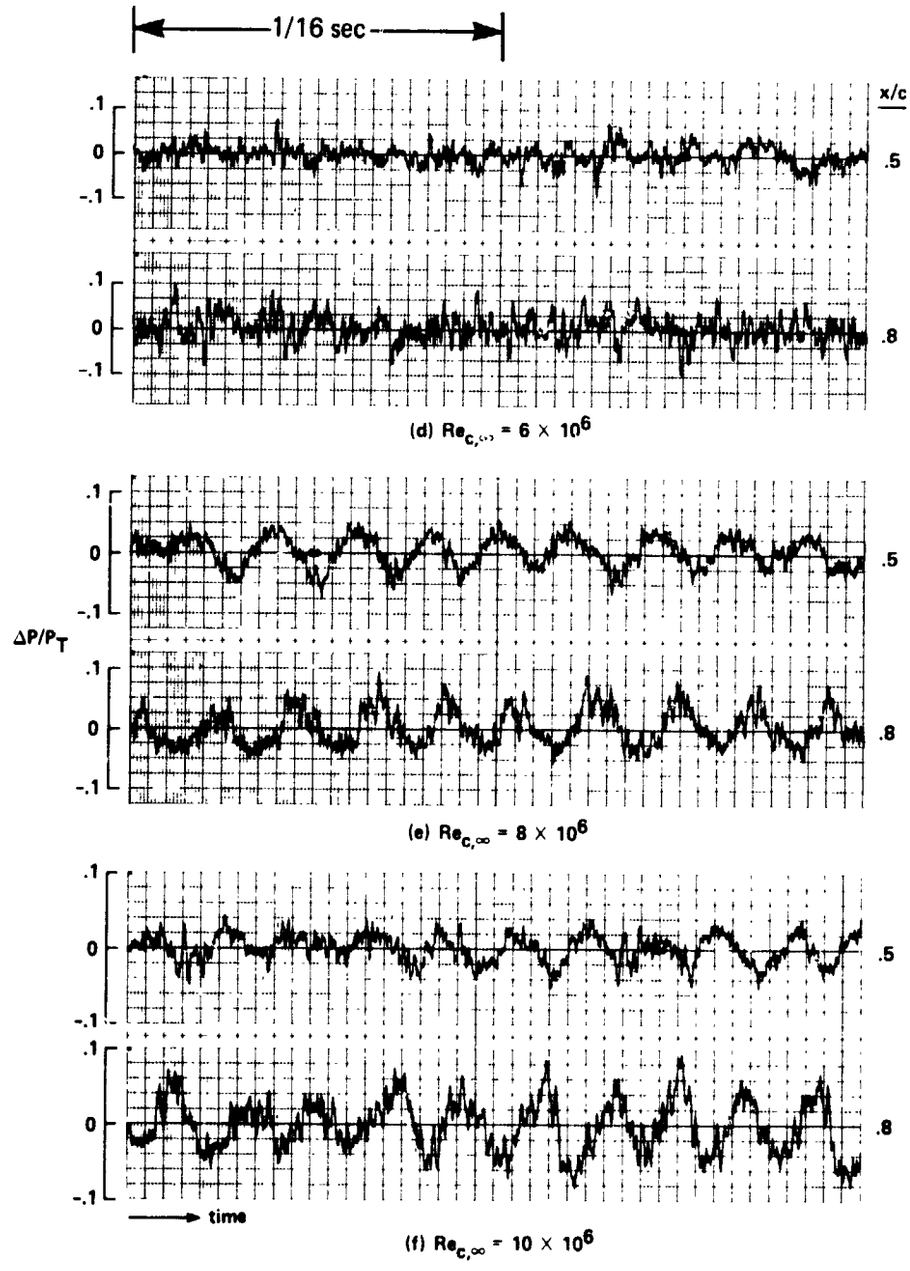

(d) $Re_{c,\infty} = 6 \times 10^6$

(e) $Re_{c,\infty} = 8 \times 10^6$

(f) $Re_{c,\infty} = 10 \times 10^6$

Figure 23.– Concluded.

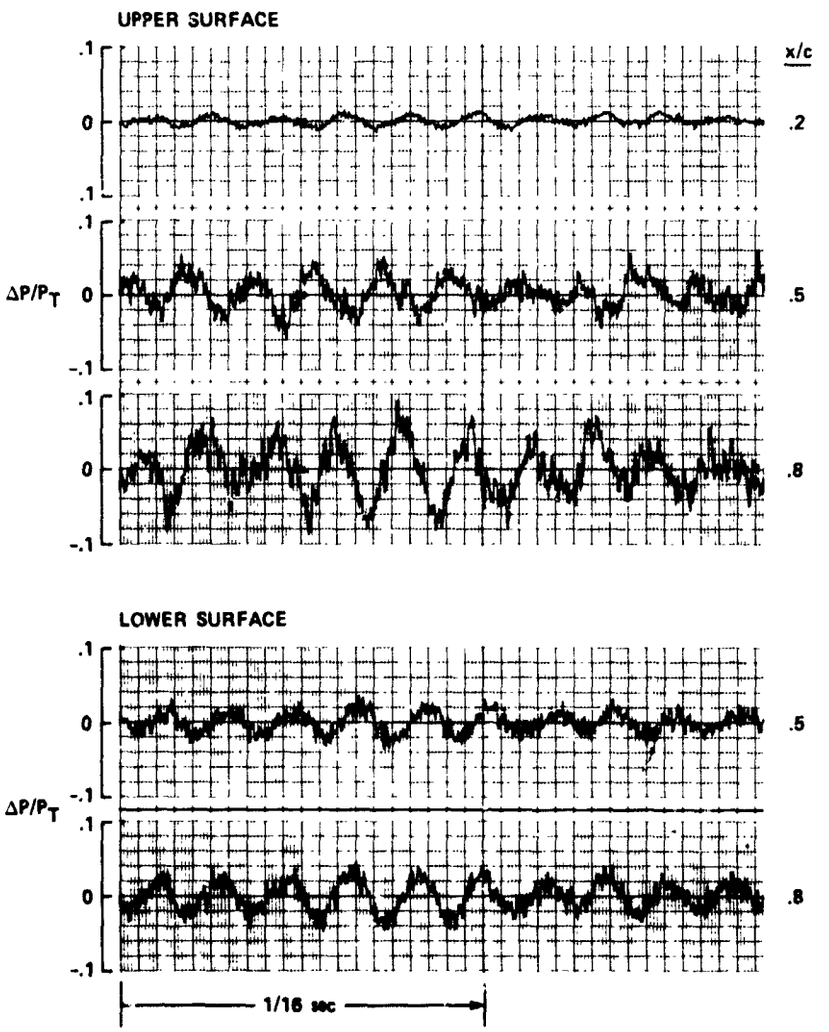

Figure 24.– Comparison of upper and lower surface wave forms; $\alpha = 4^{\circ}$, $M_{\infty} = 0.775$, $Re_{c,\infty} = 10^{7}$ (Data Set 5).

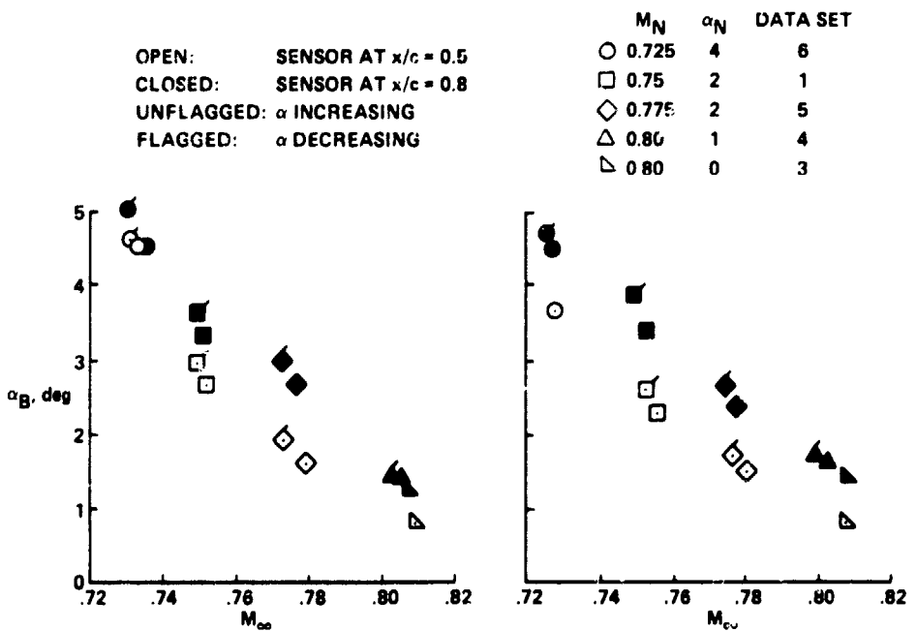

(a) $Re_{c,\infty} = 1 \times 10^6$.

(b) $Re_{c,\infty} = 2 \times 10^6$.

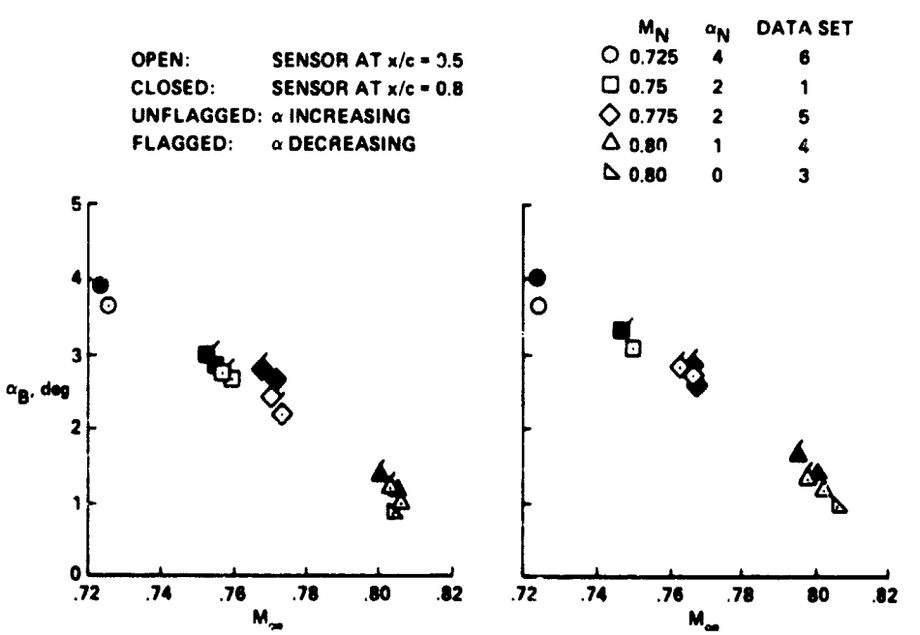

(c) $Re_{c,\infty} = 4 \times 10^6$.

(d) $Re_{c,\infty} = 6 \times 10^6$.

Figure 25.– Angle of attack for buffet onset.

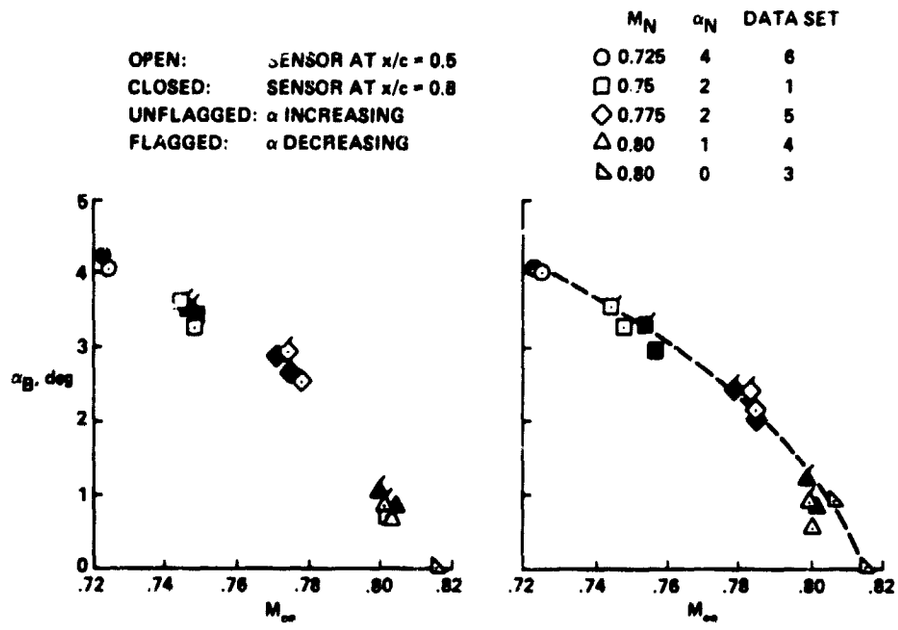

(e) $Re_{c,\infty} = 8 \times 10^6$.

(f) $Re_{c,\infty} = 10 \times 10^6$.

Figure 25.– Concluded.

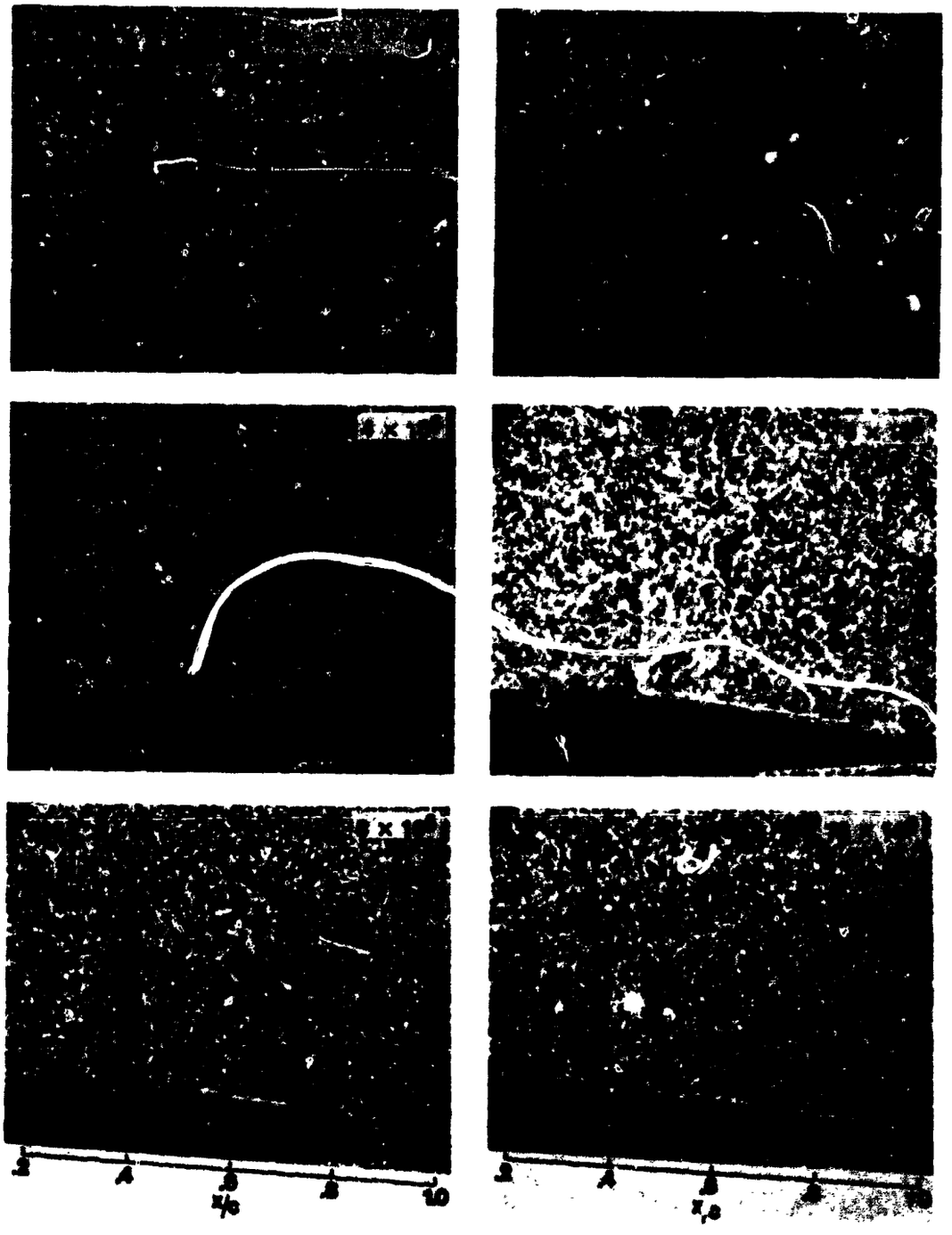

Figure 26. - Flow-field shadowgraphs; $M_\infty = 0.75$, $\alpha = 2°$ (Data Set 1, $M_N = 0.75$, $\alpha_N = 2°$).

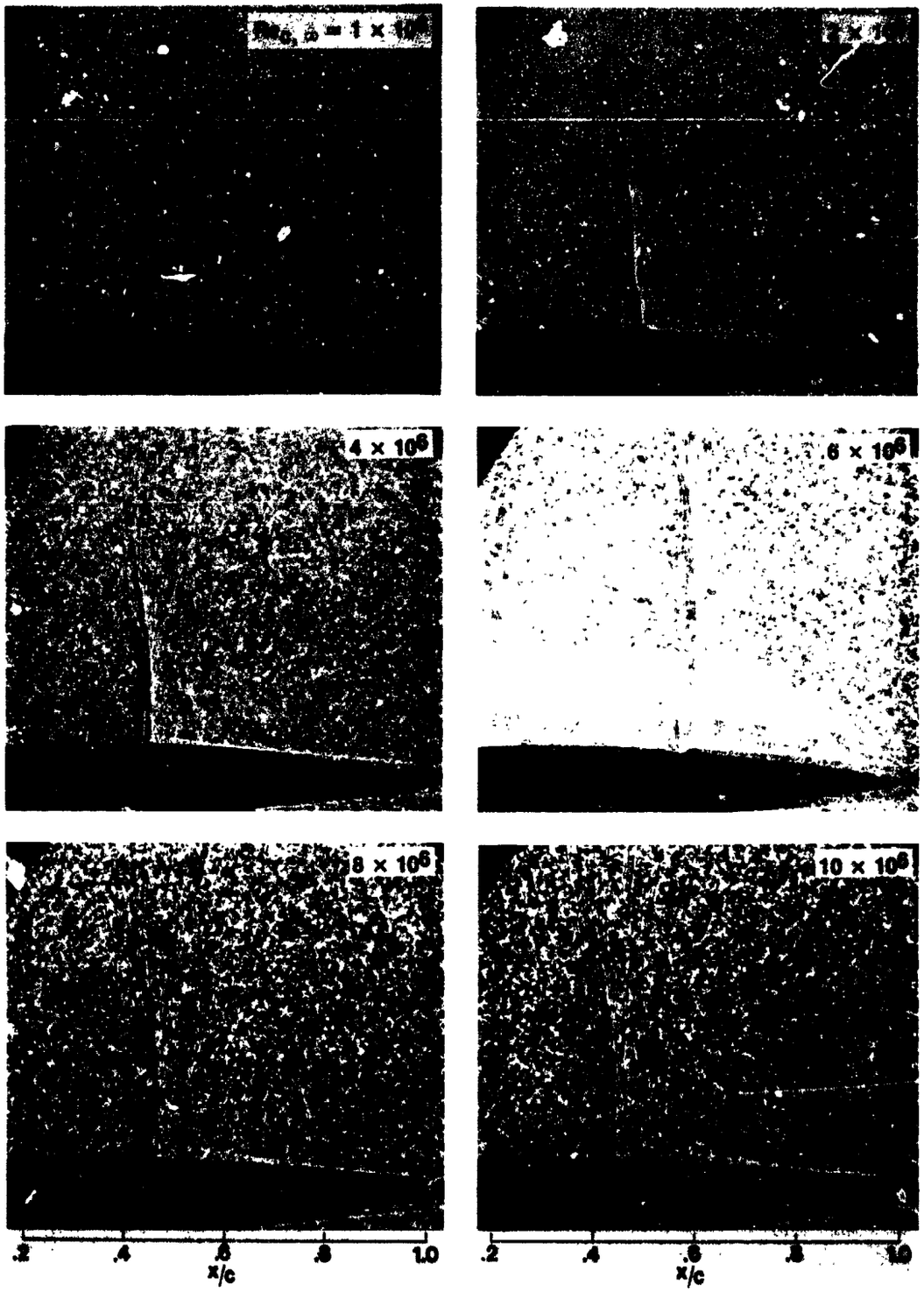

Figure 27.– Flow-field shadowgraphs; $M_\infty = 0.8$, $\alpha = 0^c$ (Data Set 3, $M_N = 0.8$, $\alpha_N = 0°$).

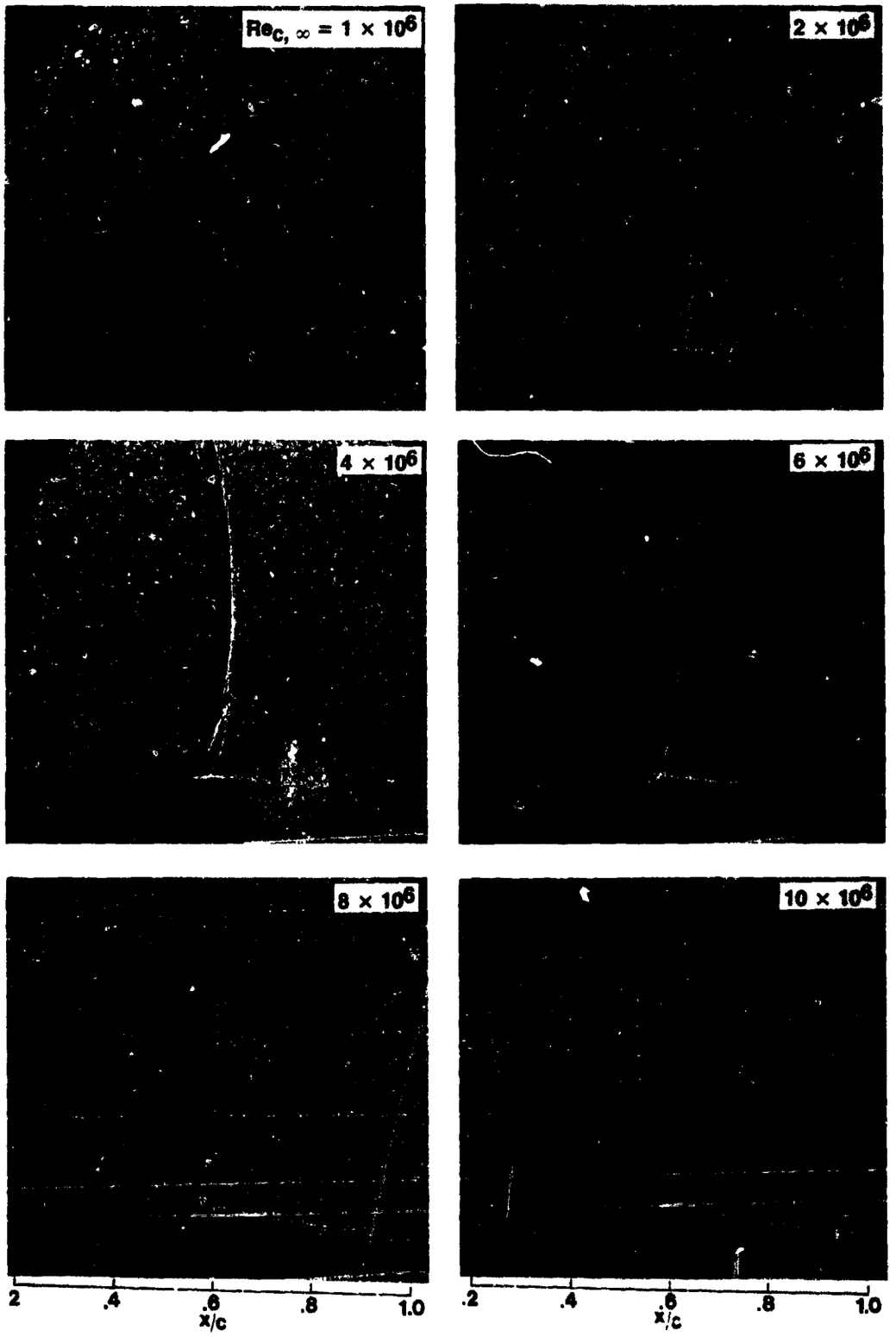

Figure 28.– Flow-field shadowgraphs; $M_\infty = 0.8$, $\alpha = 1^\circ$ (Data Set 4, $M_N = 0.8$, $\alpha_N = 1^\circ$).

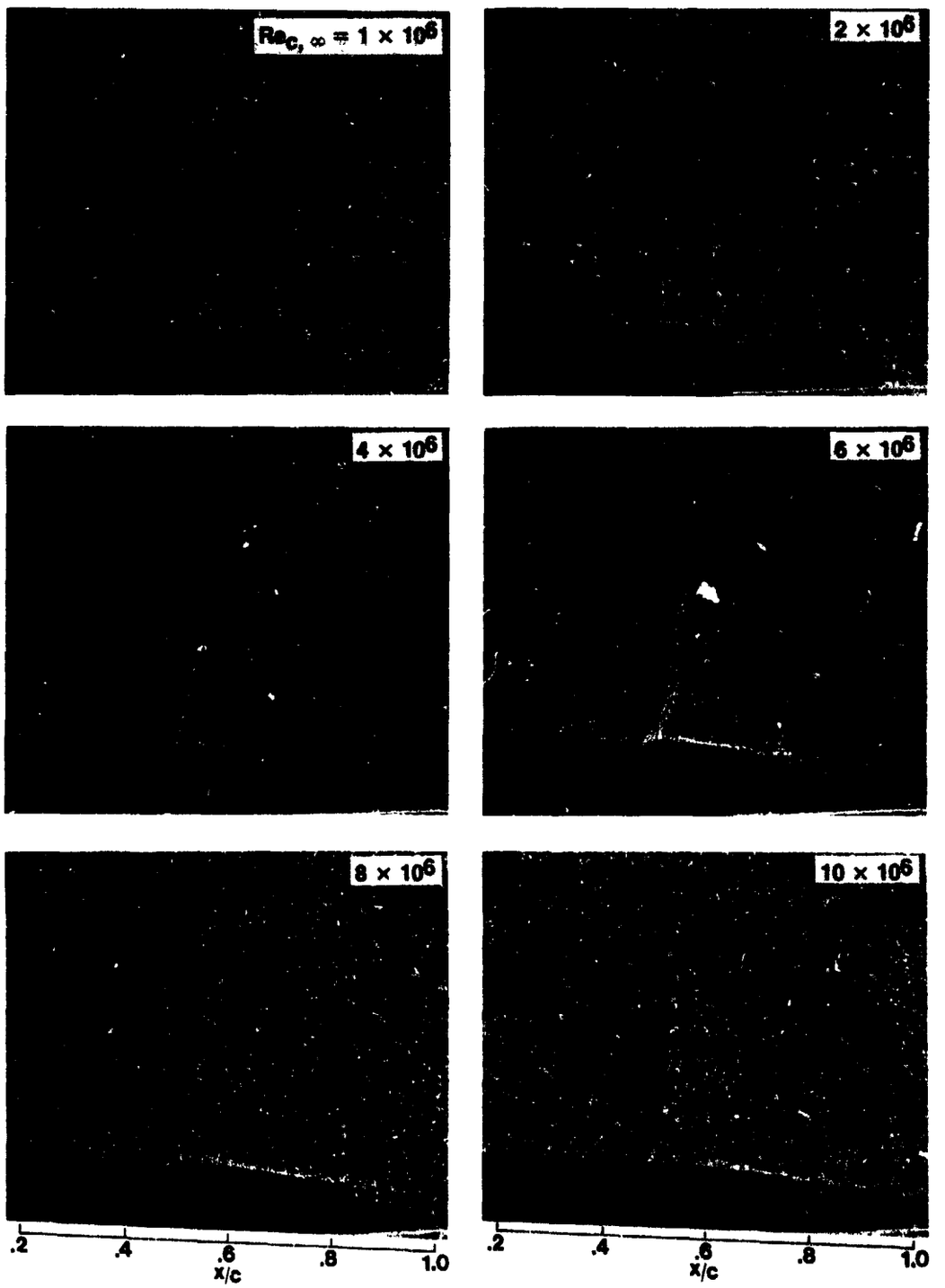

Figure 29.– Flow-field shadowgraphs; $M_\infty = 0.775$, $\alpha = 2°$ (Data Set 5, $M_N = 0.775$, $\alpha_N = 2°$).

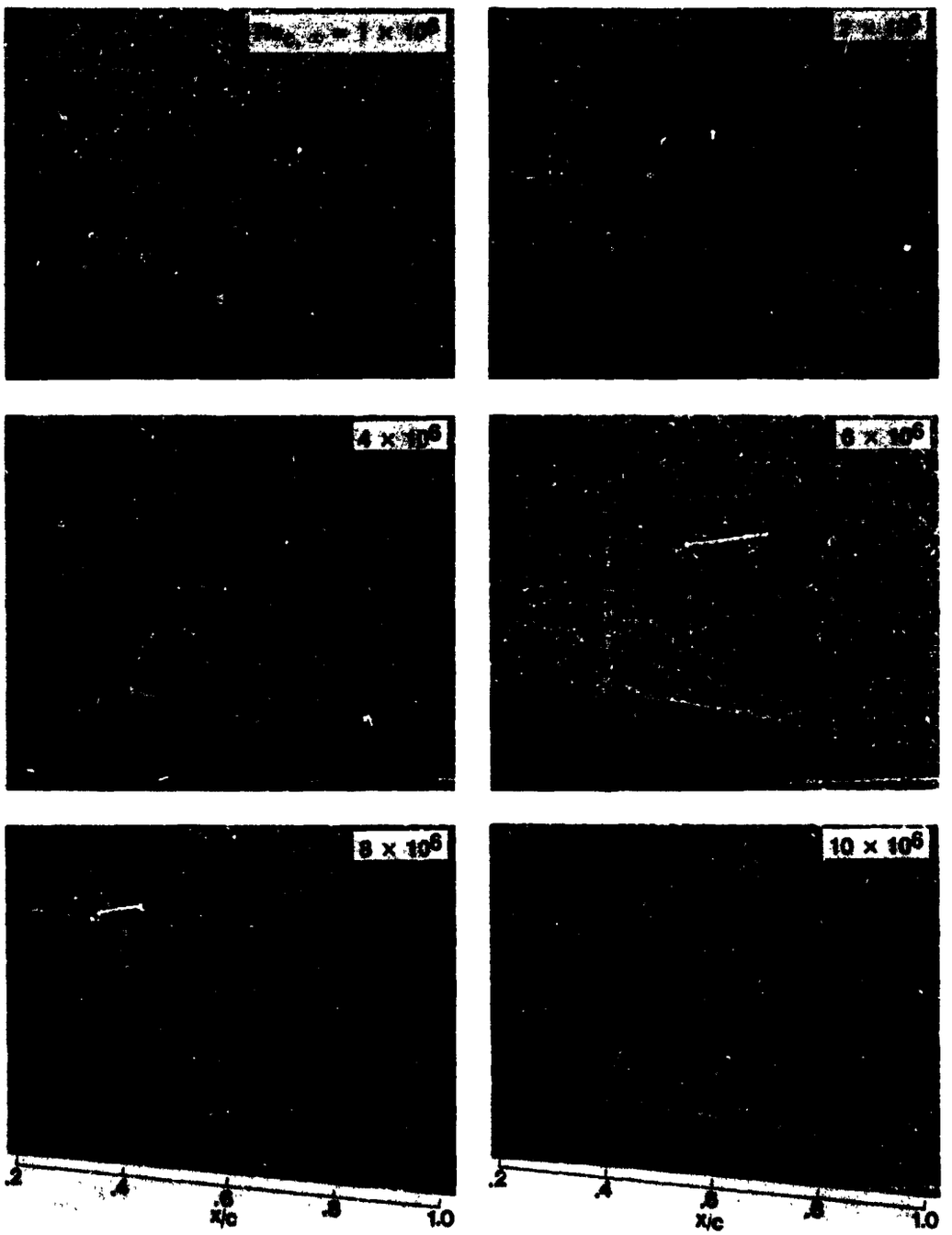

Figure 30.– Flow-field shadowgraphs; $M_\infty = 0.725$, $\alpha = 4°$ (Data Set 6, $M_N = 0.725$, $\alpha_N = 4°$).

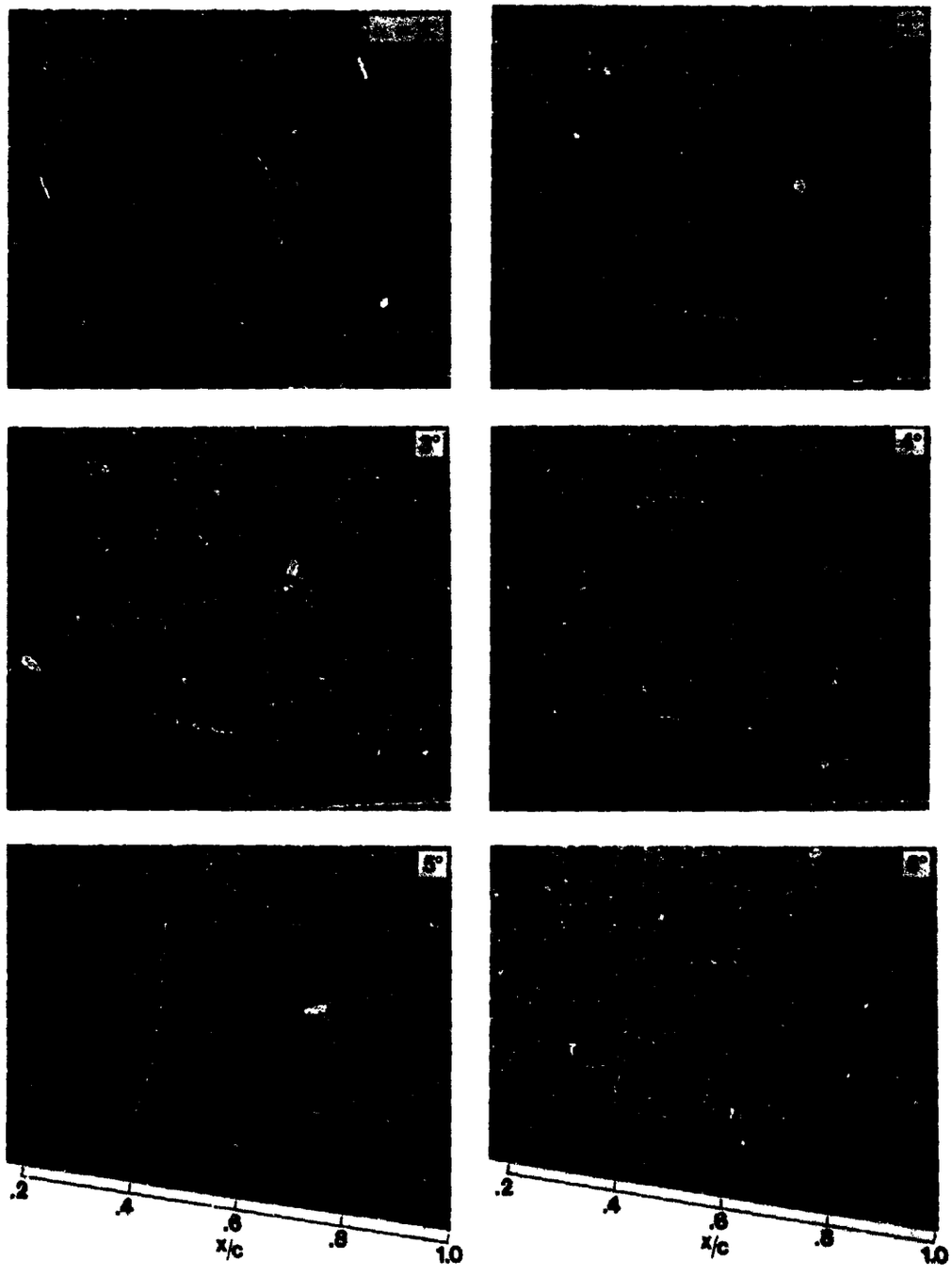

Figure 31.– Flow-field shadowgraphs showing effect of angle of attack; $M_\infty = 0.75, Re_{c,\infty} = 6 \times 10^6$ (Data Set 1, $M_N = 0.75, \alpha_N = 2^\circ$). $\alpha_B \approx 3.2^\circ$.

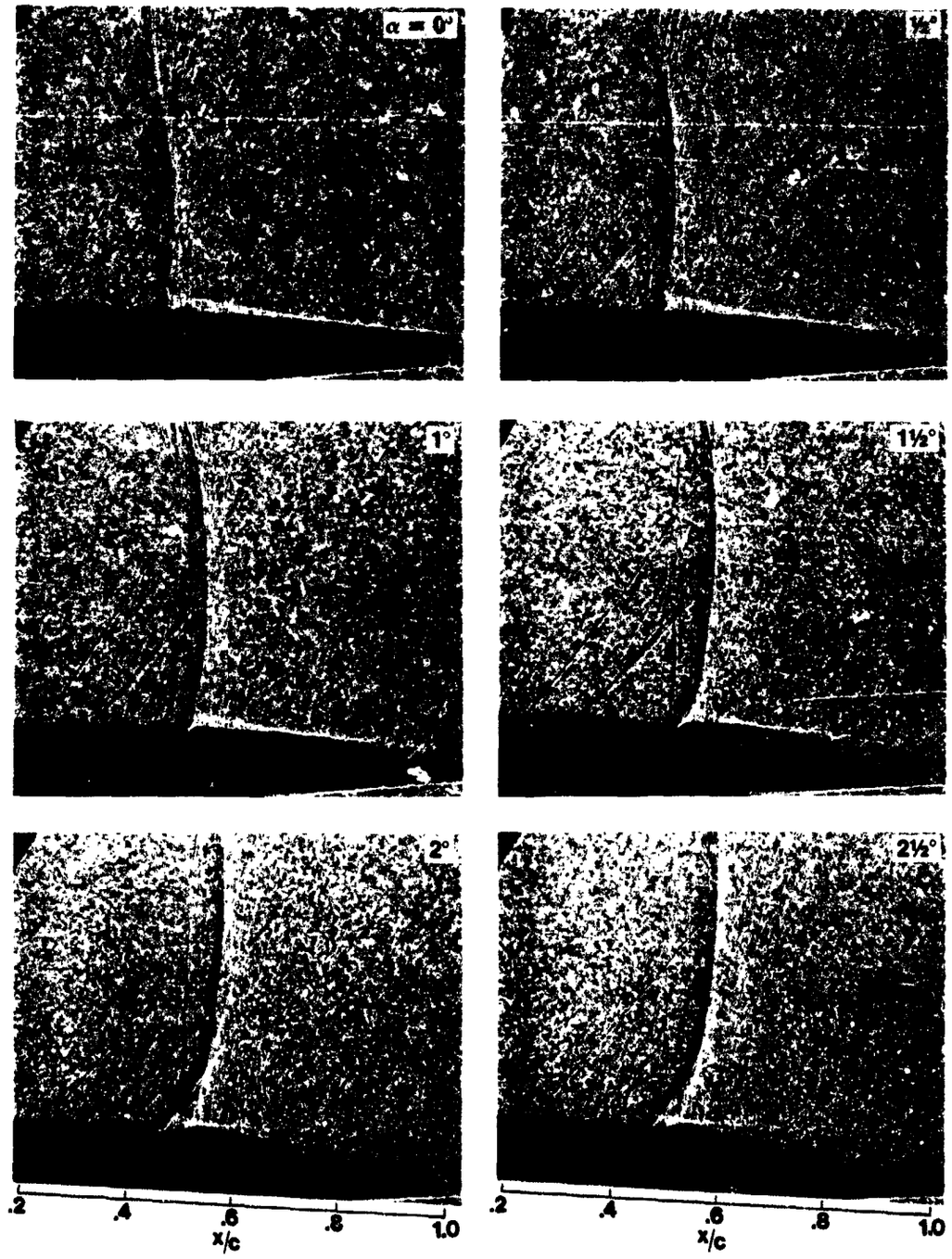

Figure 32.– Flow-field shadowgraphs showing effect of angle of attack; $M_\infty = 0.8$, $Re_{c,\infty} = 6\times10^6$ (Data Set 3, $M_N = 0.8$, $\alpha_N = 0°$). $\alpha_B \approx 1.3°$.

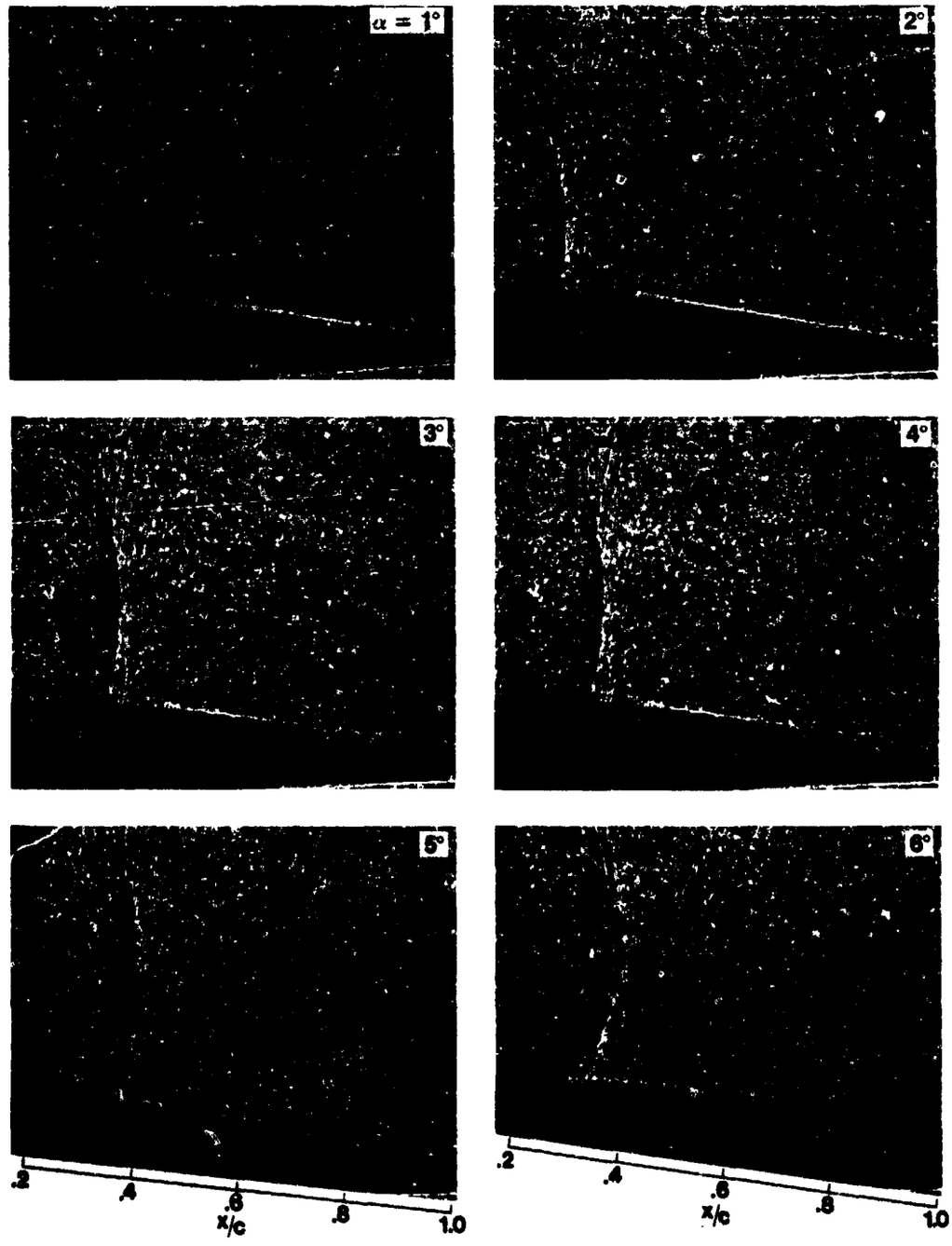

Figure 33.– Flow-field shadowgraphs showing effect of angle of attack; $M_\infty = 0.725$, $Re_{c,\infty} = 6 \times 10^6$ (Data Set 6, $M_N = 0.725$, $\alpha_N = 4°$). $\alpha_B \approx 3.9°$.

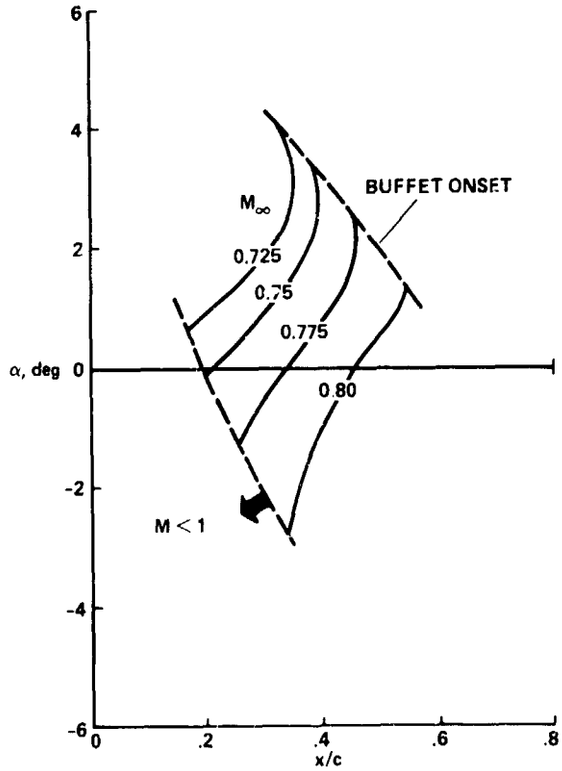

Figure 34.– Approximate chordwise location of base of shock wave, $Re_{c,\infty} = 10^7$.

1. Report No.	2. Government Accession No.	3. Recipient's Catalog No.
NASA TP-2485		

4. Title and Subtitle	5. Report Date
STATIC AND DYNAMIC PRESSURE MEASUREMENTS ON A NACA 0012 AIRFOIL IN THE AMES HIGH REYNOLDS NUMBER FACILITY	June 1985
	6. Performing Organization Code
7. Author(s)	8. Performing Organization Report No.
John B. McDevitt and Arthur F. Okuno	85100
	10. Work Unit No.
9. Performing Organization Name and Address	
Ames Research Center Moffett Field, CA 94035	11. Contract or Grant No.
	13. Type of Report and Period Covered
12. Sponsoring Agency Name and Address	Technical Paper
National Aeronautics and Space Administration Washington, DC 20546	14. Sponsoring Agency Code
	505-31-01

15. Supplementary Notes

Point of contact: Arthur F. Okuno, Ames Research Center, MS 229-1, Moffett Field, CA 94035
(415) 694-6211 or FTS 464-6211

16. Abstract

An experimental study has been conducted of the supercritical flows at high subsonic speeds over a NACA 0012 airfoil in order to acquire aerodynamic data suitable for evaluating numerical-flow codes. The measurements consisted primarily of static and dynamic pressures on the airfoil and test-channel walls. Shadowgraphs were also taken of the flow field near the airfoil. The tests were performed at free-stream Mach numbers from approximately 0.7 to 0.8, at angles of attack sufficient to include the onset of buffet, and at Reynolds numbers (based on airfoil chord) from 1 million to 14 million. A unique test section was employed which was designed specifically to obtain two-dimensional airfoil data with a minimum of wall interference effects. Boundary-layer suction panels were used to minimize sidewall interference effects. Flexible upper and lower walls allowed test-channel area-ruling to nullify Mach number changes induced by the mass removal, to correct for longitudinal boundary-layer growth, and to provide contouring compatible with the streamlines of the model in free air.

17. Key Words (Suggested by Author(s))	18. Distribution Statement
Aerodynamics Airfoils Transonic aerodynamics Buffet Flow field shadowgraphs	Unclassified - Unlimited Subject category – 02

19. Security Classif. (of this report)	20. Security Classif. (of this page)	21. No. of Pages	22. Price
Unclassified	Unclassified	76	A05

For sale by the National Technical Information Service, Springfield, Virginia 22161

NASA-Langley, 1985